SELF-TAUGHT LEARNING

A DISSERTATION
SUBMITTED TO THE DEPARTMENT OF COMPUTER SCIENCE
AND THE COMMITTEE ON GRADUATE STUDIES
OF STANFORD UNIVERSITY
IN PARTIAL FULFILLMENT OF THE REQUIREMENTS
FOR THE DEGREE OF
DOCTOR OF PHILOSOPHY

Rajat Raina
September 2009

INFORMATION TO USERS

The quality of this reproduction is dependent upon the quality of the copy submitted. Broken or indistinct print, colored or poor quality illustrations and photographs, print bleed-through, substandard margins, and improper alignment can adversely affect reproduction.
In the unlikely event that the author did not send a complete manuscript and there are missing pages, these will be noted. Also, if unauthorized copyright material had to be removed, a note will indicate the deletion.

ProQuest LLC
789 East Eisenhower Parkway
P.O. Box 1346
Ann Arbor, MI 48106-1346

I certify that I have read this dissertation and that, in my opinion, it is fully adequate in scope and quality as a dissertation for the degree of Doctor of Philosophy.

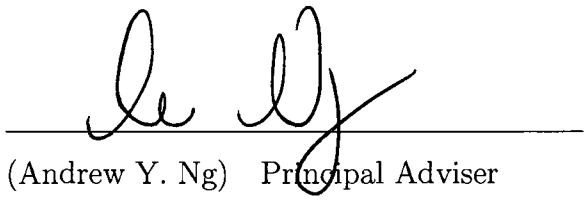

(Andrew Y. Ng) Principal Adviser

I certify that I have read this dissertation and that, in my opinion, it is fully adequate in scope and quality as a dissertation for the degree of Doctor of Philosophy.

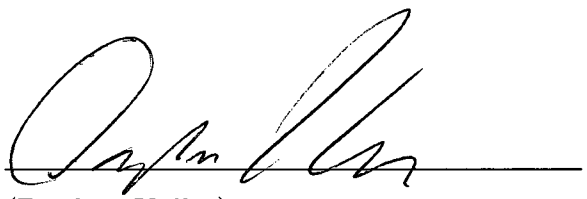

(Daphne Koller)

I certify that I have read this dissertation and that, in my opinion, it is fully adequate in scope and quality as a dissertation for the degree of Doctor of Philosophy.

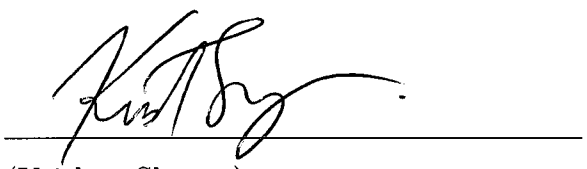

(Krishna Shenoy)

Approved for the University Committee on Graduate Studies.

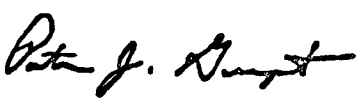

Acknowledgement

My journey at Stanford has benefitted greatly from the support of many people. First and foremost, it has been a privilege to have Andrew Ng as my advisor. Andrew has been a constant source of research advice and ideas. I am grateful that he made sure his students always had the resources, support and motivation they needed to excel. And above all, Andrew has been a wonderful and inspirational mentor. I will cherish and remember his advice for a long time to come.

Over the years, I have had several helpful discussions with professors at Stanford. I am especially grateful to Daphne Koller for her advice and for being on my dissertation reading committee. I have had several stimulating discussions with Krishna Shenoy and I thank him for being on my dissertation reading committee. I thank Christopher Manning for his guidance in my early formative years at Stanford, and Benjamin van Roy for being a wonderful teacher. I am grateful to Trevor Hastie for chairing my Orals committee.

I am indebted to my fellow students at Stanford for helping shape my research. I especially acknowledge Honglak Lee and Roger Grosse for collaborating closely on various projects. Their ideas and diligence have had a huge impact on the work presented here. I thank Ian Goodfellow and Quoc Le for help with installing graphics processor hardware. I have greatly enjoyed collaborating with Alexis Battle, Anand Madhavan and Benjamin Packer on various topics discussed in this thesis. I thank Adam Coates, Ashutosh Saxena, Chuong Do, Pieter Abbeel, Rion Snow, Stephen Gould and Zico Kolter for the many enlightening discussions.

Life has been fun at Stanford, and I owe that largely to my friends. If you are reading this, you probably know who you are. Thank you.

My family has stood by my side throughout my journey at Stanford. I am indebted to Rahul and Nirmala for being my friends over the years, and to Ajju for being a constant source of peace and happiness.

My biggest achievement at Stanford has to be that I found Penka. What would I have done without her?

Finally, my parents Rajni and Vijay made me what I am. For their unconditional support, guidance and love, this thesis is dedicated to them.

Contents

List of Tables

List of Figures

Chapter 1

Introduction

We introduce a new machine learning framework called *self-taught learning*. Algorithms in the self-taught learning framework require almost no human supervision, and can learn from easily available data sources. Machine learning algorithms are often only as good as the data they can learn from. Since self-taught learning algorithms can learn from much more data than many conventional learning algorithms, we believe that the development of such algorithms can significantly improve practical applications of machine learning. In this thesis, we develop several self-taught learning algorithms, and show that these algorithms work well on a wide variety of machine learning applications.

1.1 Supervised learning

In recent years, machine learning techniques have been used in large variety of applications, including computer vision, natural language processing, speech recognition, and recommendation systems. The vast majority of these applications rely on using labeled training data to train models. For example, state-of-the-art methods for recognizing face images rely on being trained using thousands of labeled face images; methods for document categorization use thousands of documents already labeled with the target categories; and methods for speech recognition are trained on annotated speech samples from many users.

The task of learning from labeled data is called *supervised learning*, and has been widely studied in machine learning and statistics. Over the past few decades, many sophisticated learning methods have been developed for supervised learning problems—support vector machines (Cortes & Vapnik, 1995), conditional random fields (Lafferty et al., 2001), generalized linear models (McCullagh & Nelder, 1989), neural networks (Rumelhart et al., 1987), to name just a few—and they are able to achieve good performance in a wide variety of fields. At their heart, these methods rely on being given a large number of training inputs $x \in \mathcal{X}$, with their known labels $y \in \mathcal{Y}$, which they then use to fit a function $h : \mathcal{X} \to \mathcal{Y}$ that approximates the mapping from inputs to labels; once the function h is obtained on the labeled training data, we can take a new, previously unseen input $x_{\text{new}} \in \mathcal{X}$ and predict a label $h(x_{\text{new}})$ for that input. When a sufficiently large number of labeled training examples is available, supervised learning methods are often able to learn good predictors that give very accurate predictions on new examples. In many cases, the performance of these predictors can be theoretically guaranteed (under some assumptions).

The most challenging problems in machine learning arise when the number of labeled examples is "small." To take a specific example, consider a computer vision application, where we have to predict the gender (male or female) of a person from a 100×100 pixel input image of their face. Each input image can be represented as a high-dimensional vector $x \in \mathbb{R}^{10000}$, containing the pixel intensities of each of the 10,000 pixels in the image. In principle, it should be possible to fit a function h that takes these 10,000-dimensional input vectors and predicts whether the person in the image is male or female. In practice, this can be quite hard: a slight shift in the camera angle, or lighting conditions, or facial expression, can change the 10,000 numbers (pixel intensity values) dramatically; in the face of all these variations, we need the function h to somehow sift through all of the unimportant changes in pixel values, and compute an aggregate function that captures just the gender represented by the pixels. To have any hope of recovering such a function h, it appears that we would need to fit the function using thousands of labeled examples, at least. When many fewer labeled examples are available (e.g., tens of gender-labeled face images), the straightforward supervised learning approach does not work as well.

Unfortunately, it can often be difficult to obtain sufficiently large amounts of labeled data for supervised learning. Labeled data typically requires human supervision (e.g., a human looking at thousands of face images, and labeling each as male or female), which makes it very expensive to produce. It is thus highly desirable to have machine learning methods that are able to learn with very few labeled examples, and with limited human supervision. This is especially true for modern applications, such as on those on the web or on mobile devices, where we often want to learn a good predictor from very few user interactions.

1.2 Feature engineering

With limited labeled data, since the supervised learning task is often hard to solve automatically, one possible approach is to build in more knowledge into the supervised learner. Instead of taking the raw inputs $x \in \mathcal{X}$ and labels $y \in \mathcal{Y}$, we might manually compute certain functions $\Phi(x)$, called "features," of the input that we think are informative in predicting the label y. In the previous example, we represented each face image by a vector $x \in \mathbb{R}^{10000}$; this is a fairly impoverished representation in terms of raw pixel intensities, with no knowledge encoded about images in general (e.g., that they often have slowly varying regions separated by edges) or about faces in particular (e.g., that they have two eyes and a nose). We might instead use image processing techniques to compute image functions such as:

- $\Phi_1(x) =$ (The distance between the eyes)^2 / (The length of the nose)
- $\Phi_2(x) =$ The length of the hair.
- $\Phi_3(x) =$ The width of the forehead.
- ...
- $\Phi_{10}(x) =$ The angle of the chin.

It is tough to write down new features like these that are indeed informative about the gender, and designing good features often requires significant human expertise, insight

and ingenuity. Also, some features are themselves hard to compute—for example, it is not immediately clear how we could find the exact location of the eyes, given only 10,000 numbers representing pixel intensities for the face. In fact, some of these features might themselves require *years* of image processing research to compute accurately, even for this one application domain. Once we have the output of these features $\Phi(x)$, we might finally hope to be able to learn a function $g(\Phi(x))$ that uses the computed features $\Phi(x)$ (consisting of 10 numbers) instead of the original 10,000-dimensional input space to much more easily predict the gender label y.

This approach to machine learning is not completely satisfactory—we set out to automatically learn about images (or audio, or text, etc.), but in the end, had to spend significant amounts of time manually designing features that would enable learning algorithms to find good predictors. Many of these hand-engineered features are highly specific to particular applications, and may not easily carry over to new application domains. Further, feature design is often an empirical process, that is driven at best by human intuition, and at worst by plain trial and error. Some features might be informative and useful when considered individually, but might be subsumed by other features when considered all-at-once. Humans are exceptionally good at predicting the gender given a face image, but they still may not be able to write down 10 numbers (features) that led them to making their predictions.[1] Informally, humans are not very good at number crunching, and this can make feature engineering a laborious and cumbersome process.

This example suggests that to apply supervised learning to many hard, new problems, we might need to invest several person-years into intensive research to develop high-quality features, before learning can be successfully applied.

1.3 More data, less feature engineering

The above discussion leads to one of the central problems in machine learning over the past decade: given that labeled data is expensive and hard to obtain, can we

[1]For this particular problem, there are even detailed experiments studying the visual cues that humans use to perform gender discrimination. (Dupuis-Roy et al., 2009)

use other, more easily available sources of data for learning? The hope is that by using these other sources of data to guide the learning process, we might be able get away with less labeled data, and less feature engineering. This has led to whole new ways of thinking about machine learning, and given rise to significant new machine learning formalisms, that go beyond supervised learning. We briefly discuss two relevant formalisms.

1.3.1 Semi-supervised learning

In many machine learning applications, it is hard to get labeled data, but it is relatively easy to get large amounts of *unlabeled* data. For face recognition, it is possible to get a large number of face images automatically (e.g., by running a simple face detector over images)—each of these images contains a face, we just don't know whether it is a male or a female face. One might imagine that by looking at a large number of such unlabeled input examples $x_u \in \mathcal{X}$, even without the corresponding labels $y_u \in \mathcal{Y}$, we can learn useful things about the input domain. For example, we can estimate the input-only or "marginal" distribution $P(x)$, which might inform our supervised learning algorithm that some x values, or some combinations of 10,000 pixel intensity values, are more likely to represent faces than others; by then focusing our function-fitting and learning algorithm on those parts of the input space only, we might obtain a simpler supervised learning problem, and we might be able to learn a better predictor. Viewed another way, having access to a large number of unlabeled face images $x_u \in \mathcal{X}$ might help us "expand" our labeled training set by finding images that are extremely similar to certain labeled face images; if an unlabeled image is extremely similar to a labeled image, it appears reasonable to assume that the unlabeled image has the same label. This effectively gives us more information about the mapping $x \rightarrow y$ that we can use for learning.

This formalism of using both labeled and unlabeled data to solve a supervised learning problem is called *semi-supervised learning*, as it is in between supervised learning (only labeled data) and unsupervised learning (only unlabeled data). It assumes that the unlabeled data is derived from the *same classes as the labeled data*;

each unlabeled example $x_u \in \mathcal{X}$ can be assigned a valid label $y_u \in \mathcal{Y}$ in principle, but the label is just not available for learning. This makes sense for some applications: in our running example, any unlabeled face image must be either male or female, we just don't know the label. This turns out to be an important aspect of several semi-supervised learning algorithms, and one that we will return to later in the section.

There are tens of published papers on semi-supervised learning algorithms, and we refer the reader to Zhu's survey paper (Zhu, 2005) and Chapelle et al.'s book (Chapelle et al., 2006) for a comprehensive overview. To help later discussion, we give a bird's eye view of the field. If we consider supervised learning algorithms as attempting to find predictor functions h that minimize some "loss function" $\mathcal{L}$ (such as squared-error, misclassification rate, etc.) on the labeled data: $\arg\min_f \mathcal{L}(f)$, then loosely speaking, semi-supervised learning algorithms attempt to influence this process in various ways, by using various notions of what a "good" predictor should do on the unlabeled data. To name just a few:

- A good predictor should suggest label boundaries only in areas of low input density $P(x)$, so that most inputs $x \in \mathcal{X}$ lie far from the label boundary. Intuitively, this gives the predictor some margin for error, and makes the predictions more likely to be correct. This is often also called the "cluster assumption." (Seeger, 2001) Some methods, such as transductive support vector machines (Vapnik, 1998; Joachims, 1999), attempt to directly capture this assumption in picking the supervised learning predictor.[2] Several other methods use this intuition to pose different models, including via Gaussian processes (Lawrence & Jordan, 2006) or information regularization (Szummer & Jaakkola, 2003).

- A good predictor should vary "smoothly" in its predictions on the unlabeled data—if two unlabeled examples x_u^1 and x_u^2 are very similar, then the predictions $h(x_u^1)$ and $h(x_u^2)$ should also be similar. A large number of semi-supervised learning methods construct a weighted graph over input examples (with weights specifying similarities), and then formalize the algorithm using graph-theoretic

[2]Technically, transductive learning can be considered a special case of semi-supervised learning, where the unlabeled inputs are exactly the ones that we need predictions for. For our purposes, this is not a very important distinction.

notions of connectedness or smoothness (Blum & Chawla, 2001; Belkin et al., 2005; Zhou et al., 2003).

- If the supervised learning model attempts to learn a joint distribution $P(x, y)$ to capture what inputs x are likely to occur with what labels y, semi-supervised learning provides information about the input distribution $P(x)$, which might inform us about the predictive distribution $P(y|x)$. Such information can be leveraged, for example, by "guessing" the likely labels y_u for the unlabeled inputs x_u, and then using these labels for learning. (Nigam et al., 2006)

- A somewhat different method would be to use unlabeled data to learn an encoding for inputs x, and then use that encoding to simplify the supervised learning problem. For example, the input can be represented using a decomposition such as principal components analysis (PCA), which attempts to find a low-dimensional subspace close to most input examples; representing each input example by its low-dimensional representation could then lead to a simpler supervised learning problem.[3] Many other methods fall in this category, including manifold learning methods such as ISOMAP (Tenenbaum et al., 2000) and locally-linear embedding (Roweis & Saul, 2000), and several neural network models that are contemporary to our work, including deep belief networks (Hinton & Salakhutdinov, 2006) and autoencoders (Bengio et al., 2006). Instead of finding structure in the inputs, a semi-supervised learning method can also attempt to learn structure within good predictors h, often over auxiliary learning tasks constructed by applying heuristics to the unlabeled data; this structure can be used to prefer predictors with the learnt structure. (Ando & Zhang, 2005)

This is not an exhaustive list of semi-supervised learning algorithms, but it is worth pointing out that most of these algorithms make certain assumptions about the problem at hand, and the nature of the unlabeled and labeled data. When these

[3]Such an application of principal components analysis is especially common for text documents, where it can represent documents using semantically-meaningful combinations of words (subspaces in the input word space), instead of just using the individual words. For text documents, this is often called latent semantic analysis. (Deerwester et al., 1990)

assumptions are valid, semi-supervised learning can often help predictive performance; but when the assumptions are violated, semi-supervised learning can sometimes hurt, by adding a flawed notion of good predictors to the supervised learning problem. (Cozman & Cohen, 2002)

For this thesis, we are interested in relaxing a central restriction made by many semi-supervised learning algorithms: the unlabeled data *must* be from the same classes as the labeled data. Further, many algorithms implicitly assume that the unlabeled inputs x_u are drawn from the same distribution as the labeled inputs, and that estimating this common input distribution is useful for better learning. In many real applications, these assumptions are unfortunately difficult to meet. Consider the following examples of supervised learning tasks:

- Classifying images of elephants vs. images of rhinos: To apply semi-supervised learning, the unlabeled data must consist of images just of elephants and rhinos (and no other images). Given an unlabeled image and sufficient time, one should be able to provide a label "elephant" or "rhino." This is unsatisfactory as it is difficult to get truly unlabeled images of just elephants and rhinos, and nothing else, in such a way that we don't already know the label. What we can get easily are unlabeled images of jungles, or pictures of natural environments, but these do not fit into the semi-supervised learning framework.

- Distinguishing between 5 specific speakers using their recorded speech: To apply semi-supervised learning, we need unlabeled examples (speech) from exactly those 5 speakers. This is not very helpful—if we could record from one of those 5 speakers, we would just have more *labeled* data, not more unlabeled data. Instead, the "unlabeled data" we might want to use would be speech samples from other users, possibly speaking different languages, but semi-supervised learning does not allow this.

- Categorizing webpages about pottery vs. webpages about sculptures: Again, it is unclear how we can apply semi-supervised learning, because it appears hard to get unlabeled webpages that are about pottery or sculptures, but nothing else.

Thus, the semi-supervised learning framework does not seem to capture many types of unlabeled data that we would like to use to help supervised learning. This is a central observation and we will return to it later in proposing a different framework for using unlabeled data in machine learning. We also discuss the application of some semi-supervised learning methods and other prior art to our framework in Section 1.6, and in further detail in Section 2.5.

1.3.2 Transfer learning

Recall the supervised learning problem, where we are given a classification task with limited labeled data, and we would like to learn a good predictor from this data. Transfer learning (sometimes called multitask learning) asks the following question: can access to labeled data from other supervised learning problems help? Consider our running example of predicting gender from a face image. If we are given access to many other "similar" supervised learning problems (e.g., classifying elephant images vs. rhino images, classifying car images vs. motorcycle images, etc.), we might be able to discover the properties of "good predictors" for any of these tasks—for example, a prediction probably should not change too much if we move the camera a little, leading to a displacement of pixels in the image. By developing this notion of a good predictor on the extra supervised learning problems, and then applying the notion to help the supervised problem we care about (classifying face images), we might be able to find better predictors. In this way, transfer learning might help in situations with limited labeled data.

Again, many different algorithms have been devised for transfer learning, each requiring somewhat different assumptions. (Thrun, 1996; Ando & Zhang, 2005; Caruana, 1997) For good transfer learning, we need the extra supervised learning tasks to be "related" to the supervised learning task at hand, and this relatedness has been quantified in theoretical terms. (Baxter, 1997)

However, to apply transfer learning, we require *labeled data*, even if from other supervised learning problems. Given a new supervised learning problem, it can be difficult to find related labeled data (and if we have to manually label related data,

we might as well label data for the supervised learning task at hand).

1.4 Self-taught learning

Self-taught learning is a formalism for using unlabeled data in machine learning. To motivate our discussion, consider as a running example the computer vision task of classifying images of elephants and rhinos. For this task, it is difficult to obtain many labeled examples of elephants and rhinos; indeed, it is difficult even to obtain many *unlabeled* examples of elephants and rhinos. (In fact, we find it difficult to envision a process for collecting such unlabeled images, that does not immediately also provide the class labels.) This makes the classification task quite hard with existing algorithms for using labeled and unlabeled data, including most semi-supervised learning algorithms. (Nigam et al., 2000) Instead, we ask how unlabeled images from *other* object classes—which are much easier to obtain than images specifically of elephants and rhinos—can be used. For example, given unlimited access to unlabeled, randomly chosen images downloaded from the Internet (probably none of which contain elephants or rhinos), can we do better on the given supervised classification task?

Although we use computer vision as a running example, the problem that we pose to the machine learning community is more general. Formally, we consider solving a supervised learning task given labeled and unlabeled data, where the unlabeled data does not share the class labels or the generative distribution of the labeled data. For example, given unlimited access to natural sounds (audio), can we perform better speaker identification? Given unlimited access to news articles (text), can we perform better webpage classification?

Like semi-supervised learning (Nigam et al., 2000), our algorithms will therefore use labeled and unlabeled data. But unlike semi-supervised learning as it is typically studied in the literature, *we do not assume that the unlabeled data can be assigned to the supervised learning task's class labels.* To thus distinguish our formalism from such forms of semi-supervised learning, we will call our task *self-taught learning.*

We compare our framework with transfer learning first. Given a supervised learning problem with limited labeled data, transfer learning typically requires further

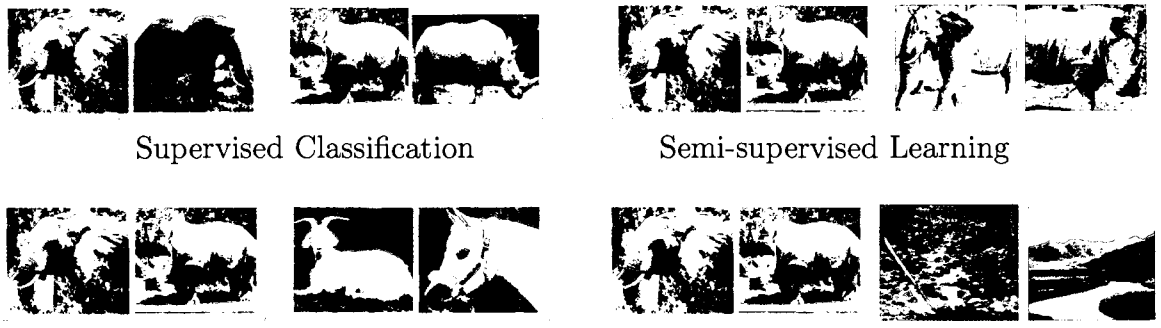

Figure 1.1: Machine learning formalisms for classifying images of elephants and rhinos. Images on orange background are labeled; others are unlabeled. Top left: Supervised classification uses labeled examples of elephants and rhinos. Top right: Semi-supervised learning uses additional unlabeled examples of elephants and rhinos. Bottom left: Transfer learning uses additional labeled datasets. Bottom right: Self-taught learning just requires additional unlabeled images, such as ones randomly downloaded from the Internet.

labeled data from a different but related task, and at its heart typically transfers knowledge from one supervised learning task to another; thus it requires additional labeled (and therefore often expensive-to-obtain) data, rather than unlabeled data, for these other supervised learning tasks. (Thrun, 1996; Caruana, 1997; Ando & Zhang, 2005) We note that these additional supervised learning tasks can sometimes be created for some domains (such as natural language modeling) via ingenious heuristics, as in Ando & Zhang (2005).

We view our self-taught learning framework as an extension of previous frameworks (such as semi-supervised learning) for incorporating more general types of unlabeled data into a supervised learning algorithm. There are many methods that use unlabeled data to assist supervised learning in various ways, with many of the published methods and results assuming a semi-supervised learning problem setup. As mentioned earlier, semi-supervised learning typically makes the additional assumption that the unlabeled data can be labeled with the same labels as the classification task, and that these labels are merely unobserved (Nigam et al., 2000). Because of this assumption, while many semi-supervised algorithms may not work well in the self-taught learning setting (where the algorithms can no longer assume that the

unlabeled data comes from the classes in the supervised task), it is possible that some semi-supervised algorithms can be successfully applied to self-taught learning problems, or can be modified to work well on self-taught learning problems.

In conventional semi-supervised learning, we assume that the unlabeled data comes from the same classes as the labeled data; in self-taught learning, we do not require this assumption. Given a supervised learning task with many classes, we can always add an extra "other" class, and assume that all the unlabeled data arises from that class. Technically, this reduces the self-taught learning to a semi-supervised learning problem, and so self-taught learning can be viewed as a specific type of semi-supervised learning problem.[4] But we note that in this reduction, the semi-supervised learning problem contains all the unlabeled data from just one ("other") class, and thus we do not expect the reduction to be practically useful in semi-supervised learning algorithms.

Over the past decade, there has been extensive research on semi-supervised learning methods (e.g., see survey papers by Seeger, 2001 and Zhu, 2005), and we discuss related work at length in the following pages, but we make particular mention of two published modifications for semi-supervised learning that appear most closely related to the self-taught learning framework:

- **Semi-supervised learning by learning predictive structures**: Ando & Zhang (2005) proposed a transfer learning method that attempts to use multiple supervised learning tasks to learn the properties of good classifiers for these tasks. While their method is based on *labeled data* from multiple learning tasks, they show that for some domains, the labeled data for these multiple learning tasks can be created automatically by applying heuristics to *unlabeled* data. For example, given unlabeled text documents, we can hide the presence/absence of a specific word w, and then label each document either as Y (if it contains the word w) or N (otherwise); this heuristic procedure thus provides labeled data for an artificially created supervised learning problem, to which the transfer learning algorithms can be applied. Using such heuristics, we can thus use both

[4] This reduction was pointed out to us by Trevor Hastie.

unlabeled and labeled data in learning a good classifier. The authors show good performance on semi-supervised learning for several text and language-related tasks.

Ando & Zhang's method can be extended to apply to several self-taught learning problems, as long as we can construct a heuristic that can create the auxiliary labeled data. While they suggest such heuristics for language problems, new heuristics need to be picked for new application domains, such as for image or audio inputs.

- **The Universum method**: Among recent methods in the literature, the Universum method (Weston et al., 2006), developed contemporarily to our method, appears to be closest in spirit to our self-taught learning framework. The Universum is a collection of unlabeled examples that specifically *do not* belong to the labeled classes of interest. For example, to learn a classifier to distinguish between images of elephants and rhinos, the unlabeled data must not contain *any* examples of elephants and rhinos. This assumption is different and more restrictive than the assumptions we consider for self-taught learning. One major point of difference is that we expect self-taught learning algorithms to work best in the semi-supervised learning setting (where the unlabeled data is from the same classes as the labeled data, and is thus very "similar"), whereas the definition of the Universum itself excludes the semi-supervised learning setting.

  The specific algorithm presented by Weston et al. (Weston et al., 2006) for learning with the Universum uses a modification of the cluster assumption—instead of encouraging the learnt predictor to pass through low input density regions for the original supervised learning problem, the algorithm encourages the learnt predictor to pass through high input density regions for the Universum. Since the Universum contains examples *only* from other classes, this encourages the predictor to be ambivalent about those other classes. In contrast, the methods we will consider for self-taught learning have a very different flavor. They rely on using unlabeled data to learn good encodings (features) of the input, and to then use these encodings for representing the labeled data. Instead of using

the distribution of the unlabeled inputs, the methods use the encoding of the unlabeled input itself and try to find patterns that recur in many input examples. In any case, it is possible that the algorithm developed for the Universum problem can apply to some self-taught learning problems as well.

How do we use the unlabeled data in self-taught learning? To give a rough idea, it is easiest to return to the discussion on feature-engineering earlier. We discussed earlier that given limited labeled examples (x, y), we can try to carefully design features $\Phi(x)$ that expose only the aspects of the input that are important for predicting the label y. The hope is that the mapping $\Phi(x) \rightarrow y$ is easier to learn than the mapping $x \rightarrow y$. In some cases, we might attempt to reduce the human feature-engineering burden by using an automatic method to suggest good features $\Phi(x)$. We will refer to these methods collectively as *feature construction* methods. Previous feature construction methods are closely related in spirit to our self-taught learning methods, so we give an introduction to some of those previous techniques now.

1.5 Automatic feature construction methods

We first discuss methods that use the labeled data itself (within the supervised learning framework) to construct features.

One of the earliest models that perform feature construction are multilayer neural network models. (Bishop, 1995) A neural network consists of multiple interconnected computing units (or neurons), where each unit receives inputs from other units, and computes an output function of its inputs. In many neural network models, the units are arranged in groups called layers, such that the n-th layer receives inputs from the $(n-1)$-th layer, and feeds its output to the $(n+1)$-th layer. The first layer typically contains the raw input $x \in \mathcal{X}$, and the last layer typically contains the predicted output $y \in \mathcal{Y}$. Thus, a two-layer neural network model would consist of an input layer that receives input x, a middle ("hidden") layer that makes intermediate predictions $f(x)$ using the input x from the previous layer, and an output layer that makes final predictions $h(x) = g(f(x))$ using input from the hidden layer. Given

a supervised learning task with labeled data (x, y), these functions g and h can be automatically learned by minimizing the error between the network's predictions $h(x)$ and the true label y. (Rumelhart et al., 1987) This learning procedure implicitly finds feature functions $f(x)$, and operates on them using another function g to compute the final output; it is thus using labeled data to construct features.

A particular type of neural network, called a convolutional neural network (LeCun & Bengio, 1998), has been applied very successfully to constructing features for image inputs. These networks capture the fact that an image should locally look similar at all locations in an image by sharing parameters at different locations in the image. By reducing the number of parameters, and carefully setting up the network architecture to combine the network units at various locations, convolutional networks often work very well on image classification tasks (Lecun et al., 1998).

There are several other supervised learning methods that can be viewed as feature construction methods. For example, linear discriminant analysis finds a linear combination of input dimensions that best discriminate between different classes in the labeled data (Fisher, 1936). This combination can be viewed as producing features for the supervised learning task. Further, in many machine learning methods such as support vector machines, we do not need to explicitly specify the feature functions $\Phi(x)$; instead, we can equivalently define a "similarity" function, or kernel function (Schölkopf & Smola, 2001), between any two inputs x_1 and x_2, and this implicitly defines the feature function, under some conditions. Methods for learning good kernel functions from labeled data are therefore also feature construction methods. (Lanckriet et al., 2004)

The feature construction methods mentioned thus far do not really solve our problem, though. We are interested in supervised learning with limited amounts of labeled data. If it is difficult to learn a predictor for the mapping $x \rightarrow y$ from the labeled data, it is not clear whether we can also learn a feature function $\Phi(x)$ and a mapping $\Phi(x) \rightarrow y$ only using the labeled data. Ideally, we would like to construct features using other, more readily available sources of data. In this thesis, our algorithms will construct features using unlabeled data, which we call *unsupervised feature construction* in this thesis.

1.6 Unsupervised feature construction methods

We mention at the outset that many semi-supervised learning algorithms, as well as many unsupervised learning algorithms, can be applied or modified to construct features from unlabeled data. We discuss some of these methods in further detail below.

Principal components analysis (PCA) is an example of an algorithm that can be applied to unlabeled data to construct features (Pearson, 1901). Given many unlabeled examples $x_u \in \mathbb{R}^n$, PCA finds a low-dimensional linear subspace that is "closest" to the unlabeled data (in Euclidean distance). The PCA problem has the nice property that it can be solved by solving an eigenvalue (or singular value decomposition) problem, for which very good numerical methods are available. This makes PCA particularly efficient. Once the eigenvalue problem is solved, the result can be represented using a matrix of numbers $P \in \mathbb{R}^{q \times n}$ (where $q \leq n$ is the dimension of the PCA subspace), and features can be computed by applying a simple linear operation: $\Phi(x) = Px$, with $\Phi(x) \in \mathbb{R}^q$. Since $\Phi(x)$ is in a lower-dimension than x itself, PCA is often called a dimensionality-reduction algorithm.

The features constructed by some other algorithms can be written in the canonical form $\Phi(x) = Px$, for a matrix P that is found in different ways by different algorithms. Independent component analysis (ICA) finds the matrix P by optimizing a different objective: making the elements in $\Phi(x) = Px$ as independent of each other as possible.[5]

Since PCA and ICA define a linear mapping from input x to features $\Phi(x)$, PCA and ICA have only limited use as feature-construction algorithms. Some other dimensionality-reduction algorithms embed the data into lower-dimensional manifolds (instead of just a linear lower-dimensional subspace). This includes algorithms such as ISOMAP (Tenenbaum et al., 2000) and locally-linear embedding (Roweis & Saul, 2000). As studied in the literature, these algorithms are focused on finding structure within a given dataset and we are not aware of applications of these methods to self-taught learning problems.

[5]Two random variables X_1 and X_2 are independent when knowing one does not affect the distribution over the other: $P(X_1|X_2) = P(X_1)$.

Mathematically, many algorithms for handling unlabeled data (including PCA and ICA) can be grouped in the general class of *matrix factorization* algorithms. Given a large number of unlabeled inputs $x_u \in \mathbb{R}^n$, each arranged as a separate column in a matrix X, matrix factorization algorithms attempt to find two matrices U and V such that $X \approx UV$, by expressing various preferences over the types of matrices U and V. For example, low-rank matrix factorization constrains the number of columns in U (or the number of rows in V) to be less than the input dimension n. Such a factorization can be viewed as representing each input x_u in a low-dimensional linear subspace, and like PCA, can be computed easily using a singular value decomposition (Horn & Johnson, 1985; Srebro, 2004). A different criterion for picking U and V would be to encourage many of the entries in U and V to be zero (using various problem formulations), so that the matrices U and V are *sparse*; this subclass of methods is often called sparse matrix factorization (Srebro & Jaakkola, 2001; Zou et al., 2004). Another well-known technique constrains the values of U and V to be nonnegative; by constraining the reconstruction $X \approx UV$ to use only additive nonnegative terms, the factorization can find useful substructure for many input domains (Lee & Seung, 1999; Lee & Seung, 1997). We will return to a technical comparison with matrix factorization methods in Section 2.5.

Matrix factorization methods typically represent input examples using many varying factors (e.g., PCA represents input examples using several principal components). Technically, in the factorization $X \approx UV$, a single column of X (corresponding to a single example x_u) is represented approximately as a linear combination of the columns of U, with the weights on those columns denoted by (nonzero) values in V. In the extreme case, each input example can be mapped to exactly one factor, or "codeword." Such methods that learn a set of codewords, and then quantize every input x_u to one codeword, are broadly called *vector quantization* (VQ) methods. These methods are widely used, especially in speech processing and computer vision. The codewords can be learnt on unlabeled data by clustering the unlabeled examples, and then using each cluster centroid as a codeword. Since VQ maps inputs to closely related prototypes, the feature mapping can be highly localized, selective

and nonlinear.[6] However, this also means that VQ may need a very large number of prototypes, especially to sufficiently tile a high-dimensional input space; but with a very large number of centroids, VQ might also lose the ability to generalize across small variations in the inputs. Further, VQ is very dependent on a distance metric that finds the closest codeword to a given input, and a Euclidean distance metric may work poorly for inputs such as image pixels. In our experiments in Section 2.5, we show that the above VQ method does not work well for self-taught learning.

Many neural network models can be used for unsupervised feature construction, often by applying the supervised feature construction techniques to reconstruct the input x itself. For example, an autoencoder is a special neural network model in which the input layer is fed the input x, and we expect the output layer to return an output close to the original input x; the middle hidden layers act as a funnel through which the input x must pass. By forcing the network to condense the information in input x into a possibly low-dimensional hidden layer, in such a way that the input can be recovered at the output layer, the autoencoder often finds hidden layer representations that capture interesting features in the data (Caruana, 1997). However, when the neural network has multiple layers (also called a "deep" network), the error signal propagated from the output layer is weak and ineffective for layers deep inside the network—we usually do not have any information about intermediate representations, and no direct error signal in the hidden layers. It is thus usually hard to learn multiple layers of feature representation using this model.

In recent years, a different neural network model called a deep belief network (Hinton & Salakhutdinov, 2006) has been widely used for unsupervised feature construction. Instead of training all the layers at once, it trains the network one layer at a time, all the while using only unlabeled data. This line of work is very closely related to the central contributions of this thesis, and we return to it in Chapter 5.

Apart from the methods discussed above, there have been several domain-specific

[6]This extreme selectivity of VQ, where each codeword is chosen for all of a set of closely related inputs, but for no other inputs, is reminiscent of the "grandmother cell" neuron hypothesized in the brain. The grandmother cell is a hypothetical highly specific neuron that activates whenever you perceive your grandmother (or more generally, some other specific concept), and thus represents an extremely selective neuron. (Gross, 2002) The existence of grandmother cells is a controversial topic in neuroscience, with partial evidence for such cells in the human brain. (Quiroga et al., 2005)

algorithms and experiments reported in the literature, that use unlabeled data in various ways to construct features for a particular domain (such as images or text documents). In this thesis, we are most interested in methods that can be applied to multiple domains, and methods that are tuned only minimally to each particular domain. For the sake of completeness, we discuss previous domain-specific methods for two application domains, and note that the ideas in some of these methods could be applicable in a more domain-general method for learning from unlabeled data.

1.6.1 Text documents

Supervised learning has been widely applied to text document categorization, for example in spam filtering applications (where the task is to predict whether an email is spam, given the text contained in the email). In these text problems, the input x is typically represented as a bag-of-words vector, which is a n-length vector for a text vocabulary of n words, such that the j-th element of the bag-of-words vector for a document is 1 if the j-th word in the vocabulary occurs in that document, and 0 otherwise. (The case where we maintain word counts, instead of just a binary 0 or 1 value, is similar.) Since a single text document usually contains only a small fraction of all the words in the vocabulary, a small labeled training set can not directly provide information about many of the words in the vocabulary. For example, the training set might associate the words "moon" and "space" with a particular label, but the training documents might never use related words such as "astronaut" or "planet." In this situation, a straightforward supervised learning algorithm without any additional information cannot determine that related words such as "astronaut" or "planet" are also likely to be related to the same label as "moon" or "space." This problem arises very frequently in text applications (Essen & Steinbiss, 1992), but also in other applications with high-dimensional input vectors, and is often called the *data sparsity* problem. Since the problem of data sparsity is particularly pervasive in text applications, many text-specific methods have been developed for dealing with it. Of special interest to us are some methods that use unlabeled data in various ways to help supervised learning.

An influential idea in the field is as follows: we might be able to reduce data sparsity issues if we represent not just the occurence (or not) of a word by keeping a 1 or 0 input element, but also use the *co-occurence* statistics across different words. If the word "moon" occurs in many documents that also contain the word "astronaut," then this might lead us to believe that these words are related, and might occur in documents with the same label. Crucially, such co-occurence statistics can be obtained reliably and easily from purely unlabeled text documents. This idea is formalized in the *distributional similarity* method, in which we represent the semantic "meaning" of a word by using the typical context (surrounding words) for that word in unlabeled text documents (Harris, 1968; Lee, 1999; Lin, 1998). In the simplest version of this method, given a single word w, we compute a bag-of-words vector $v_w \in \mathbb{R}^n$ for that word (not the document) by setting the j-th element of v_w to the fraction of unlabeled documents containing word w that also contain the j-th vocabulary word; the representation x for a given document can then be computed as a sum of the vectors v_w for each of the words w in the document. This can thus be viewed as a way of constructing features on unlabeled data, by estimating the hidden, semantic meaning of each word using the typical context around it.

Distributional similarity has been applied widely in text and natural language processing applications, including for clustering similar words (Lin, 1998), disambiguation problems (Pantel & Lin, 2000), and others. Methods based on distributional similarity appear to be applicable to self-taught learning problems for text, but to the best of our knowledge, there are no generalizations of this method that work on domains such as images or audio as well.

A different text-specific model for constructing features using unlabeled data is based on using the unlabeled data to learn a generative model for text documents, and to then apply this generative model to represent new documents. (Hofmann, 1999; Blei et al., 2002) A specific class of these models, often called "topic models," uses a particular flavor of generative model, in which each word in the document is generated by a two-step process: first, a "topic" (concepts or related groups of words) is picked, and then the individual word is generated from that topic's word distribution. The topics are most often learned on unlabeled data (Blei et al., 2002).

Topic models can be used to map a document into the inferred list of topics that occur in the document, and are among the best-known generative models of text documents. We show in Chapter 4 that one of the best known topic models, latent Dirichlet allocation (Blei et al., 2002), can be applied to self-taught learning problems, but that it does not work as well as the methods we develop in this thesis.

The problem of data sparsity in text problems often arises because we model the various words (or input dimensions) as independent of each other, but in real usage, these words are highly correlated. If the word "moon" occurs in a document, there is a higher chance that the word "space" will also occur, but there might be a somewhat lower chance that completely unrelated words will occur. Distributional similarity can be viewed as capturing such word similarity using co-occurence statistics. Other methods can more directly try to capture specific types of word relations. For example, one can look for patterns such as "w_1 is a type of w_2" in unlabeled text (for some words w_1 and w_2) to find "hypernym" relations[7] similar to those found in linguistic resources such as WordNet (Miller, 1995; Hearst, 1992; Snow et al., 2005). Such methods can be generalized to some other types of word relations, and can be used to better engineer word features.

In mapping a natural language sentence to its semantic meaning, linguists often find it useful to compute intermediate, latent representations, such as part-of-speech tags on words, the semantic sense of ambiguous words, or the parse tree for the whole sentence. Some methods for learning these latent representations use unlabeled data, by assuming models for these latent representations and then using probabilistic techniques (such as the EM algorithm) to iteratively refine these models. To take one example, such a method can be used for automatically learning a context-free grammar for a language, given access to unlabeled sentences. (Manning & Schütze, 1999) While the motivations for some of these unsupervised methods are fairly different from self-taught learning problems, they might be applicable to some self-taught learning problems in the domain of natural language processing.

We also mention the problem of "domain adaptation" where the task is to learn

[7] A word w_1 is said to be a hypernym of word w_2 if w_1 is more generic than w_2. For example, *animal* is a hypernym for *horse*.

on input labeled data, from some input distribution $P_{\text{train}}(x)$, and then testing on another input distribution $P_{\text{test}}(x)$ (III & Marcu, 2006). While this is cosmetically similar to self-taught learning in that we use different sources of data for learning, domain adaptation has a different focus, and typically assumes that the data sources being adapted over are all labeled; in self-taught learning, on the other hand, one of the data sources is unlabeled, in addition to being different from the the labeled data source.

1.6.2 Computer vision

A challenge faced by many computer vision methods is to produce global predictions (e.g., does an input image contain an elephant?) by aggregating local analysis of the pixels (e.g., is there a horizontal edge in the top-left corner of the image?). Many methods for performing local analysis rely on vector quantization style (VQ) methods. In current practice, the following is a standard method for mapping an input image to a set of VQ codewords:

1. Use an *interest-point detector* to find locations in the image where local features should be extracted. These detectors often look for the presence of edges or corners in images.

2. Extract local features at the locations output by the above step. The simplest feature would correspond to extracting the image pixel intensities around each location.

3. Map each local feature to a codeword. This reduces the input-image to a set of codewords, much like a text document consists of a set of words, and is called a bag-of-visual-words representation.

The VQ codewords themselves can be learnt by clustering similarly extracted local features (from labeled or unlabeled data), assigning a unique codeword to each learnt cluster, and computing the codeword for a local feature by finding the closest codeword in Euclidean distance. Given a bag-of-visual-words representation, standard supervised learning classifiers can then be applied.

Unfortunately, as presented above, the method does not work very well on standard computer vision applications (such as image classification), and additional special-purpose techniques are required. By using a classifier specially hand-designed for images (called a pyramid match kernel), and by using special image features such as the SIFT features (Lowe, 1999), variations of this method can produce good performance on image classification tasks. (Grauman & Darrell, 2007) However, to the best of our knowledge, this method has not been successfully applied to use unlabeled data—the codewords are typically learned using the labeled training data itself, and it is not clear whether the mapping of local features to codewords will work when the codewords are extracted from other, unlabeled images.

A different method relies on extracting many small fragments from labeled training images, and using the computed "similarity" with those fragments as a local feature extractor for images. (Vidal-Naquet & Ullman, 2003) Typically, these local feature extractors are combined into a global image-level predictor via a statistical method such as boosting. (Torralba et al., 2007) This method constructs features from data, and often performs reasonably on computer vision tasks, when the fragments are extracted from labeled training data itself. We can envision an application of this method to a self-taught learning problem, by extracting fragments from unlabeled data instead of from labeled data, but this runs the risk of extracting features that are not informative about the classes in the supervised learning problem (because they were extracted from images not in the training data). We are not aware of any such application in the literature.

1.6.3 Discussion

Because self-taught learning places significantly fewer restrictions on the type of unlabeled data, in many practical applications (such as image, audio or text classification) it is much easier to apply than typical semi-supervised learning or transfer learning methods. For example, it is far easier to obtain 100,000 Internet images than to obtain 100,000 images of elephants and rhinos; far easier to obtain 100,000 newswire articles

than 100,000 webpages on pottery and sculpture, and so on. Using our running example of image classification, Figure 1.1 illustrates these crucial distinctions between the self-taught learning problem that we pose, and previous, related formalisms.

We note that even though semi-supervised learning was originally defined with the assumption that the unlabeled and labeled data follow the same class labels (Nigam et al., 2000), it is sometimes conceived as "learning with labeled and unlabeled data." Under this broader definition of semi-supervised learning, self-taught learning would be an instance (a particularly widely applicable one) of it.

Examining the last two decades of progress in machine learning, we believe that the self-taught learning framework introduced here represents the natural extrapolation of a sequence of machine learning problem formalisms posed by various authors—starting from purely supervised learning, through semi-supervised learning and other formalisms using unlabeled data, to transfer learning—where researchers have considered problems making increasingly little use of expensive labeled data, and using less and less related data. In this light, self-taught learning can also be described as "unsupervised transfer" or "transfer learning from unlabeled data."

We pose the self-taught learning problem mainly to formalize a machine learning framework that we think has the potential to make learning significantly easier and cheaper. And while we treat any biological motivation for algorithms with great caution, the self-taught learning problem perhaps also more accurately reflects how humans may learn than previous formalisms, since much of human learning is believed to be from *unlabeled* data. Consider the following informal order-of-magnitude argument.[8] A typical adult human brain has about 10^{14} synapses (connections), and a typical human lives on the order of 10^9 seconds. Thus, even if each synapse is parameterized by just a one bit parameter, a learning algorithm would require about $10^{14}/10^9 = 10^5$ bits of information per second to "learn" all the connections in the brain. It seems extremely unlikely that this many bits of labeled information are available (say, from a human's parents or teachers in his/her youth). While this argument has many (known) flaws and is not to be taken too seriously, it strongly

[8]This argument was first described to us by Geoffrey Hinton (personal communication) but the conclusionappears to reflect a view that is fairly widely held in neuroscience.

suggests that most of human learning is only weakly supervised, requiring primarily unlabeled data without any explicit labels (such as whatever natural images, sounds, etc. one may encounter in one's life).

1.7 Summary of contributions

We believe that the reliance on expensive labeled data and on hand-engineered feature functions for high-performance machine learning severely limits the applicability of machine learning to many new problems. For this reason, the ability to use readily available unlabeled data, and to avoid hand-engineering of feature functions, has the potential to significantly expand the applicability of machine learning methods.

1.7.1 Self-taught learning

This thesis introduces a machine learning framework called "self-taught learning" for using unlabeled data in learning algorithms. This framework requires very few restrictions on the unlabeled data, and is widely applicable.

The issue of what data there is to learn from lies at the heart of all machine learning methods. In supervised learning, even an inferior learning algorithm can often outperform a superior one if it is given more data (Banko & Brill, 2001b; Brants et al., 2007). Self-taught learning uses a type of unlabeled data that is often easily obtained even in massive quantities, and that thus can provide a large number of "bits" of information for algorithms to try to learn from. Thus, we believe that if good self-taught learning algorithms can be developed, they hold the potential to make machine learning significantly more effective for many problems.

1.7.2 Algorithms for self-taught learning

We present an algorithm for self-taught learning that requires almost no hand-engineered features, and that can work well even with very few labeled examples. The algorithm uses the unlabeled examples to discover the "basic elements" present in all inputs, and then uses those basic elements to describe any new examples.

For example, consider the task of image classification. Images are most easily represented as a high-dimensional vector of pixel intensity values—this representation contains a single intensity value per pixel in the image, capturing absolutely no correlations between pixels, and is thus an extremely *low-level* representation. When our self-taught learning algorithm is applied to image inputs, it may discover (through examining the statistics of the unlabeled images) certain strong correlations between neighboring pixels, and therefore learn that most images have many *edges*. Through this, it then learns to represent images in terms of the edges that appear in it, rather than in terms of the raw pixel intensity values. This representation of an image in terms of the edges that appear in it (rather than the raw pixel intensity values) is a *higher-level*, or more abstract, representation of the input. By applying this learned representation to the input examples in a supervised classification task, we can then obtain a higher level representation of those examples also, and consequently obtain a simpler supervised learning task than the one we started with. Indeed, we demonstrate that this self-taught learning algorithm leads to improved performance on problems with image, text and audio inputs.

1.7.3 Self-taught learning for audio classification

We consider specifically the application of self-taught learning to audio classification problems. For audio inputs, the feature-engineering step is usually crucial for application of machine learning, as each input example is naturally represented as a very high-dimensional vector. For example, just 1 second of speech recorded at moderate quality (sampled at 16KHz) would be represented as a 16000-dimensional real-valued vector of intensities. The application of machine learning algorithms to such high-dimensional inputs has to be invariably mediated by carefully hand-designed filters, which compute a summary description of the high-dimensional inputs in terms of only a few feature values. One such summary description is given by the Mel-frequency cepstral coefficient (MFCC) representation, developed in the 1970s and derived by applying a sequence of filters to the frequency-domain representation (spectrogram) of the audio input. This hand-designed MFCC representation is used ubiquitously in

audio applications—even to this day, machine learning applications to audio (speech or music) problems invariably use the MFCC (or similar) representation to represent the inputs.

We consider an application of self-taught learning to audio classification, where we use a sparse coding model to automatically learn a succinct description of the high-dimensional audio input. This description is learnt with almost no feature engineering, using only access to a large collection of unlabeled audio samples. Further, we show that our automatically learned features often outperform the hand-crafted MFCC features, especially when the audio signal is corrupted with noise.

For audio inputs, it is highly desirable to have a representation that is invariant to temporal shifts of the input. The earlier sparse coding models can be modified to capture such invariance; unfortunately, learning and inference in this specific model is extremely slow with our earlier sparse coding algorithms. We develop new algorithms for this model, which allow us to tractably apply the model to speech and music classification tasks.

1.7.4 Self-taught learning for discrete inputs

Our self-taught learning algorithms for image and audio classification use the sparse coding model to learn a succinct, higher-level representation of the inputs. Sparse coding uses a Gaussian noise assumption and a quadratic loss function, which are both well-suited to continuous valued inputs (such as image and audio). However, these assumptions do not hold for binary-valued, integer-valued, non-Gaussian or discrete input types, such as text documents. The sparse coding models thus perform poorly if applied to such data types, as in text classification problems.

Drawing on ideas from generalized linear models (GLMs), we present a generalization of sparse coding to learning with data drawn from any exponential family distribution (such as Bernoulli, Poisson, etc). This gives a method that we argue is much better suited to model other data types than Gaussian. In our view, the ability to handle such data types is essential in a general self-taught learning algorithm.

The corresponding optimization problems are significantly harder than the problems encountered for (Gaussian) sparse coding. We present an algorithm for solving the optimization problem defined by this model; this algorithm is especially efficient for our sparse coding model. We also show that the new model results in significantly improved self-taught learning performance when applied to text classification and to 3D point-cloud classification (for a robotic perception task).

1.7.5 Large-scale deep unsupervised learning

The promise of self-taught learning methods (and unsupervised learning methods in general) lies in their potential to use vast amounts of unlabeled data to learn complex, highly nonlinear models with millions of free parameters. This is especially true when we are interested in unsupervised learning of "deep" models with multiple levels (or layers) of processing, in which the output of one layer is fed as input to the next layer. We consider the sparse coding model we developed for self-taught learning, as well as a well-known unsupervised learning model, deep belief networks (DBNs); both of these models have recently been applied to a flurry of machine learning applications (Hinton & Salakhutdinov, 2006; Raina et al., 2007). Unfortunately, current learning algorithms for both models are too slow for large-scale applications, forcing researchers to focus on smaller-scale models, or to use fewer training examples.

We suggest massively parallel methods to help resolve these problems. We argue that modern graphics processors far surpass the computational capabilities of multicore CPUs, and have the potential to revolutionize the applicability of deep unsupervised learning methods. We develop general principles for massively parallelizing unsupervised learning tasks using graphics processors. We show that these principles can be applied to successfully scaling up learning algorithms for both DBNs and sparse coding. Our implementation of DBN learning is up to 70 times faster than a dual-core CPU implementation for large models. For example, we are able to reduce the time required to learn a four-layer DBN with 100 million free parameters from several weeks to around a single day. For sparse coding, we develop a simple, inherently parallel algorithm, that leads to a 5 to 15-fold speedup over previous methods.

1.8 First published appearances of the described work

Most of the research described in this this thesis appeared first in various publications. The following is a list of references to papers that are relevant to each of the chapters, with papers listed roughly in decreasing order of importance for the contents of the chapter:

- Chapter 2:
  - Self-taught learning: Transfer learning from unlabeled data. Rajat Raina, Alexis Battle, Honglak Lee, Benjamin Packer and Andrew Y. Ng. *ICML 2007.* (Raina et al., 2007)
  - Self-taught learning: Transfer learning from unlabeled data. Rajat Raina, Alexis Battle, Honglak Lee, Benjamin Packer and Andrew Y. Ng. *NIPS 2006 Workshop on Learning when Test and Training Inputs Have Different Distributions.* (Raina et al., 2006)
  - Efficient sparse coding algorithms. Honglak Lee, Alexis Battle, Rajat Raina, and Andrew Y. Ng. *NIPS 2006.* (Lee et al., 2007a)
- Chapter 3:
  - Shift-invariant sparse coding for audio classification. Roger Grosse, Rajat Raina, Helen Kwong, and Andrew Y. Ng. *UAI 2007.* (Grosse et al., 2007)
- Chapter 4:
  - Exponential Family Sparse Coding with Application to Self-taught Learning for Text Documents. Honglak Lee, Rajat Raina, Alex Teichman, and Andrew Y. Ng. *ICML 2008 Workshop on Prior Knowledge for Text and Language Processing.* (Lee et al., 2008)
  - Exponential Family Sparse Coding with Application to Self-taught Learning. Honglak Lee, Rajat Raina, Alex Teichman, and Andrew Y. Ng. *IJCAI 2009.* (Lee et al., 2009b)

- Chapter 5:
  - Learning Large Deep Belief Networks using Graphics Processors. Rajat Raina, Andrew Y. Ng. *NIPS 2008 Workshop on Parallel Implementations of Learning Algorithms.* (Raina & Ng, 2008)
  - Large-scale Deep Unsupervised Learning using Graphics Processors. Rajat Raina, Anand Madhavan, Andrew Y. Ng. *ICML 2009.* (Raina et al., 2009)

Chapter 2

Self-taught Learning

2.1 Problem Formalism

A self-taught learning problem consists of a supervised learning problem, with some labeled data, and a much larger set of unlabeled examples. We assume we are given a labeled training set of m examples $\{(x_l^{(1)}, y^{(1)}), (x_l^{(2)}, y^{(2)}), \ldots, (x_l^{(m)}, y^{(m)})\}$ drawn i.i.d. from some distribution $\mathcal{D}$, as in a typical supervised learning problem. Here, each $x_l^{(i)} \in \mathbb{R}^n$ is an input feature vector (the "l" subscript indicates that it is a labeled example), and $y^{(i)} \in \{1, \ldots, C\}$ is the corresponding class label.

In addition, we are given a set of k unlabeled examples $x_u^{(1)}, x_u^{(2)}, \ldots, x_u^{(k)} \in \mathbb{R}^n$. Crucially, we do not assume that the unlabeled data $x_u^{(i)}$ was drawn from the same distribution as, nor that it can be associated with the same class labels as, the labeled data. Clearly, as in transfer learning (Thrun, 1996; Caruana, 1997), the labeled and unlabeled data should not be completely irrelevant to each other if unlabeled data is to help the classification task. For example, we would typically expect that $x_l^{(\cdot)}$ and $x_u^{(\cdot)}$ come from the same input "type" or "modality," such as images, audio, text, etc.

Given the labeled and unlabeled training set, a self-taught learning algorithm outputs a hypothesis $h : \mathbb{R}^n \to \{1, \ldots, C\}$ that tries to mimic the input-label relationship represented by the labeled training data. This hypothesis h is then tested under the same distribution $\mathcal{D}$ from which the labeled data was drawn. In situations where the labeled training data is limited (m is small), a self-taught learning algorithm attempts

to use information from the weakly related unlabeled data to better select the output hypothesis h.

2.2 A Self-taught Learning Algorithm

In this chapter, we introduce the approach that we use to develop self-taught learning algorithms. While the approach is general and can be applied to any self-taught learning problem, we first illustrate the method using our earlier image classification example — we would like to classify images of elephants vs. rhinos, and have access to a few labeled examples of each, as well as to a large number of unlabeled images randomly downloaded from the Internet.

Our approach is motivated by the observation that even many randomly downloaded images will contain basic visual patterns (such as edges) that are similar to those in images of elephants and rhinos. We would expect this to be true even though the unlabeled data may or may not contain any images containing elephants or rhinos themselves. If, therefore, we can learn to recognize such patterns from the unlabeled data, these patterns can be used for the supervised learning task of interest, such as recognizing elephants and rhinos.

Our algorithm uses the unlabeled data $x_u^{(i)}$ to learn a slightly higher-level, more succinct, representation of the inputs. For example, if the inputs $x_u^{(i)}$ (and $x_l^{(i)}$) are vectors of pixel intensity values that represent images, our algorithm will use $x_u^{(i)}$ to learn the "basic elements" that comprise an image. It may discover (through examining the statistics of the unlabeled images) certain strong correlations between rows of pixels, and therefore learn that most images have many *edges*. Through this, it then learns to represent images in terms of the edges that appear in it, rather than in terms of the raw pixel intensity values. This representation of an image in terms of the edges that appear in it—rather than the raw pixel intensity values—is a *higher level,* or more *abstract,* representation of the input. By applying this learned representation to the labeled data $x_l^{(i)}$, we obtain a higher level representation of the labeled data also, and thus an easier supervised learning task.

To put things in perspective, our algorithms here learn to represent images using

edges instead of individual pixels, but we view this line of work more generally as constructing even higher-level representations of inputs. Instead of hand-engineered representations, we use an automatic recipe for building these representations, given access to a large dataset of unlabeled examples. Thus, while our algorithms learn to represent images using edges instead of individual pixels, in the longer term, we strive to obtain even higher-level representations of the input. In the limit, we could imagine a representation based on presence or absence of objects—for example, if we are able to learn a representation in which an image feature has the value 1 if an elephant occurs in the image, and 0 otherwise, then our image classification task would be trivially easy. The challenge, of course, is learning a suitably high-level representation. We view our algorithms for learning higher-level representations as steps in this direction.

2.3 Learning higher-level representations

We first explain our algorithm for learning a higher-level representation using a simple example. Given an input image, such as the one on the left in Figure 2.3, our algorithm will find a large number of patterns or "basis vectors," such as the images on the right, such that the image can be represented using *only a few* basis vectors. In the example, the input image contains a complex combination of pixel intensities; our algorithm instead represents the input image using a combination of just 3 basis vectors, thus providing a simple, succinct representation of the input. If each image contains 30×30 pixels, then the input image is represented using the pixel intensities as a 900-dimensional vector. By capturing the 3 patterns that occur in the image, rather than the 900 individual pixels, our representation is a *higher-level* representation of the input in terms of patterns (edges) rather than input dimensions (pixels). We would thus expect that it might be easier to learn a classifier over such a higher-level representation, than over the pixel-based input itself. Our algorithm will thus use unlabeled data to find a large number of basis vectors, and then use those basis vectors to construct a representation for the labeled data.

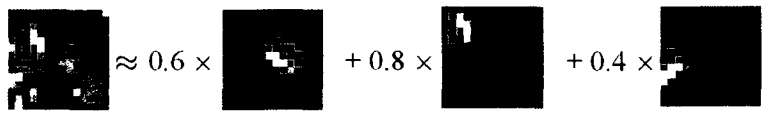

Figure 2.1: An illustration of the idea behind our algorithm for learning higher-level representations. The input image (left) is represented as a linear combination of basis vectors (right).

Concretely, our algorithm for learning a higher-level representation works as follows: given inputs $x \in \mathbb{R}^n$, the algorithm attempts to find patterns or *basis vectors* $b = \{b_1, b_2, \ldots, b_s\}$, $b_j \in \mathbb{R}^n$ such that any individual input x can be represented using only a few basis vectors. The total number of basis vectors k can be very large—in particular, the number of basis vectors k might be larger than the input dimension n. Specifically, the algorithm attempts to represent each input x as a linear combination of a few basis vectors: $x \approx \sum_j a_j b_j$, where the weights on the basis vectors $a = (a_1, a_2, \ldots, a_s)$ will be called the *activations*. To enforce the constraint that only a few basis vectors are used for a given input x, only a few activations values a_j can be nonzero. In other words, most of the activation values a_j must be *exactly* zero, i.e., the vector of activations $a \in \mathbb{R}^s$ must be "sparse."

To learn such a representation, we first need to learn the basis vectors b. Since each basis vector $b_j \in \mathbb{R}^n$ contains $O(n)$ free parameters, to learn s different basis vectors, we need to learn a total of $O(ns)$ free parameters. For example, if the input is 1000-dimensional ($n = 1000$), and we want to learn 1000 basis vectors ($s = 1000$), the basis vectors contain about a million free parameters. In many practical supervised learning tasks where only a few labeled training examples are available, it would be difficult to reliably pick good values for each of these million free parameters using only the labeled data. This suggests that other sources must be used in learning the basis vectors. Our algorithm will thus learn the basis vectors b using unlabeled examples $\{x_u^{(i)}\}$, which are typically easy to obtain in large quantities—it is relatively easy to obtain millions of unlabeled images (or text documents, or audio examples, etc.) from the Internet.

2.3.1 Sparse Coding

Our algorithm for learning basis vectors is based on the "sparse coding" optimization problem posed by Olshausen & Field (1996) as an unsupervised computational model of low-level sensory processing in humans. Given unlabeled data $\{x_u^{(1)}, ..., x_u^{(k)}\}$, sparse coding is posed as the problem of minimizing a cost function E over the basis vectors b and the corresponding activations $\{a^{(1)}, ..., a^{(k)}\}$:

$$E(b, a) = \sum_i \|x_u^{(i)} - \sum_j a_j^{(i)} b_j\|^2 + \beta \sum_{i,j} \Psi(a_j^{(i)}) \tag{2.1}$$

where the sparsity penalty function $\Psi(t)$ is chosen to be some function that is minimized at $t = 0$, and increases for larger values of t. Olshausen & Field suggest several sparsity functions such as $-e^{-t^2}$, $\log(1 + t^2)$ and $|t|$ that all share these properties. The first term in the cost function E encourages each input $x_u^{(i)}$ to be represented accurately using the linear combination $\sum_j a_j^{(i)} b_j$, and the second term encourages only a few activations to have large nonzero values. The nonnegative value $\beta \in \mathbb{R}$ controls the relative importance assigned to each of these terms—the value $\beta = 0$ corresponds to not enforcing sparsity at all, and solutions are sparser for higher values of β, till all the activations are zero as $\beta \to \infty$.

The cost function E can be optimized by starting at randomly picked values for b and a, and then alternating between two steps:

1. Change a by gradient descent on the cost function E, while keeping b fixed.

$$a \longleftarrow a - \eta \frac{\partial E}{\partial a}$$

2. Change b by gradient descent on the cost function E, while keeping a fixed.

$$b \longleftarrow b - \eta \frac{\partial E}{\partial b}$$

where η is the learning rate. An additional normalization condition bounding the norm of each basis vector $\|b_j\|$ is needed, to avoid the trivial solution where the

basis vectors have very large elements and the corresponding activations can have infinitesimally small elements, all while keeping the first term in the cost function fixed, and setting the second term infinitesimally close to zero. Olshausen & Field suggest adapting the norm of each basis vector b_j separately so that the variance of the corresponding activations a_j is held at a fixed level (Olshausen & Field, 1997).

The basis vectors learned by applying this procedure to unlabeled data capture interesting patterns. For example, when trained on small 8×8 pixel patches extracted from images of outdoor scenes, the basis vectors represent edge-like patterns ("Gabor filters") that are very similar to those observed in low-level vision in the mammalian cortex. However, this optimization procedure requires a large number of small gradient descent steps, and is extremely slow in practice, rendering it practically unusable for self-taught learning applications.

2.3.2 A different sparse coding formulation

We consider a modification of Olshausen & Field's original sparse coding formulation, and henceforth refer to this formulation whenever we refer to "sparse coding." We solve the following optimization problem for learning higher-level representations (Lee et al., 2007a):

$$\text{minimize}_{b,a} \quad \sum_i \|x_u^{(i)} - \sum_j a_j^{(i)} b_j\|^2 + \beta \sum_i \|a^{(i)}\|_1 \tag{2.2}$$

$$\text{s.t.} \qquad \|b_j\| \leq 1, \quad \forall j \in 1, ..., s \tag{2.3}$$

We capture the basis normalization requirement explicitly by posing a constraint on the norm $\|b_j\|$; this will also help us devise efficient convex optimization techniques for solving the optimization problem. We have also focused on one particular sparsity penalty function, the L_1-norm penalty function $\Psi(t) = |t|$, because we found in our experiments that this form of the penalty function performed well on self-taught learning problems. The derivative of this penalty function $\Psi(\cdot)$ remains constant even when an activation is close to zero (unlike say $\Psi(t) = \|t\|^2$ for which the derivative is close to zero when the activation is close to zero), and this forces many of the activations to be exactly zero at the optimum (Tibshirani, 1996a), as desired in our

sparse coding formulation. Further, in other machine learning contexts, L_1-norm regularization in parameter estimation has been shown to have attractive feature selection properties, and to lead to strong learning guarantees for high-dimensional problems (Tibshirani, 1996a; Ng, 2004).

The optimization variables in this problem are the basis vectors $b = \{b_1, b_2, \ldots, b_s\}$ with each $b_j \in \mathbb{R}^n$, and the activations $a = \{a^{(1)}, \ldots, a^{(k)}\}$ with each $a^{(i)} \in \mathbb{R}^s$; here, $a_j^{(i)}$ is the activation of basis b_j for input $x_u^{(i)}$. The number of bases s can be much larger than the input dimension n. The optimization objective (2.2) balances two terms: (i) The first quadratic term encourages each input $x_u^{(i)}$ to be reconstructed well as a weighted linear combination of the bases b_j (with corresponding weights given by the activations $a_j^{(i)}$); and (ii) it encourages the activations to have low L_1 norm. The latter term encourages the activations a to be *sparse*—in other words, for most of its elements to be zero. (Tibshirani, 1996a; Ng, 2004)

Our formulation in Equation (2.2) can be solved significantly more efficiently than Olshausen & Field's formulation. Specifically, the problem (2.2) is convex separately in the a and b variables (though not jointly convex in a and b). Instead of a procedure involving alternating gradient descent steps, we can now efficiently perform alternating *minimization* steps. In other words, starting at randomly initialized values of a and b, we can now repeat the following steps:

1. Minimize the objective function over the activations a, while keeping the basis vectors b fixed. In this case, the optimal activation $a^{(i)}$ for an example $x^{(i)}$ is independent of the activations for the other input examples, and it suffices to solve the following optimization problem separately over each activation vector $a^{(i)}$:

$$\text{minimize}_{a^{(i)}} \quad \|x_u^{(i)} - \textstyle\sum_j a_j^{(i)} b_j\|^2 + \beta \, \|a^{(i)}\|_1 \tag{2.4}$$

   This is an unconstrained convex optimization problem, and thus has a global minimum. The problem is also related to the "Lasso" problem in statistics, and has been widely studied; several custom algorithms have been designed to use the special structure of the problem (Tibshirani, 1996a; Roth, 2004; Osborne

et al., 2000b; Osborne et al., 2000a; Perkins et al., 2003; Goodman, 2004; Andrew & Gao, 2007; Koh et al., 2007). However, for moderate-sized sparse coding problems, these algorithms still take a few seconds *per unlabeled example.* Since we would usually want to use a large number of unlabeled examples for self-taught learning, sparse coding with those algorithms can take days or weeks to converge.

We use a new method based on the following observation: If we were to know the sign $\theta_j^{(i)}$ of each of the activations $a_j^{(i)}$ ($\theta_j^{(i)} \in \{-1, 0, +1\}$), then problem (2.4) reduces to an unconstrained optimization problem with a differentiable objective function:

$$\text{minimize}_{a^{(i)}} \quad \|x_u^{(i)} - \textstyle\sum_j a_j^{(i)} b_j\|^2 + \beta \textstyle\sum_j \theta_j^{(i)} a^{(i)}\|_1 \tag{2.5}$$

In fact, this problem has a closed form solution. Using this observation, problem (2.4) can be solved efficiently by performing a greedy search over the signs, in such a way that we also guarantee convergence to the optimal activations. We call this algorithm the *feature-sign search* algorithm (Lee et al., 2007a).

2. Minimize the objective function over the basis vectors b, while keeping the activations a fixed. This leads to the following problem:

$$\begin{aligned} \text{minimize}_b \quad & \textstyle\sum_i \|x_u^{(i)} - \sum_j a_j^{(i)} b_j\|_2^2 \\ \text{s.t.} \quad & \|b_j\| \leq 1, \quad \forall j \in 1, ..., s \end{aligned} \tag{2.6}$$

This optimization problem is convex, as both the objective and feasible set are convex; as such, it can be solved using off-the-shelf convex optimization solvers. The problem is that there are a very large number of optimization variables—for example, with 1000-dimensional inputs and 1000 basis vectors, the basis vectors b have about a million free parameters. Even with efficient solvers, a direct solution to the above problem with a million optimization variables is too slow.

Instead of solving the above problem directly, we can use the simple form of the

constraints to analytically compute the dual optimization problem. This dual problem involves just one dual variable per constraint—or one dual variable per basis vector—and thus involves much fewer optimization variables. In our earlier example, the dual problem has only 1000 optimization variables (instead of a million). Once we solve the dual problem, we can then reconstruct the optimal basis vectors from the optimal dual solution. (See Lee et al., 2006 (Lee et al., 2007a) for details.)

Using these efficient algorithms for the two convex subproblems—one optimizing over activations a, and the other optimizing over basis vectors b—we can find good basis vectors in an order of magnitude less time than using off-the-shelf solvers. As an example, when this algorithm is applied to learning basis vectors from unlabeled 14x14 pixel images (i.e., $x^{(i)} \in \mathbb{R}^{196}$), it learns to detect different edges in the image, as shown in Figure 2.2 (left). We have used images as our running example, but exactly the same algorithm can also be applied to other input types. To take a different example, we can learn a representation for speech audio, where each input example corresponds to a 25ms segment of speech, and is represented as a vector of amplitudes (e.g., for speech at 16KHz, each 25ms segment contains .025×16000=400 amplitude samples, and thus each input $x^{(i)} \in \mathbb{R}^{400}$). When applied to such speech sequences, sparse coding learns to detect different patterns of frequencies, as shown in Figure 2.2 (right).

Importantly, by using an L_1 regularization term, we obtain extremely sparse activations—only a few bases are used to reconstruct any input $x_u^{(i)}$; this gives us a succinct representation for $x_u^{(i)}$. We note that some other regularization terms, such as the ones considered by Olshausen & Field, result in most of the $a_j^{(i)}$ being non-zero, and do not lead to good self-taught learning performance; this is described in more detail in Section 2.6.

2.4 Unsupervised Feature Construction

A fundamental problem in supervised learning is the following: given a supervised learning problem with inputs x, we would like to compute a feature function (or

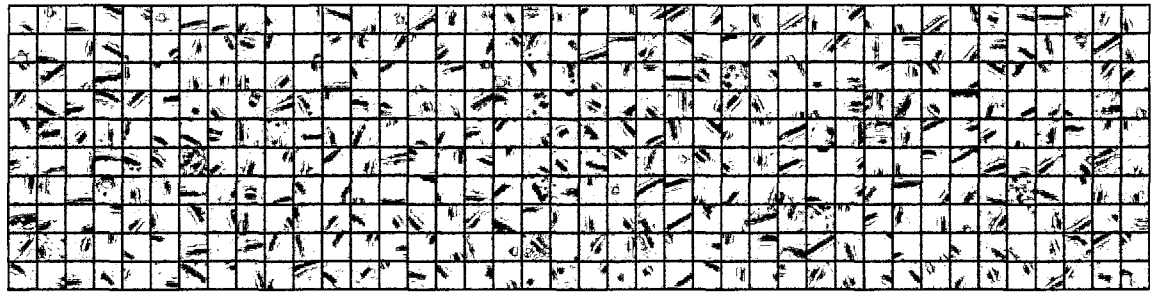

(a) Sparse coding on image inputs.

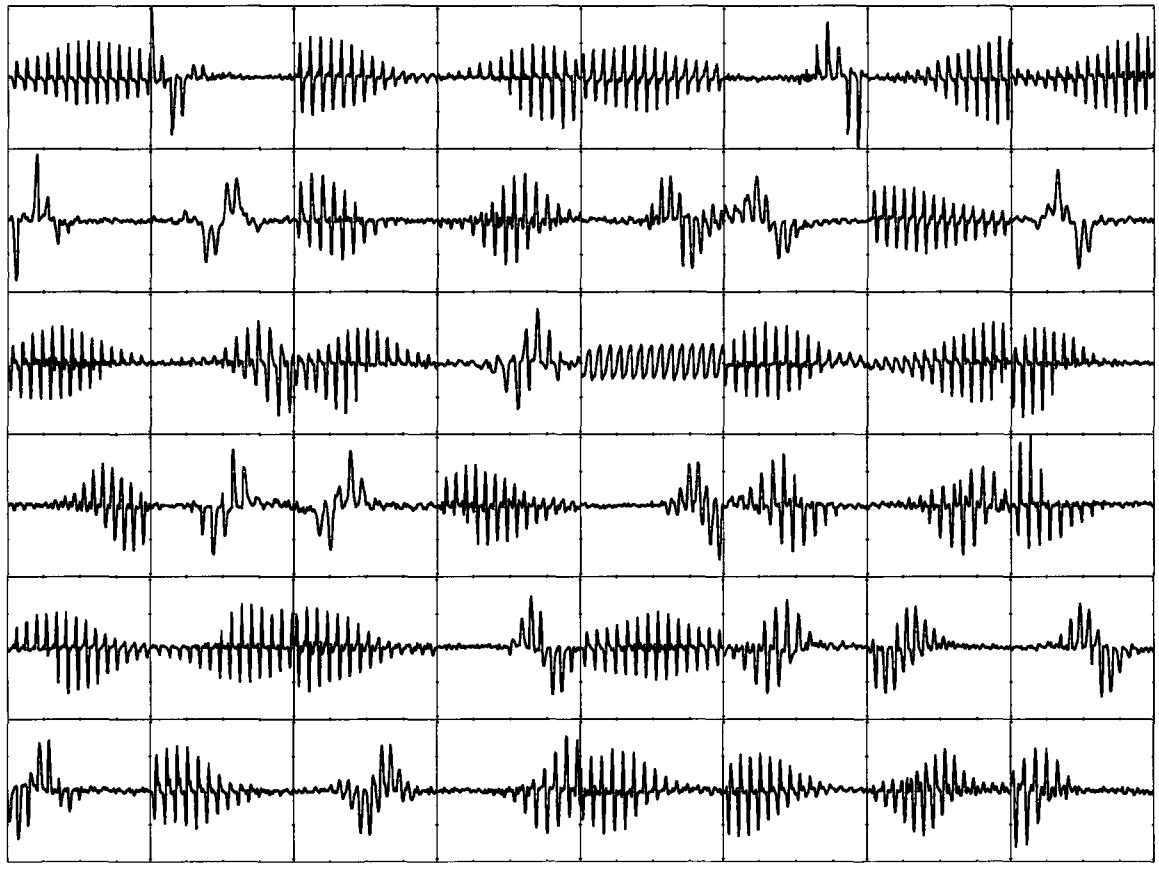

(b) Sparse coding on speech audio inputs.

Figure 2.2: (a) Example sparse coding basis vectors learned from image patches (14x14 pixels) extracted at random from grayscale images of natural scenery. Each square in the grid represents one basis vector. (b) Example basis vectors learned by the *same algorithm*, using 25ms sound samples from speech data. Each of the 48 rectangles in the grid shows the 25ms long acoustic signal represented by a basis vector.

"features") of those inputs $f(x)$, such that the feature representation $f(x)$ is easier to reason with. For example, given an image x represented as a vector of pixel intensities, we might want features that detect various kinds of patterns (such as edges) in the image. In typical applications of machine learning, including in computer vision, audio processing, and text processing, significant amount of time is needed carefully finding good features, even before any machine learning algorithm can be applied. We refer to this (usually laborious) task of finding good feature functions $f(x)$ as "feature construction."

Instead of hand-designing feature functions, we are interested in automatic methods for constructing these feature functions. In cases where large amounts of labeled data is available, it can be feasible to use the labeled data to suggest good feature functions. For example, neural network models with one hidden layer (trained by backpropagation on the labeled data) are essentially learning an intermediate feature function in the hidden layer, that is then used for classification (Rumelhart et al., 1987; Caruana, 1997). However, these methods for *supervised* feature construction are not feasible for problems where only limited amounts of labeled data is available. In particular, we will now develop an *unsupervised* method to automatically construct good features.

Our method relies on the following observation: It is often easy to obtain large amounts of unlabeled data that shares several salient patterns with the labeled data from the classification task of interest. In image classification, most images contain many edges and other visual structures; in optical character recognition, characters from different scripts mostly comprise different pen "strokes"; and for speaker identification, speech even in different languages can often be broken down into common sounds (such as phones). If the unlabeled data shares these salient patterns (edges, pen strokes, sounds, etc.) with the labeled data, then we could try to learn those patterns from large amounts of unlabeled data, and then simply apply the patterns on labeled data to get good features.

Building on this observation, we propose the following approach to self-taught learning: We first apply sparse coding to the unlabeled data $x_u^{(i)} \in \mathbb{R}^n$ to learn a set of bases b, as described in Section 2.3. Then, for each training input $x_l^{(i)} \in \mathbb{R}^n$ from

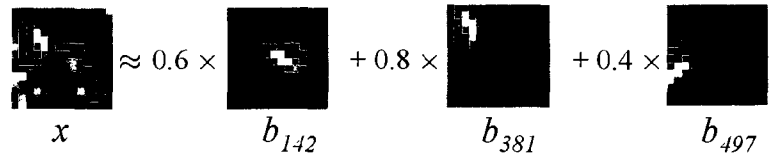

Figure 2.3: An illustration of the idea behind our algorithm for unsupervised feature construction. The input image (left) is represented using just 3 numbers.

the classification task, we compute features $\hat{a}(x_l^{(i)}) \in \mathbb{R}^s$ by solving the sparse coding optimization problem, but with the basis vectors held fixed at the previously learned values:

$$\hat{a}(x_l^{(i)}) = \arg\min_{a^{(i)}} \|x_l^{(i)} - \sum_j a_j^{(i)} b_j\|_2^2 + \beta \|a^{(i)}\|_1 \tag{2.7}$$

By solving this problem, we approximately express the input $x_l^{(i)}$ as a sparse linear combination of the bases b_j. This is a convex optimization problem, and is an L_1-regularized least squares problem similar to the one solved during basis learning. We can use the same methods to solve this problem efficiently (Efron et al., 2004; Lee et al., 2007a). As before, the optimal activations $\hat{a}(x_l^{(i)})$ will be mostly zero, and the activation vector will be sparse. Since the basis vectors capture higher-level patterns, the activations for an input example encode the patterns that occur in that example. Thus, we would expect the sparse vector $\hat{a}(x_l^{(i)})$ to be a higher-level representation for $x_l^{(i)}$, and also that the activation values would provide good features for a supervised learning algorithm.

Using a set of 512 learned image bases over 14x14 pixel image inputs (as in Figure 2.2), Figure 2.3 illustrates a solution to this optimization problem, where the input image x is approximately expressed as a combination of three basis vectors $b_{142}, b_{381}, b_{497}$. The image x can now be represented via the vector $\hat{a} \in \mathbb{R}^{512}$ with $\hat{a}_{142} = 0.6$, $\hat{a}_{381} = 0.8$, $\hat{a}_{497} = 0.4$, and all other $\hat{a}$ coordinates set to zero.

In many applications to images, the input can be very high-dimensional (e.g., a 500×500 pixel image has 250,000 pixels in total). In these cases, a direct application of the above method would force the algorithm to find patterns or basis vectors that

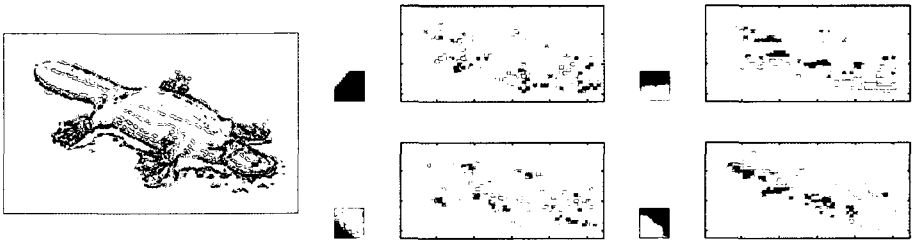

Figure 2.4: Left: An example image taken from the Caltech 101 image dataset from the *platypus* class. Right: Features computed for the platypus image using four sample image patch bases (trained on color images, and shown in the small colored squares) by computing features at different locations in the image. In the large figures on the right, white pixels represents highly positive feature values for the corresponding basis, and black pixels represents highly negative feature values. These activations capture higher-level structure of the input image. (Bases have been magnified for clarity; best viewed in color.)

are the same size as the input images; with such full-image basis vectors, we might need a very large number of basis vectors, to encode all the various types of patterns redundantly at all locations in the image. Instead, we can set up the algorithm to learn local patterns (over small image patches), and to then find occurences of those same patterns at various locations in the image. For example, given a 500×500 pixel image, we could still learn basis vectors over 14×14 pixel image patches, and then compute activations (features) for the 500×500 pixel image by taking 14×14 pixel patches at various offsets and solving problem (2.7). This gives an activation vector *for each offset* in the image, and these can be used as features for learning (as described in Section 2.6).

Figure 2.4 shows such features $\hat{a}$ computed for a large image. The sparse coding algorithm was applied to learn basis vectors over 14×14 pixel color image patches (represented as 196×3-dimensional RGB vector), and then used to compute activations at various offsets in a large platypus image. The figure shows the activations computed for the platypus image using four sample image patch bases (shown in the small colored squares) by computing features at different locations in the image. In the large figures on the right, white pixels represent highly positive activation values

for the corresponding basis vector, and black pixels represents highly negative activation values. These activations capture various types of higher-level structure of the input image, and as we show in Section 2.6, allow us to learn a good classifier for image categories.

These observations are not limited to images. The same method applies equally well to other input types; the features computed on audio samples or text documents similarly detect useful higher-level patterns in the inputs, and can be used to learn good classifiers for audio or text categories respectively.

On all applications, we use these features as input to standard supervised classification algorithms (such as SVMs). Using labeled training data, the supervised classification algorithm learns a classifier over our activation features. To classify a test example, we solve (2.7) to obtain feature vector $\hat{a}$ for the example, and use that as input to the trained classifier. Algorithm 1 summarizes our algorithm for self-taught learning.

2.5 Comparison with Related Methods

It seems that any algorithm for the self-taught learning problem must, at some abstract level, detect structure using the unlabeled data. Many unsupervised learning algorithms have been devised to model different aspects of "higher-level" structure, for example by constructing features automatically using unlabeled data (as discussed in Chapter 1). However, their application to self-taught learning is more challenging than might be apparent at first blush.

Principal component analysis (PCA) is among the most commonly used unsupervised learning algorithms. It identifies a low-dimensional subspace of maximal variation within unlabeled data. Interestingly, the top $T \leq n$ principal components $b_1, b_2, \ldots, b_T$ are a solution to an optimization problem that is cosmetically similar to our formulation in (2.2):

$$\begin{aligned} \text{minimize}_{b,a} \quad & \textstyle\sum_i \|x_u^{(i)} - \sum_j a_j^{(i)} b_j\|_2^2 \\ \text{s.t.} \quad & b_1, b_2, \ldots, b_T \text{ are orthogonal} \end{aligned} \tag{2.8}$$

Algorithm 1 Self-taught Learning via Sparse Coding

input Labeled training set for a classification task:

$$T = \{(x_l^{(1)}, y^{(1)}), (x_l^{(2)}, y^{(2)}), \ldots, (x_l^{(m)}, y^{(m)})\}.$$

Unlabeled data $\{x_u^{(1)}, x_u^{(2)}, \ldots, x_u^{(k)}\}$

Test example x.

output Predicted label for test example x.

algorithm

Initialize basis vectors b randomly, s.t. $\|b_j\| \leq 1 \ \forall j$.
while convergence criterion is not satisfied **do**
  Compute activations $a_j^{(i)}$ by solving problem (2.4):
    $\min_{a^{(i)}} \ \|x_u^{(i)} - \sum_j a_j^{(i)} b_j\|^2 + \beta \ \|a^{(i)}\|_1$
  Compute basis vectors b by solving problem (2.6):
    $\min_b \ \sum_i \|x_u^{(i)} - \sum_j a_j^{(i)} b_j\|_2^2$ s.t. $\|b_j\| \leq 1, \ \forall j$
end while
Fix the basis vectors b at the learned values.

} Basis learning

For each labeled example $x_l^{(i)}$, compute features $\hat{a}(x_l^{(i)})$:
  $\hat{a}(x_l^{(i)}) = \arg\min_{a^{(i)}} \|x_l^{(i)} - \sum_j a_j^{(i)} b_j\|^2 + \beta \ \|a^{(i)}\|_1$.
Construct the new labeled training set:
  $\hat{T} = \{(\hat{a}(x_l^{(1)}), y^{(1)}), (\hat{a}(x_l^{(2)}), y^{(2)}), \ldots, (\hat{a}(x_l^{(m)}), y^{(m)})\}$
Learn a classifier C by applying a supervised learning algorithm (e.g., SVM) to the labeled training set $\hat{T}$.

} Construct features

Compute features $\hat{a}(x)$ for test input x:
  $\hat{a}(x) = \arg\min_a \|x - \sum_j a_j b_j\|^2 + \beta \ \|a\|_1$.
return prediction of the classifier C on the features $\hat{a}(x)$.

} Prediction

The basis vectors are constrained to be orthogonal to each other—the resulting formulation has the useful properties that the subspace spanned by the basis vectors $b_1, b_2, \ldots, b_T$ is optimal among all T-dimensional subspaces (in terms of Euclidean distance of the points from the subspace), and that there is no redundancy in the activations as they capture orthogonal basis vector directions (technically, the activations corresponding to any two basis vectors, a_{j_1} and a_{j_2}, are uncorrelated with each other in the training data $\{x_u^{(i)}\}$). When formulated in this way, PCA differs from our sparse coding formulation in two ways: PCA does not enforce sparsity of the activations, and PCA constrains basis vectors to be orthogonal (or orthonormal if the basis vectors are also normalized to have unit norm).

PCA is convenient because the above optimization problem can be solved efficiently using standard numerical software; the absence of an L_1-sparsity penalty term leads to a solution that can be computed simply via an eigenvector decomposition, without the need for an iterative alternating minimization procedure. Further, given basis vector b_j, the corresponding features $a_j^{(i)}$ can be computed easily because of the orthogonality constraint, and are simply $a_j^{(i)} = b_j^T x_u^{(i)}$ (independent of the basis vectors other than b_j).

When compared with sparse coding as a method for constructing self-taught learning features, PCA has two limitations. First, PCA results in *linear* feature extraction, in that the features $a_j^{(i)}$ are simply a linear function $a_j^{(i)} = b_j^T x_u^{(i)}$ of the input $x_u^{(i)}$. This appears to be a severe restriction. As an example of a nonlinear but useful feature for images, consider the phenomenon called *end-stopping* (which is known to occur in biological visual perception (Sceniak et al., 2001)) in which a feature is maximally activated by edges of only a specific orientation and length; increasing the length of the edge further significantly decreases the feature's activation. A linear response model cannot exhibit end-stopping. Second, since PCA assumes the bases b_j to be orthogonal, the number of PCA features cannot be greater than the dimension n of the input. Sparse coding does not have either of these limitations. Its features $\hat{a}(x)$ are an inherently nonlinear function of the input x, as they are computed by solving an optimization problem in Equation (2.7), where the L_1-term provides a strong incentive to set many features exactly to zero. In fact, we have shown that sparse coding can

exhibit end-stopping behavior (Lee et al., 2007a). Note also that even though sparse coding attempts to express x as a *linear* combination of the bases b_j, the optimization problem (2.7) results in the activations $\hat{a}(x)$ being a *nonlinear* function of x. Further, sparse coding can use more basis vectors/features than the input dimension n. By learning a large number of basis vectors but using only a small number of them for any particular input, sparse coding gives a higher-level representation in terms of the many possible "basic patterns," such as edges, that may appear in an input.

As we noted earlier, sparse coding differs from PCA in two major ways: it adds an L_1-penalty enforcing sparsity of activations, and it replaces the orthogonality constraint on the basis vectors by a much weaker normalization constraint. PCA can be modified in various ways to make it more similar to sparse coding. The simplest way would be to add in the L_1-penalty term to the PCA formulation (2.8-2.9), thus leading to a *sparse PCA* formulation such as the following:[1]

$$\begin{array}{ll} \text{minimize}_{b,a} & \sum_i \|x_u^{(i)} - \sum_j a_j^{(i)} b_j\|^2 + \beta \sum_i \|a^{(i)}\|_1 \\ \text{s.t.} & b_1, b_2, \ldots, b_T \text{ are orthogonal} \end{array} \tag{2.9}$$

This sparse PCA formulation can be solved efficiently using the alternating minimization algorithm used for sparse coding, because the additional orthogonality constraint simplifies each of the minimization steps: (i) We can optimize the activations a while keeping basis vectors b by a linear operation, as for PCA, followed by an additional thresholding step that pulls every individual activation value a_j closer to zero by resetting it to $\max(0, a_j - \text{sign}(a_j) \cdot \beta)$. Intuitively, the effect of the L_1-term acts individually on the activation values, and we do not need to explicitly solve an optimization problem jointly over all the activation values, because the basis vectors are orthogonal and act on orthogonal input subspaces. (ii) We can optimize the basis vectors b while keeping the activations a fixed via a singular value decomposition, as

[1]Note that simply relaxing the orthogonality constraint in the PCA formulation, without adding the L_1-penalty term, would not help, as one of the optimal solutions for such a formulation would consist of orthogonal basis vectors. In other words, without a sparsity constraint on activations, there is no incentive against making any two basis vectors orthogonal to each other, as long as the subspace spanned by the basis vectors does not change.

in PCA.

Unfortunately, this sparse PCA formulation also did not perform well on self-taught learning problems in our experiments. One significant drawback this formulation shares with PCA is that the number of basis vectors is still limited by the input dimension, due to the requirement that basis vectors be orthogonal to each other. In particular, the number of basis vectors must still be less than the input dimension (as in the case of PCA), and overcomplete basis vectors cannot be learned. In practice, input data from many domains often lies close to a low-dimensional subspace (of lower dimension that the input dimension n), and this further exacerbates the problem—if the data lies close to a 20-dimensional subspace, 20 basis vectors are sufficient to span the subspace, and there is little extra information to learn further basis vectors (even considering the L_1-penalty term to encourage sparsity).

The differences between sparse coding, PCA, and the above sparse PCA formulation can be illustrated through a sample of the basis vectors learnt by them. Figure 2.5(a)-(c) shows 100 basis vectors obtained when the respective optimization problems were solved with 100,000 input images, each representing a 14×14 pixel image extracted at random from unlabeled grayscale images of natural scenes.[2] Each input $x_u^{(i)} \in \mathbb{R}^{196}$ lies in a 196-dimensional space of pixel intensities, but even 100 principal components are sufficient to explain over 97% of the variance in the input data, and consequently, it appears hard to learn any more than 100 useful basis vectors (or features) by using PCA. In Figure 2.5(a), PCA basis vectors are ordered top to bottom by decreasing variance of the input data along the basis vector. The differences between PCA and sparse coding have been well-documented—sparse coding learns basis vectors that are oriented and spatially localized, modeling various types of edges, but PCA does not learn such basis vectors. (Olshausen & Field, 1996a) The sparse PCA formulation in Figure 2.5(b) learns some edge-like basis vectors, but as expected, cannot learn more than a few such vectors. The basis vectors are ordered from top to bottom by decreasing fraction of input examples that have a nonzero

[2]Other details: For sparse coding and sparse PCA, we used the same sparsity penalty parameter $\beta = 0.7$, which lead to 7% nonzero activations per input example on average. Following standard preprocessing, we centered the data by subtracting the mean pixel intensity for each pixel in the dataset.

activation value for the basis vector, and the basis vectors in the bottom half are activated only for a small fraction of the input examples. For example, the bottom 20 basis vectors were active for less than 1% of the input examples.

By not imposing the orthogonality constraint, sparse coding can learn a much larger number of usable basis vectors. Each sparse coding basis vectors displayed in Figure 2.5(c) had a nonzero activation for between 6% to 9% of the examples. (The basis vectors are ordered by decreasing fraction of input examples that have a nonzero activation value for the basis vector.) Sparse coding can be applied to learn more basis vectors, and Figure 2.5(d) shows an example with 400 basis vectors. Even in this case, all basis vectors had nonzero activations for between 2% to 4% of the examples (the average fraction of activations per example in this case was 3%).

There are other modifications of PCA that enforce sparsity by formulating the problem differently. For example, Zou et al. (2004) use an "elastic net penalty" instead of our L_1-penalty, but still constrain the basis vectors to be orthogonal. A different method consists of finding a matrix factorization for the input matrix $X \approx UV$, for matrices U and V, by additionally constraining U and V to be sparse (Srebro & Jaakkola, 2001), or by placing linear constraints on the entries of U and V variables (Lee & Seung, 1997). Some of these methods can produce basis vectors that look similar to basis vectors learned by sparse coding, in that they learn edge-like features on natural images (e.g., see Lee & Seung, 1997), but they differ in the details of their formulation, and in the way that a new input is mapped to activations (features). Lee & Seung (1997) show that their factorization method can be used for classification of handwritten digits, but the basis vectors were learned on the labeled training data itself (by learning a separate set of basis vectors per label class). Variations of these methods might be applicable to self-taught learning problems, but we are not aware of any previous applications.

A different modification of PCA can also address the concern that PCA learns a linear mapping $a_j^{(i)} = b_j^T x_u^{(i)}$ from input $x_u^{(i)}$ to features $a_j^{(i)}$. Kernel dimensionality reduction algorithms such as kernel PCA (Mika et al., 1999) implicitly operate linearly in a potentially high-dimensional space, but due to the implicit mapping to a high-dimensional space, they can behave very nonlinearly in the input space. (For example,

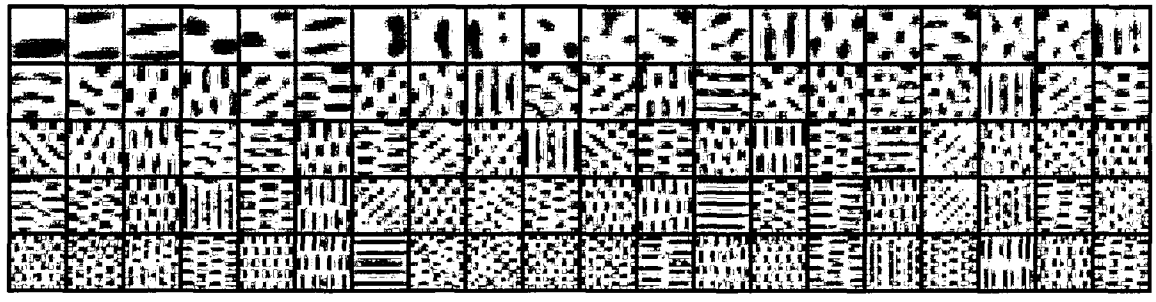

(a) PCA

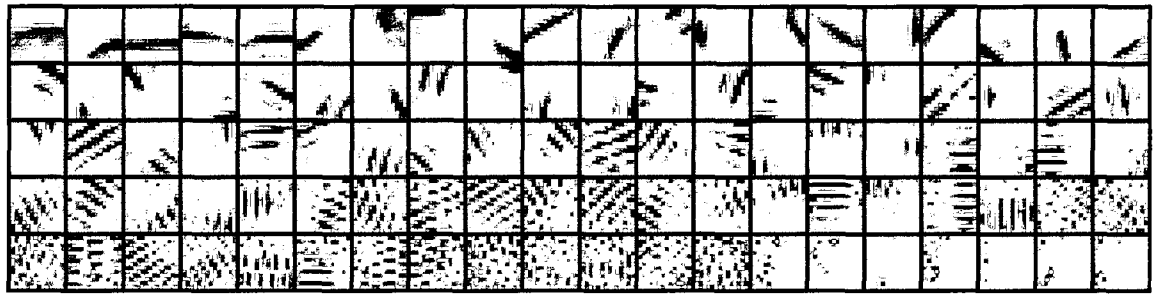

(b) Our sparse PCA formulation

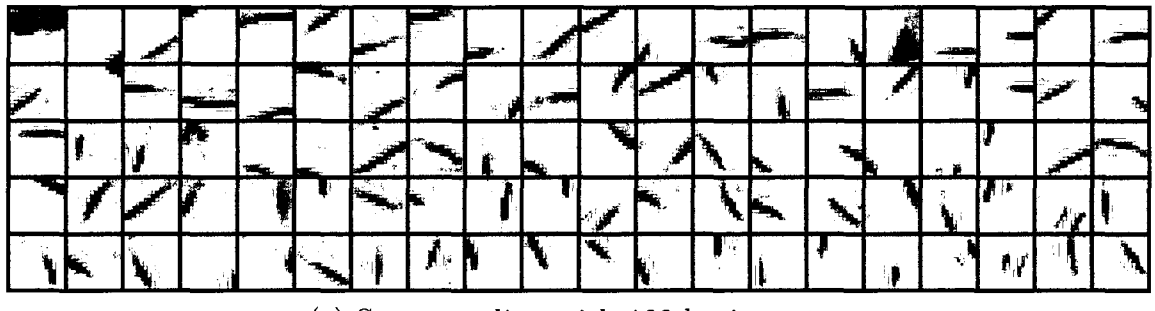

(c) Sparse coding with 100 basis vectors

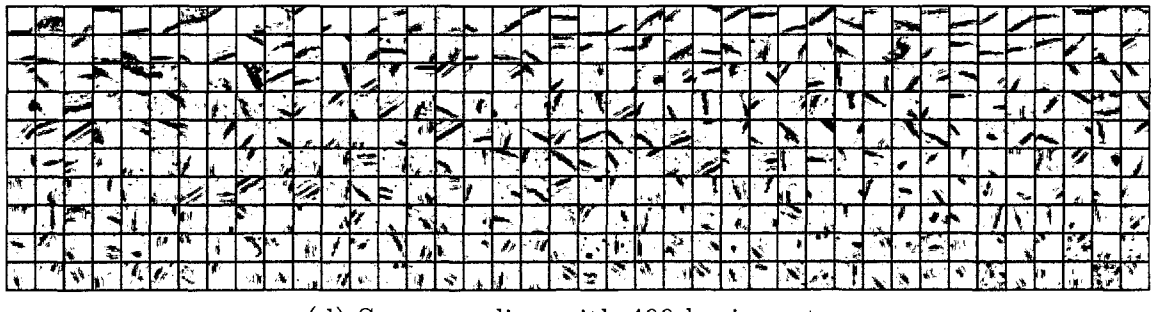

(d) Sparse coding with 400 basis vectors

Figure 2.5: Basis vectors learned by PCA, PCA with sparsity, and sparse coding on unlabeled input images. A single square box in each figure denotes a basis vector.

a linear function in the space of "all-pairs" features with elements $x_{j_1}x_{j_2}$, for any two input dimensions j_1 and j_2, is equivalent to a quadratic function in the space of the original feature space x.) This removes the restriction to linear mappings in PCA, while still allowing an efficient solution. But kernel PCA still requires a "kernel function" that captures a useful similarity metric over the input data (we give a brief introduction to kernel functions in 2.7.2), and such a kernel function can be hard to hand-design or learn from unlabeled data.

The independent components analysis (ICA) algorithm attempts to find basis vectors b_j such that the activation $a_j^{(i)} = b_j^T x_u^{(i)}$ is maximally independent from the activations for other basis vectors. (Bell & Sejnowski, 1995) By encouraging independence of the activations (features), ICA produces a representation that has very low redundancy. ICA is also known to learn basis vectors similar to sparse coding basis vectors, and has been widely studied in computational neuroscience. (van Hateren & van der Schaaf, 1998) Unfortunately, as a self-taught learning method for learning features, ICA did not work well in our experiments. One reason for this could be that ICA still defines a *linear* mapping from inputs $x_u^{(i)}$ to features $a_j^{(i)}$. It is possible that some nonlinear ICA methods (Hyvärinen & Pajunen, 1999) can be applied to self-taught learning problems.

Nonnegative matrix factorization (NMF) is a matrix factorization method that represents the input data matrix X approximately as a product of two matrices U and V with only nonnegative elements: $X \approx UV$. Nonnegative matrix factorization has been shown to learn "parts" of images automatically from data. (Lee & Seung, 1999) However, we are not familiar with previous applications to problems where the parts are learned on a very different, unlabeled source of data, and then applied to represent a target labeled dataset. Some of the ideas in nonnegative matrix factorization might be applicable to self-taught learning problems.

In Chapter 1, we discussed the vector quantization method (VQ) for transforming input vectors $x_u^{(i)}$ (or hand-designed features of $x_u^{(i)}$) to a single "codeword," where the codewords are themselves learnt on the unlabeled data. In comparison with sparse coding, which represents each input vector using a few patterns (basis vectors), VQ represents every input vector by using exactly one pattern (codeword). When VQ is

used with the Euclidean distance measure to map inputs to codewords, this link can be further formalized: with the k-means clustering algorithm used for learning the codewords, VQ is mathematically identical to our sparse coding formulation, with β set to a high value that guarantees exactly one nonzero activation, and with the activations only allowed to take the values 0 or 1.[3] The typical application of VQ thus appears more restrictive than sparse coding, and in Section 2.6.3 we demonstrate that sparse coding works better than a VQ method that is used widely in computer vision applications.

Methods based on VQ have been further customized to certain applications such as computer vision (Grauman & Darrell, 2007) and speech processing (Rabiner & Juang, 1993), though the codewords are usually learnt on the labeled training data itself. Nevertheless, it is plausible that such methods can be applied to self-taught learning problems as well.

In the semi-supervised learning setting, several authors have previously constructed features using labeled or unlabeled data from the *same* domain as the labeled data (e.g., see Chapter 1 for a detailed discussion of several such methods). A recent example is provided by the influential work of Hinton & Salakhutdinov (2006),, in which the authors train a multilayer neural network to learn features for handwritten digit images. They obtain striking results by using handwritten digit images themselves to construct features. In contrast, self-taught learning poses a harder problem, and requires that the structure learned from unlabeled data from a different domain (such as handwritten digit images) be "useful" for representing data (such as handwritten English character images) from the classification task.

Several existing methods for unsupervised and semi-supervised learning can be applied to self-taught learning, though many of them do not lead to good performance. For example, consider the task of classifying images of English characters ("a"—"z"), using unlabeled images of digits ("0"—"9"). For such a task, manifold learning algorithms such as ISOMAP (Tenenbaum et al., 2000) or LLE (Roweis & Saul, 2000) can learn a low-dimensional manifold using the unlabeled data (digits); however, these

[3]Technically, β must be set to a separate value per input example to ensure that only one activation is nonzero.

manifold representations do not generalize straightforwardly to the labeled inputs (English characters) that are dissimilar to any single unlabeled input (digit). As discussed in Chapter 1, neural network models such as autoencoders can also be applied to self-taught learning problems. To the best of our knowledge, they have only been applied to learning features from the same domain as the labeled data, and not to self-taught learning problems.

2.6 Experiments

We apply our algorithm to several self-taught learning tasks shown in Table 2.1. Note that the unlabeled data in each case cannot be assigned the labels from the labeled task. For each application, the raw input examples x were represented in a standard way with almost no hand-engineered preprocessing: raw pixel intensities for images, the frequency spectrogram for audio, and the bag-of-words (vector) representation for text documents.

2.6.1 Implementation details

For computational reasons, the unlabeled data was preprocessed by applying PCA to reduce its dimension;[4] the sparse coding basis learning algorithm was then applied in the resulting principal component space. We note that reasonable basis vectors can often be learned even using a smooth approximation such as $\Psi(a) = (\sum_j \sqrt{a_j^2 + \epsilon})$ to the L_1-norm sparsity penalty $\Psi(a) = \|a\|_1$; the smooth approximation leads to a differentiable objective function, and a much faster sparse coding algorithm. However, such approximations do *not* produce sparse features, and in our experiments, we found that classification performance is significantly worse if such approximations are used to compute $\hat{a}(x_l^{(i)})$.[5]

[4] We picked the number of principal components to preserve approximately 96% of the unlabeled data variance. This allowed us to apply sparse coding over a lower-dimensional input space, while preserving almost all of the input information.

[5] There is recent work showing that a smooth sparsity penalty based on the KL divergence measure can also work well for self-taught learning problems (Bradley & Bagnell, 2008).

Domain	Unlabeled data	Labeled data	Classes	Raw features
Image classification	10 images of outdoor scenes	Caltech101 image classification dataset (Fei-Fei et al., 2004)	101	Intensities in 14x14 pixel patch
Handwritten character recognition	Handwritten digits ("0"–"9") (LeCun & Cortes, 1998)	Handwritten English characters ("a"–"z") (Taskar, 2004)	26	Intensities in 28x28 pixel character/digit image
Font character recognition	Handwritten English characters ("a"–"z") (Taskar, 2004)	Font character images ("a"/"A" –"z"/"Z") obtained using Linux fonts	26	Intensities in 28x28 pixel character image
Song genre classification	Song snippets from 10 genres (Magnatune dataset: `http://magnatune.com`)	Song snippets from 7 *different* genres (Magnatune dataset: `http://magnatune.com`)	7	Log-frequency spectrogram over 50ms time windows
Webpage classification	100,000 news articles from the Reuters corpus (Rose et al., 2002)	Categorized webpages from the DMOZ hierarchy (`http://www.dmoz.org`)	2	Bag-of-words with 500 word vocabulary
UseNet article classification	100,000 news articles from the Reuters corpus (Rose et al., 2002)	Categorized UseNet posts from the "SRAA" dataset (McCallum, 2000)	2	Bag-of-words with 377 word vocabulary

Table 2.1: Details of self-taught learning applications evaluated in the experiments.

Once the basis vectors were learned on unlabeled data, they were used to construct features for each input from the supervised classification task.[6] The basis vectors were trained on the unlabeled data source, and are thus optimized to represent those examples with sparse activations (using very few basis vectors per input example). When the basis vectors are applied to computing activations for labeled data, to which the basis vectors were not tuned in advance, the same value of sparsity penalty β can lead to a higher number of nonzero activation values. Since the labeled and unlabeled data can sometimes lead to very different numbers of non-zero coefficients a_j, in our experiments β was also recalibrated prior to computing the labeled data's representations $\hat{a}(x_l^{(i)})$. We recommend that β used for computing this labeled data representation be picked by cross-validation on the labeled data.

For each such task, we report the result from the better of two standard, off-the-shelf supervised learning algorithms: a support vector machine (SVM) and Gaussian discriminant analysis (GDA). We used completely standard, off-the-shelf SVM and GDA classifiers that were not customized to the sparse coding features in any way, to demonstrate the utility of the learned features. A classifier specifically customized to sparse coding features is described in Section 2.7.

Partly for scaling and computational reasons, an additional feature aggregation step was applied to the image and audio classification tasks (since a single image is several times larger than the individual/small image patch bases that can be learned tractably by sparse coding). We aggregated features for large input images by extracting features for small image windows ("patches") in different locations in the large image, and then aggregating the features per-basis by taking the feature value with the maximum absolute value. The aggregation procedure effectively looks for the "strongest" occurrence of each basis pattern within the image. (Even better performance is obtained by aggregating features over a KxK grid of regions, thus looking for strong activations separately in different parts of the large image; see Table 2.2.) These region-wise aggregated features were used as input to the classification

[6] If PCA was used to reduce the dimensionality of inputs at basis learning time, by transforming input vector $x_u^{(i)}$ to the vector $Px_u^{(i)}$ for a matrix P containing the PCA parameters, the same PCA transform was applied on the labeled data as well to transform input $x_l^{(i)}$ to $Px_l^{(i)}$.

algorithms (SVM or GDA). Features for audio snippets were similarly aggregated by computing the maximum activation per basis vector over 50ms time windows in the snippet.

In the previous section, we compared our sparse coding formulation with many other methods for learning from unlabeled data. In this section, we compare our self-taught learning algorithm against two baselines, also trained with an SVM or GDA: using the raw inputs themselves as features, and using principal component projections as features, where the principal components were computed on the unlabeled data (as described in Section 2.5). In the PCA results presented in this paper, the number of principal components used was always fixed at the number of principal components used for preprocessing the raw input before applying sparse coding. This control experiment allows us to evaluate the effects of PCA preprocessing and the later sparse coding step separately, but should therefore not be treated as a direct evaluation of PCA as a self-taught learning algorithm (where the number of principal components could then also be varied). There is a vast variety of methods that can be used for "learning from unlabeled data," though we are not aware of previous applications of such methods to general self-taught learning problems. In Section 2.6.3, we delve deeper into the computer vision domain, and compare our results more broadly with previous techniques that use various kinds of unlabeled data.

2.6.2 Results

Tables 2.2-2.6 report the results for various domains. Sparse coding features, possibly in combination with raw features, significantly outperform the raw features alone as well as PCA features on most of the domains.

On the 101-way Caltech 101 image classification task with 15 training images per class (Table 2.2), sparse coding features achieve a test accuracy of 46.6%. In comparison, the first published supervised learning algorithm for this dataset achieved only 16% test accuracy even with computer vision specific features (instead of raw pixel intensities). Further, at the time we ran our experiments, our results were competitive with the best reported results on the dataset (Fei-Fei et al., 2004; Berg

Features	Number of regions			
	1	4	9	16
PCA	20.1%	30.6%	36.8%	37.0%
Sparse coding	30.8%	40.9%	46.0%	**46.6%**
Published baseline (Fei-Fei et al., 2004)				16%

Table 2.2: Classification accuracy on the Caltech 101 image classification dataset. For PCA and sparse coding results, each image was split into the specified number of regions, and features were aggregated *within* each region by taking the maximum absolute value.

et al., 2005; Holub et al., 2005; Serre et al., 2005). This is quite remarkable, since those other results required extensively researched computer vision specific techniques, and often used carefully hand-designed features or classifiers, while our method was based on an almost completely unsupervised algorithm with almost no explicit computer vision specific methods or human hand-engineering of features.[7]

Figure 2.6 shows example input images from the three character datasets, and some of the learned basis vectors. The learned basis vectors appear to represent "pen strokes." In Table 2.3, it is thus not surprising that sparse coding is able to use basis vectors ("strokes") learned on digits to significantly improve performance on handwritten characters—it allows the supervised learning algorithm to "see" the characters as comprising strokes, rather than as comprising pixels.

For audio classification, our algorithm outperforms the raw (spectral) features (Table 2.4).[8] In Chapter 4, we present a more sophisticated sparse coding algorithm for audio classification, and show that sparse coding methods outperform spectral features as well as some hand-engineered music/speech specific features.

When applied to text, sparse coding discovers word relations that might be useful

[7]Since the time we ran our experiments, other researchers have reported even better results using *highly specialized* computer vision algorithms (Zhang et al., 2006: 59.1%; Lazebnik et al., 2006: 56.4%). (Zhang et al., 2006; Lazebnik et al., 2006) Some of the computer vision specific ideas in these methods, such as Lazebnik's spatial pyramid kernel for aggregating local image features into global predictions, can also be applied directly to sparse coding features. This would give a computer vision specific self-taught learning method that might work better on this image classification dataset.

[8]Details: We learned bases over songs from 10 genres, and used these bases to construct features for a music genre classification over songs from 7 *different* genres (with different artists, and possibly different instruments). Each training example comprised a labeled 50ms song snippet; each test example was a 1 second song snippet.

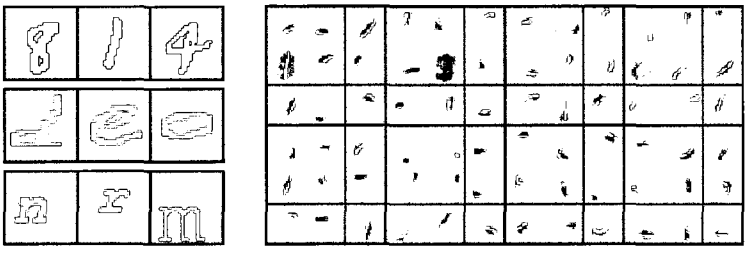

(a) (b)

Figure 2.6: (a) Example images from the handwritten digit dataset (top), the handwritten character dataset (middle) and the font character dataset (bottom). (b) Example sparse coding bases learned on handwritten digits.

Digits → English handwritten characters			
Training set size	Raw	PCA	Sparse coding
100	**39.8%**	25.3%	39.7%
500	54.8%	54.8%	**58.5%**
1000	61.9%	64.5%	**65.3%**
Handwritten characters → Font characters			
Training set size	Raw	PCA	Sparse coding
100	8.2%	5.7%	7.0% (**9.2%**)
500	17.9%	14.5%	16.6% (**20.2%**)
1000	25.6%	23.7%	23.2% (**28.3%**)

Table 2.3: Top: Classification accuracy on 26-way handwritten English character classification, using basis vectors trained on handwritten digits. Bottom: Classification accuracy on 26-way English font character classification, using basis vectors trained on English handwritten characters. The numbers in parentheses denote the accuracy using raw and sparse coding features together. Here, sparse coding features alone do not perform as well as the raw features, but perform significantly better when used in combination with the raw features.

Training set size	Raw	PCA	Sparse coding
100	28.3%	28.6%	**44.0%**
1000	34.0%	26.3%	**45.5%**
5000	38.1%	38.1%	**44.3%**

Table 2.4: Classification accuracy on 7-way music genre classification, using basis vectors trained on songs from 10 different genres.

Design	design, company, product, work, market
Business	car, sale, vehicle, motor, market, import
vaccine	infect, report, virus, hiv, decline, product
movie	share, disney, abc, release, office, movie, pay

Table 2.5: Text basis vectors learned on 100,000 Reuters newswire documents. Top: Each row represents the basis vector most active on average for documents with the class label at the left. For each basis vector, the words corresponding to the largest magnitude elements are displayed. Bottom: Each row represents the basis vector that contains the largest magnitude element for the word at the left. The words corresponding to other large magnitude elements are displayed.

for classification (Table 2.5). The performance improvement over raw features is small (Table 2.6).[9] This might be because the bag-of-words representation of text documents is already sparse, unlike the raw inputs for the other applications, and because the bag-of-words representation contains either binary (0/1) or integer-valued features, which are poorly approximated by the quadratic term in the sparse coding objective function. In Chapter 4, we elaborate further on this problem, and show that a more general sparse coding model works even better on text classification; that model also outperforms Latent Dirichlet Allocation (Blei et al., 2003), a method that is widely used for unsupervised learning with text documents.

We envision self-taught learning as being most useful when labeled data is scarce. Table 2.7 shows that with small amounts of labeled data, classification performance deteriorates significantly when the basis vectors (in sparse coding) or principal components (in PCA) are learned on the labeled data itself, instead of on large amounts of

[9]Details: Basis vectors were learned on 100,000 news articles from the Reuters corpus (Rose et al., 2002), and then evaluated on 30 binary webpage category classification tasks, and on 2 binary UseNet article classification tasks. PCA applied to text documents is commonly referred to as latent semantic analysis. (Deerwester et al., 1990)

Reuters news → Webpages			
Training set size	Raw	PCA	Sparse coding
4	62.8%	63.3%	**64.3%**
10	73.0%	72.9%	**75.9%**
20	79.9%	78.6%	**80.4%**
Reuters news → UseNet articles			
Training set size	Raw	PCA	Sparse coding
4	61.3%	60.7%	**63.8%**
10	**69.8%**	64.6%	68.7%

Table 2.6: Classification accuracy on webpage classification (top) and UseNet article classification (bottom), using bases trained on Reuters news articles.

additional unlabeled data.[10] This demonstrates that our method is in fact using the unlabeled data, and cannot simply be applied successfully to a supervised learning problem with no unlabeled data. As more and more labeled data becomes available, the performance of sparse coding trained on labeled data approaches (and presumably will ultimately exceed) that of sparse coding trained on unlabeled data.

2.6.3 Other methods of using unlabeled data

To the best of our knowledge, the self-taught learning framework places significantly fewer restrictions than previous formalisms for using unlabeled data for a supervised learning task. However, there are many published algorithms in the literature that use some form of "weakly related" unlabeled data for a specific application, and as such, those algorithms can be applied to self-taught learning problems. As a case study, we consider experimental results for the Caltech101 image classification dataset, as it is a standard dataset with a significant body of published results, and compare the results obtained by our self-taught learning algorithm with other data-driven methods. For comparison, our sparse coding method achieves an accuracy of 46.6% on the Caltech101 dataset with 101 image classes and 15 training examples per class.

A widely used method in computer vision is based on the vector quantization or "bag-of-visual-words" technique (see Section 1.6.2 for an introduction). Briefly, this

[10]For the sake of simplicity, we performed this comparison only for the domains that the basic sparse coding algorithm applies to, and that do not require the extra feature aggregation step.

Domain	Training set size	Unlabeled	Labeled	
		SC	PCA	SC
Handwritten characters	100	**39.7%**	36.2%	31.4%
	500	**58.5%**	50.4%	50.8%
	1000	**65.3%**	62.5%	61.3%
	5000	73.1%	**73.5%**	73.0%
Font characters	100	**7.0%**	5.2%	5.1%
	500	**16.6%**	11.7%	14.7%
	1000	**23.2%**	19.0%	22.3%
Webpages	4	**64.3%**	55.9%	53.6%
	10	**75.9%**	57.0%	54.8%
	20	**80.4%**	62.9%	60.5%
UseNet	4	**63.8%**	60.5%	50.9%
	10	**68.7%**	67.9%	60.8%

Table 2.7: Accuracy on the self-taught learning tasks when sparse coding bases are learned on unlabeled data (third column), or when principal components/sparse coding bases are learned on the labeled training set (fourth/fifth column). Since Tables 2.2-2.6 already show the results for PCA trained on unlabeled data, we omit those results from this table. The performance trends are qualitatively preserved even when raw features are appended to the sparse coding features.

technique uses a large number of example images to learn a set of local patterns, also called codewords or "visual words," and then uses a single pattern to describe any local image feature. Grauman & Darrell (2007) performed an extensive study of such bag-of-visual-words methods. They used the hand-designed SIFT features as local image features (Lowe, 1999), and preprocessed the features by applying a principal component analysis (PCA) transform to give the so-called "PCA-SIFT" features (Ke & Sukthankar, 2004). These PCA-SIFT features have been shown to be comparable to, or outperform, various other types of local features for image classification (Mikolajczyk & Schmid, 2005), including a large number of local descriptors developed over the past decade in computer vision research.[11] Given the extensive comparisons with

[11]The descriptors compared by Mikolajczyk & Schmid included gradient location and orientation histograms or GLOH (Mikolajczyk & Schmid, 2005), shape context (Belongie et al., 2002), sift (Lowe, 1999), spin images (laz, 2005), steerable filters (Freeman & Adelson, 1991), differential invariants (Koenderink & van Doom, 1987), complex filters (Schaffalitzky & Zisserman, 2002), moment invariants (Gool et al., 1996), and cross-correlation of sampled pixel values.

other feature types, we are not aware of a better local feature type that could have been used instead of the PCA-SIFT features. In their study, Grauman & Darrell learnt the codewords on labeled training data itself (and not on unrelated unlabeled data); they also extensively tuned various parameters in the classification algorithm, including the number of patterns (codewords), the distance metric used to map to a local PCA-SIFT feature to the closest pattern, and also the SVM classification hyperparameters. Even with all these customizations, the best results reported using a standard support vector machine classifier were around 38% accuracy on the Caltech101 dataset, which is much lower than the 46.6% obtained by our method. In addition, Grauman & Darrell note that the bag-of-visual-word approach's accuracy was fairly sensitive to the exact parameter settings; in comparison our algorithm requires little parameter tuning.[12]

The above results with bag-of-visual-words were obtained when codewords were trained by clustering the labeled training data itself. We would expect that the results might be comparable or worse if the codewords are trained on other unlabeled images, as the trained codewords would be optimized for representing features from those unlabeled images. We confirmed this in the following control experiment. We trained codewords in two different ways: either using the labeled training set, or using a set of unlabeled images different from the labeled training set. We found that the final results did not change significantly in these two experiments. Combined with Grauman & Darrell's study, this indicates that using standard supervised learning classifiers, the typical bag-of-visual-words method does not perform as well as our sparse coding method on self-taught learning applied to image classification.

[12]In their paper, Grauman & Darrell use the study reported here as a baseline. They design an ingenious method called the pyramid match kernel for matching local features from one image with local features from another image. Such a matching method does not penalize for the presence of extra local features, and is thus more robust to clutter, changing backgrounds or occlusions. With this pyramid match kernel, Grauman & Darrell obtain 50% accuracy for this task which is better than the 46.6% accuracy we report here. We note that a similar pyramid match kernel can be applied to the sparse coding features as well, replacing our simplistic grid-wise-maximum feature aggregation procedure with a more sophisticated matching algorithm. In any case, we find it remarkable that our algorithm achieves an accuracy of 46.6% even though it is almost completely unsupervised, uses only unlabeled data to train the representation (unlike the codewords learnt in typical bag-of-visual-words applications), uses almost no hand-designed features, and required almost no computer vision specific tuning.

For image classification, Serre et al. (2005) present a method that was hand-designed to match observed biological processing. The method is superficially similar to our method, in that the local image filters were hand-designed Gabor filters, and qualitatively resemble the basis vectors learned automatically by our method. A crucial difference is that the filters used by Serre et al. are linear, and are computed by applying the Gabor filter to local image patches. In contrast, the local features in our method are obtained by solving an optimization problem that tries to find the best few filters for matching the input. Serre et al. report a final accuracy of 35%, compared to the 46.6% accuracy attained by our method. The facts that our filters are automatically adapted to images (and not hand-designed), and that our feature construction is nonlinear, might explain the observed differences, and also help validate the utility of self-taught learning for image classification.

2.7 A classifier for sparse coding features

We have presented a method that can automatically use unlabeled data to learn a higher-level representation; this representation can then provide useful features for the labeled data. In our discussions and experiments thus far, we have largely ignored what we do next with those features—we have simply used an off-the-shelf supervised learning classifier (such as an SVM or GDA), without giving any special consideration to the source or characteristics of the features. This could be unsatisfactory for some applications, as the features produced by our model, especially for high values of the sparsity penalty β, can be atypical—the features are extremely sparse, and sometimes, a feature value can change by a lot even if the input x changes only by a little (e.g., if the input changes such that a different basis vector matches it best). It is likely that such features are poorly modeled by some off-the-shelf classifiers (e.g., GDA assumes that features from each class are distributed according to a Gaussian distribution)

It does not have to be this way, however, since we know the *exact* model (specified by the basis vectors) that generated these features $\hat{a}(x)$ from the input vectors x. In this section, we describe a different interpretation of sparse coding based on a probabilistic model. This model will in turn suggest a supervised learning classifier

that is customized to the specific model that generated those features.

2.7.1 A probabilistic model for sparse coding

We will first pose a generative model for the input vector $x_u^{(i)} \in \mathbb{R}^n$, and then demonstrate that the sparse coding formulation in Equations (2.2-2.3) can be interpreted as performing learning/inference over that model. The generative model assumes that given the basis vectors $b = \{b_1, \ldots, b_s\}$, and the activation vector $a^{(i)} = ({a^{(i)}}_1, \ldots, {a^{(i)}}_s)^T$, input $x_u^{(i)}$ is generated from a multivariate Gaussian distribution with mean $\eta = \sum_j b_j a_j^{(i)}$ and (known) covariance $\sigma^2 I$:

$$x_u^{(i)} \mid b, a^{(i)} \sim \mathcal{N}(\eta, \sigma^2 I) \quad \forall i = 1, 2, \ldots, k$$

Another interpretation for this is that the input $x_u^{(i)}$ is generated by the reconstruction $\eta = \sum_j b_j a_j^{(i)}$, with additive Gaussian noise with mean zero and covariance $\sigma^2 I$. This is a fairly standard probabilistic assumption that is used, for example, also in the probabilistic justification for PCA. (Tipping & Bishop, 1999)

To fully specific the generative model, we also need to specify the prior probabilities for activations $a^{(i)}$ and basis vectors b. The prior distribution of each activation vector $a^{(i)}$ is defined using the Laplacian distribution parameterized by a sparsity parameter β':

$$P(a^{(i)}) \propto \exp(-\beta' \|a^{(i)}\|_1) \tag{2.10}$$

This distribution gives low probability to large, nonzero activation values; compared to the Gaussian distribution, the Laplacian distribution also has a fatter tail, because large values are not penalized as much—as an activation value a_j increases, the Laplacian probability decays as $\exp(-\beta'|a_j|)$ whereas the Gaussian probability decays as $\exp(-\beta'|a_j|^2)$. Because of these properties, the Laplacian prior encourages activations with many values set exactly to zero, and only some nonzero activations with large values. (Tibshirani, 1996a; Ng, 2004)

Finally, each basis vectors b_j is constrained to the set $\{b_j | b_j \in \mathbb{R}^n\}$, and assigned

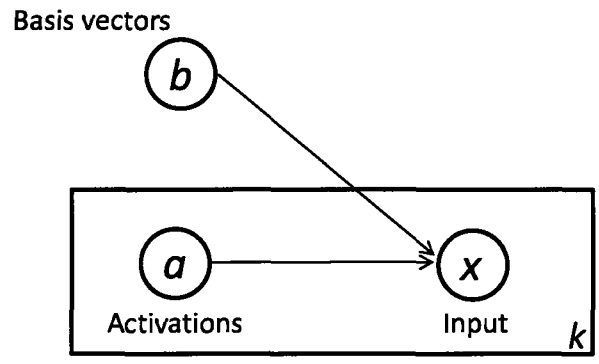

Figure 2.7: A probabilistic model for sparse coding.

uniform prior probability within this feasible set. Different basis vectors are assumed to be generated independently.

$$P(b) = \prod_j P(b_j)$$

$$P(b_j) = \begin{cases} 1/Z & \text{if } \|b_j\| \leq 1 \\ 0 & \text{otherwise} \end{cases}$$

where Z is a normalization constant.

Figure 2.7 shows a qualitative graphical model representation. The box or "plate" in the figure denotes replication. The basis vectors b are generated just once, and are shared across all input vectors; the input vector x and activations a are unique to any one example, and are regenerated for any new example. The number k in the plate denotes that there are k copies (one per input example).

Given a large number of unlabeled examples $\{x_u^{(i)}\}$, the task of basis learning can be posed as finding the maximum-a-posteriori value of the basis vectors b in this

probabilistic model:

$$\begin{aligned}
\arg\max_b P(b|\{x_u^{(i)}\}) &= \arg\max_b P(\{x_u^{(i)}\}|b)P(b) \\
&= \arg\max_{\{b:\|b_j\|\leq 1\}} \prod_i P(x_u^{(i)}|b) \\
&= \arg\max_{\{b:\|b_j\|\leq 1\}} \prod_i \int_{a^{(i)}} P(x_u^{(i)}|b,a^{(i)})P(a^{(i)})da^{(i)}
\end{aligned}$$

where the second line uses the fact that the prior probability over b is uniform if $\|b_j\| \leq 1\ \forall j$, and zero otherwise; the third line uses the fact that $P(a^{(i)}|b) = P(a^{(i)})$ because $a^{(i)}$ is independent of b (when x is not given). The integral over $a^{(i)}$ cannot be computed in closed form—this is partly because of our choice of the Laplacian prior on $a^{(i)}$ to promote sparsity, as the Laplacian is not a conjugate prior for the Gaussian observation model for $x_u^{(i)}|b,a^{(i)}$. Instead, we approximate the integral over all $a^{(i)}$ values by just the maximum over $a^{(i)}$:

$$\begin{aligned}
\arg\max_b P(b|\{x_u^{(i)}\}) &\approx \arg\max_{\{b:\|b_j\|\leq 1\}} \prod_i \max_{a^{(i)}} P(x_u^{(i)}|b,a^{(i)})P(a^{(i)}) \\
&= \arg\max_{\{b:\|b_j\|\leq 1\}} \max_{\{a^{(i)}\}} \prod_i P(x_u^{(i)}|b,a^{(i)})P(a^{(i)}) \\
&= \arg\max_{\{b:\|b_j\|\leq 1\}} \max_{\{a^{(i)}\}} \sum_i \left(\log P(x_u^{(i)}|b,a^{(i)}) + \log P(a^{(i)})\right) \\
&= \arg\min_{\{b:\|b_j\|\leq 1\}} \min_{\{a^{(i)}\}} \sum_i \left(-\log P(x_u^{(i)}|b,a^{(i)}) - \log P(a^{(i)})\right)
\end{aligned}$$

where the second line follows because each $a^{(i)}$ can be maximized separately from other activation for other examples, so the product and maximization can be swapped; the third line follows by taking logarithms, as we are just interested in the arg max over b.

Substituting the model probabilities from Equations (2.10) and (2.10), changingand setting $\beta = 2\sigma^2\beta'$, this leads exactly to the sparse coding optimization problem in Equations (2.2-2.3). Thus, the sparse coding optimization problem corresponds to performing approximate learning for the probabilistic model described in this section.

2.7.2 Obtaining a classifier for sparse coding

A fundamental problem in supervised classification is defining a "similarity" function between two input examples. One way of formalizing this similarity function is by using a kernel function K, that takes two input examples $x^{(r)}$ and $x^{(t)}$, and computes a nonnegative similarity value $K(x^{(r)}, x^{(t)})$ for them.[13] For example, support vector machines (and many other machine learning algorithms, including GDA, logistic regression, principal components analysis, etc.) can be "kernelized," meaning that the algorithm can be written in an equivalent form where it accesses inputs only via computing the kernel function K between two input examples; by changing this kernel function, the algorithm can handle other definitions of similarity. In the experiments described above, we used the regular notions of similarity (i.e., standard SVM kernels, including linear and polynomial kernels) to allow a fair comparison with the baseline algorithms. However, we now show that the sparse coding model also suggests a specific specialized similarity function (kernel) for the learned representations.

In particular, an explicit generative model, such as the one we learned in the previous section, can suggest a similarity function between input examples—instead of just comparing the input vectors $x^{(r)}$ and $x^{(t)}$, we can compare the generative process for $x^{(r)}$ and $x^{(t)}$. There are many methods for formalizing this intuition into a supervised learning classifier (Lasserre et al., 2006), and we demonstrate just one of them here. Loosely speaking, the method we consider is based on comparing the difference in the way the various generative model parameters contribute to generating the input vectors $x^{(r)}$ and $x^{(t)}$; the method achieves this by comparing the *gradient* of the (log) input probabilities with respect to the model parameters (Jaakkola & Haussler, 1998). More precisely, given a generative model $P(x|\theta)$, with model parameters θ, the method considers the *Fisher score* $U_x = \nabla_\theta \log P(x|\theta)$, and then computes the *Fisher kernel* as $K(x^{(r)}, x^{(t)}) = U_{x^{(r)}}^T U_{x^{(t)}}$.[14]

[13] A kernel function K, as conventionally defined, must satisfy a technical condition that the kernel function $K(x^{(r)}, x^{(t)})$ between inputs $x^{(r)}$ and $x^{(t)}$ is equivalent to computing dot products between vectors $\Phi(x^{(r)})$ and $\Phi(x^{(t)})$ for some function Φ: $K(x^{(r)}, x^{(t)}) = \Phi(x^{(r)})^T \Phi(x^{(t)})$. See Bishop's textbook (Bishop, 2006) for further details.

[14] For simplicity, we set the Fisher information matrix to the identity matrix (Jaakkola & Haussler, 1998).

In the probabilistic model for sparse coding, the basis vectors b are the model parameters, and the generative model is obtained by marginalizing out the hidden variable a:

$$P(x|b) = \int_a P(x|b,a)P(a)da$$

For this model, the Fisher score is:

$$U_x = \nabla_b \log \int_a P(x|b,a)P(a)da$$

A kernel based on this Fisher score can be computed (e.g., by numerically estimating the integral using MCMC sampling), but we found that a much simpler kernel based on a point estimate of a performs as well.[15] We approximate the integral using a point estimate $\hat{a} = \arg\max_a P(x|b,a)P(a)$ (which also corresponds to finding the optimal activations for input x given fixed basis vectors b), and get $U_x \propto \nabla_b \log P(x|b,\hat{a}) \propto (x - B\hat{a})\hat{a}^T$, where B is the basis matrix with b_j as its j-th column. Ignoring constant multiplicative factors, the corresponding Fisher kernel can be simplified to the following form:

$$K(x^{(r)}, x^{(t)}) = \left(\hat{a}(x^{(r)})^T \hat{a}(x^{(t)})\right) \cdot \left(r^{(r)^T} r^{(t)}\right),$$

where $r = x - \sum_j b_j \hat{a}_j$ represents the residual vector corresponding to the activations $\hat{a}$. This kernel has an intuitive interpretation. For the inputs $x^{(r)}$ and $x^{(t)}$, we first construct the features $\hat{a}(x^{(r)})$ and $\hat{a}(x^{(t)})$ (according to Equation 2.7). Then, the kernel is a product of two terms: the first term is simply the inner product of the sparse coding features $\hat{a}(x^{(r)})$ and $\hat{a}(x^{(t)})$, and corresponds to using a linear kernel over the sparse coding features; the second term is the inner product of the residuals for the input examples.

[15] For generative models with hidden variables, the kernel obtained by marginalizing out the hidden variable in the Fisher kernel is also called a marginalized kernel (Tsuda et al., 2002). Marginalized kernels have been found useful for certain generative models, such as hidden Markov models.

Training set size	Standard kernel	Sparse coding
100	35.4%	**41.8%**
500	54.8%	**62.6%**
1000	61.9%	**68.9%**

Table 2.8: Classification accuracy using the learned sparse coding kernel in the Handwritten Characters domain, compared with the accuracy using the *best* choice of standard kernel and input features.

Further, since we already compute the features $\hat{a}(x)$ for inputs x in our earlier method, we can additionally compute the Fisher kernel very efficiently. We can thus use this customized kernel (instead of a standard SVM kernel) to learn a support vector machine classifier with very little overhead. This gives us a supervised learning classifier that is partially tuned to the sparse coding features, and might be better able to handle the atypical characteristics of these features.

2.7.3 Experimental comparison

We evaluate the performance of the learned kernel on the handwritten character recognition domain. As a baseline, we compare against some choices of standard kernels (linear/polynomials of degree 2 and 3/RBF) and features (raw features/PCA/sparse coding features). To give the baseline a slightly unfair advantage, we also pick the best combination of these choices for kernels and features, based on performance on the *test data*. Table 2.8 shows that an SVM with the new kernel outperforms the *best* choice of standard kernels and features. Using the generative model via the Fisher kernel gives a classifier customized specifically to the distribution of sparse coding features.

2.8 Discussion

In this chapter, we have introduced an algorithm for self-taught learning. The algorithm is based on applying sparse coding to unlabeled data to learn a higher-level representation of inputs, and then using this representation to construct features for

a supervised learning classifier. We conclude the chapter with a discussion of some unexplored connections and open questions for future work.

2.8.1 Biological comparisons

A longstanding hypothesis in computational neuroscience states that human perceptual processing is tuned to the statistics of its natural surroundings. (Atick, 1992) For example, it states that visual processing occurs the way it does because of the visual nature of the world we live in; or, audio processing occurs the way it does because of the audio surroundings we live in, and so on. This suggests that there might be a general organizing principle, or a computational algorithm, that when applied to percepts (images, audio, etc.) in the natural surroundings, can lead to human-like perceptual processing. In fact, some neuroscientists believe that a lot of human intelligence can be attributed to a single algorithm (Mountcastle, 1978), a hypothesis that has recently become popular with a broader public audience. (Hawkins & Blakeslee, 2004) As partial validation of this hypothesis, experiments have demonstrated that the same piece of brain tissue can learn to process very different input modalities, such as sight and sound, just by being exposed to inputs of those modalities (Sharma et al., 2000). This further suggests that we may not need a different organizing principle each for vision, audio, touch, etc., but that a single organizing principle, or a single learning algorithm, could be used to replicate intelligent, human-like perceptual processing.

Against this background, the sparse coding model was originally developed as a model for low-level mammalian perception, and it was demonstrated that sparse coding (as well as some other algorithms, such as independent components analysis (van Hateren & van der Schaaf, 1998)) applied to unlabeled input data (images, audio, etc.) can learn basis vectors that resemble filters found in perceptual processing in the mammalian brain (Hubel & Wiesel, 1962; Olshausen & Field, 1996a; Olshausen & Field, 1997). For example, when sparse coding was applied to small image patches extracted from images of natural scenes, the basis vectors converged to various kinds of Gabor filters (edges), and closely matched the filters observed in low-level visual

processing in the brain (in the visual cortex layer called "V1") (Olshausen & Field, 1997). When sparse coding was applied to audio inputs, the basis vectors converged to audio patterns called gammatones, almost identical to those observed in low-level audio processing in the brain (Smith & Lewicki, 2005). Sparse coding has also been shown to exhibit other kinds of nonlinear phenomena, such as end-stopping (Sceniak et al., 2001) and center-surround suppression (Cavanaugh et al., 2002; Series et al., 2003), observed in the brain (Lee et al., 2007a).

In our view, the observed match between the results of sparse coding algorithms and measured biological data is a significant bonus. While it is difficult to motivate a machine learning algorithm *purely* based on match with biological data, a comparison with biological data may help direct future research via the following question: given that sparse coding mimics characteristics of low-level visual/audio processing in the brain, and that it also performs well on self-taught learning applications, what new modifications or extensions are needed to also mimic higher-level visual/audio processing, and thus hopefully obtain even better self-taught learning performance? As a specific example, a different unsupervised learning algorithm, called the sparse deep belief network (Lee et al., 2007b), was recently developed to explain observed higher-level filters in the visual cortex layer called V2 (Ito & Komatsu, 2004; Boynton & Hegde, 2004; Levitt et al., 1994)—while the model was primarily validated by showing that it matches measured biological data, the model also performs well on machine learning tasks, such as image classification. With more detailed computational studies of the brain being produced regularly, we believe that such fruitful synergies between analysis of artificial (machine learning) and biological systems will only increase in the future.

2.8.2 Theoretical guarantees

We posed the self-taught learning problem mainly to reduce the restrictions on the types of data that we are allowed to learn from. As Table 2.1 shows, the unlabeled and labeled data in our experiments were obtained in a natural way, with only a minimal attempt to obtain both unlabeled and labeled data from the same "data

type." Across these domains, self-taught learning empirically leads to significant gains in classification accuracy. An important theoretical question is characterizing how the "similarity" between the unlabeled and labeled data affects the self-taught learning performance (similar to the analysis by Baxter, 1997, for transfer learning).

The self-taught learning formalism itself does not make restrictions on the types of unlabeled data, but of course, we do need the unlabeled data to be "similar" to the labeled data in some way—to take an extreme example, if the unlabeled data were to consist of random (noise) images with random pixel intensities, while the labeled data consists of handwritten characters, it is unlikely that we can benefit from using the unlabeled data for learning. Similar theoretical statements have been made about other formalisms such as semi-supervised learning (Ando & Zhang, 2005; Ben-David et al., 2008; Zhu, 2005; Seeger, 2001) and transfer learning (Baxter, 1995; Thrun, 1996; Ben-David & Schuller, 2003; Caruana, 1997), and we leave a similar theoretical understanding of self-taught learning as an important open question for future research.

We note that in our self-taught learning algorithm, the same probabilistic model for sparse coding was used for both unlabeled and labeled data—the parameters b were estimated using the unlabeled data, and then the latent activation variables a were inferred for the labeled data using the learnt parameters b; these inferred activations were finally used as features. While we did not make explicit assumptions about the unlabeled and labeled data arising from the same distribution in self-taught learning (as done in some semi-supervised learning algorithms, such as Nigam et al., 2000), and did not use such distributional considerations explicitly in picking the unlabeled and labeled data for our experiments, our sparse coding algorithm can be interpreted as relying on the fact that both the labeled and unlabeled data can be fit well with a common sparse coding probabilistic model, as shown in Figure 2.7. In our view, since the model can use a large number of basis vectors, even larger than the original input dimension,[16] and multiplex different subsets of basis vectors for each input using the latent activation variables a, this is a moderately weak restriction in practice.

[16]This is unlike PCA, for example, where the number of "basis vectors" (principal components) must be less than the input dimension due to the orthogonality constraint between principal components.

We believe that further exploration of this modeling assumption could lead to a better theoretical understanding of precisely when our self-taught learning algorithm might be expected to perform well, and answer a central question: Given labeled data from a supervised classification problem, under what minimal theoretical assumptions can we expect benefits from using unlabeled data?

2.8.3 Extensions to the sparse coding model

Our sparse coding formulation uses a nondifferentiable L_1-penalty term. Especially with a large number of basis vectors, the formulation encourages activations to be sparse, and to only have nonzero activations for the few basis vectors that best match the input vector. Sparse coding can have the property that a small modification in the input x leads to a large change in the activations or features $\hat{a}(x)$, because a different basis vector is now the best match for the modified input. In other words, the features computed by our sparse coding algorithm can be "unstable," and this might affect performance on some self-taught learning tasks. Recent work has shown that the nondifferentiable L_1-penalty can be replaced by a differentiable penalty based on the KL divergence measure, to produce better self-taught learning performance (Bradley & Bagnell, 2008). Other forms of regularization might also reduce the problems due to instability—one such option could be an elastic net penalty (Zou et al., 2004), that empirically leads to sparsity across groups of activations, instead of encouraging sparsity for individual activations as in our sparse coding model.

In our work, we have not used the labeled data at all in the unsupervised feature construction phase. When labeled data is extremely scarce (only a few available examples), there is little other choice. But when moderate amounts of labeled data are available, the sparse coding formulation can be modified to also encourage basis vectors to model the labeled data well. One way to implement this modification would be to explicitly encourage the learnt activations to be discriminative for the target

classes, by adding an extra term to the sparse coding objective function:

$$\text{minimize}_{b,a} \quad \sum_i \|x_u^{(i)} - \sum_j a_j^{(i)} b_j\|^2 + \beta \sum_i \|a^{(i)}\|_1 + \gamma \sum_i q\left(\hat{a}(x_l^{(i)})\right) \tag{2.11}$$

$$\text{s.t.} \quad \|b_j\| \leq 1, \quad \forall j \in 1, ..., s \tag{2.12}$$

where q is some functon that measures the quality of the learnt features on the labeled data (for example, by computing the log-likelihood achievable on labeled data), and γ is a parameter that specifies the relative importance given to the labeled data. If q is a convex differentiable function of a and b separately, then our previous alternating minimization algorithm can be adapted to this setting. A different way of using labeled data to influence basis vectors would be to train initial basis vectors on unlabeled data, and then fine tune the basis vectors on labeled data as well (Bradley & Bagnell, 2008).

Our sparse coding algorithm is able to learn low-level features of the inputs. This includes edge-like features for images, simple sound patterns for audio, and text topics for text documents. For high-performance self-taught learning, we would want to learn more complex features also. For example, for images, we might hope to learn features that represent parts of objects ("wheel", "face", etc.), or whole objects ("car", "apple", etc.). One way to achieve this would be to use a hierarchical model, that computes not just features of the input, but also features of those features, features of the features-of-features, and so on. This corresponds to learning a multilayer representation, where each layer computes more complex features as output, given the previous layer's features as input. Sparse coding has indeed been applied in two layers (Hoyer & Hyvrinen, 2002), and it learns interesting, slightly higher-level filters (such as larger contours instead of edges), though such a two-layer extension did not lead to large gains on self-taught learning in our experiments. There is a lot of recent work in learning such multilayer representations from unlabeled data using neural network models (Hinton & Salakhutdinov, 2006; Lee et al., 2009a), and we expect those models to be widely applicable to self-taught learning problems.

Chapter 3

Self-taught Learning for Audio Classification

In this chapter, we focus on the application of our self-taught learning algorithms to audio classification. To motivate later discussion, consider a speaker identification task in which we'd like to distinguish between Adam and Bob from their speech with only a few seconds of labeled speech samples from Adam and Bob as training data. Given only a few seconds of speech samples as labeled training data, this is a difficult task to solve well using only supervised learning techniques. For such a task, semi-supervised learning algorithms can make use of additional unlabeled data that has the same class labels as the classification task (Nigam et al., 2000). Thus, to apply most semi-supervised learning methods (such as the method of Nigam et al. (Nigam et al., 2006)) to distinguish between Adam and Bob, we must obtain additional unlabeled data from Adam and Bob specifically. This sort of unlabeled data is hard to obtain; indeed, short of eavesdropping on conversations between Adam and Bob, it is hard to envisage a data collection method that results in unlabeled speech samples from Adam and Bob—*and no one else*—that does not also automatically result in our having the class labels as well. Transfer learning typically attempts to use additional labeled data to construct supervised classification problems that are related to the task of interest (Caruana, 1997; Thrun, 1996; Ando & Zhang, 2005). Thus, for speaker identification, transfer learning may require labeled data from other speech

classification tasks. Since these additional classification tasks are supervised and thus require labeled examples, data for even transfer learning is often difficult to obtain.

In contrast, the self-taught learning framework introduced in the previous chapter attempts to use easily obtainable unlabeled data to improve classification performance. For the task of distinguishing between Adam and Bob, this means we may use unlabeled data from speakers *other* than Adam and Bob (or perhaps even use non-speech audio samples). Given the ease with which such data can be obtained—one can envisage recording audio from radio broadcasts or downloading audio clips randomly off the internet—we believe that self-taught learning holds the promise of much easier applicability than most semi-supervised learning and transfer learning algorithms.

In principle, the sparse coding algorithm discussed in the previous chapter can be directly applied to audio classification. For illustration, consider a 500ms speech signal sampled at 16kHz. The raw acoustic signal is a vector $x \in \mathbb{R}^{8000}$ containing the time-domain amplitude values that constitute the signal. This unwieldy representation can be extremely difficult to reason over. Instead, our self-taught learning algorithm discovers statistical correlations from unrelated unlabeled data, and thus learns a "dictionary" of 200 basis vectors (say) that, when superposed only a few at a time, suffice to adequately describe most input audio signals. Given a 500ms speech signal, the algorithm might be able to represent the signal using just 10 (say) of these learnt basis functions. Informally, the algorithm is able to describe the 8000 numbers succinctly using only 10 numbers corresponding to the activated basis vectors, leading to a succinct representation that is significantly easier to reason with. (See Figure 1a.)

In the example of speech, we can informally think of the audio speech signal as being generated by a small number of distinct acoustic events, such as vibrations of the vocal cords. These underlying acoustic events might provide a concise and relatively noiseless representation of the signal; they also provide a slightly higher-level representation that might be easier to reason with than the raw acoustic signal. This is analogous to the image representation example considered in the previous chapter—visual signals (images) can be encoded efficiently as a combination of only

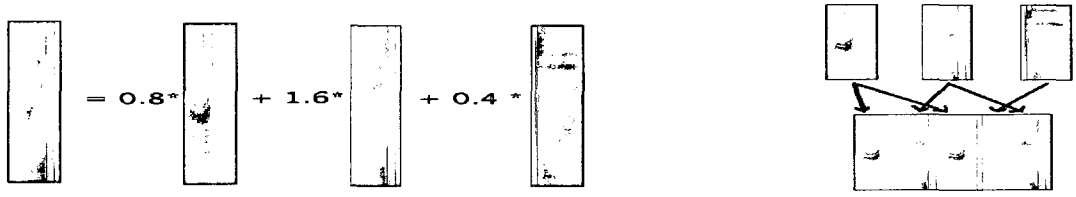

Figure 3.1: Illustration of our sparse coding algorithm for audio (spectrogram) data. Left: Regular sparse coding applied to the spectrogram of an input signal. The input is represented approximately as a linear combination of a small number of basis functions (spectrograms). Right: Shift-invariant sparse coding allows the input (bottom) to be represented by reusing the same basis functions (top) at different time offsets in the signal. Each arrow represents a nonzero coefficient corresponding to a basis and a time offset.

a few oriented edges (or Gabor filters). (Atick, 1992; Olshausen & Field, 1996a)

However, when sparse coding is applied to audio signals, there is a significant technical problem: sparse coding is required to learn the occurrence of each acoustic pattern *at each time offset* as a wholly different basis vector. This is clearly undesirable—in the example of speech data, we want a basis vector to be capable of representing a particular phone (or acoustic event) at *any* time in the signal. Shift-invariant sparse coding (SISC) is an extension of sparse coding that allows each basis function to be replicated at each time offset within the signal (Figure 3.1b). (Lewicki & Sejnowski, 1999; Smith & Lewicki, 2005) However, current algorithms for SISC rely on heuristic solutions, and finding exact solutions has been intractable. (Lewicki & Sejnowski, 1999; Smith & Lewicki, 2005; Blumensath & Davies, 2006) In neuroscience, such heuristically-computed variants of SISC have been used to model the responses of cells in the cochlea (ear) and auditory nerve (Smith & Lewicki, 2005); for music, they have also been used to separate musical instruments in an audio recording. (Blumensath & Davies, 2006) We present an efficient algorithm for computing SISC solutions, and apply it to self-taught learning.

3.1 Shift-invariant Sparse Coding

Recall the sparse coding model used in the previous chapter: given unlabeled examples $\{x_u^{(1)}, x_u^{(2)}, \ldots, x_u^{(k)}\}$ where $x_u^{(i)} \in \mathbb{R}^n$, the sparse coding model finds basis vectors $\{b_1, b_2, \ldots, b_s\}$ where $b_j \in \mathbb{R}^n$, and activations $a_j^{(i)}$ by solving the following optimization problem:

$$\text{minimize}_{b,a} \quad \sum_i \|x_u^{(i)} - \sum_j a_j^{(i)} b_j\|^2 + \beta \sum_i \|a^{(i)}\|_1 \tag{3.1}$$

$$\text{s.t.} \qquad \|b_j\| \leq 1, \quad \forall j \in 1, ..., s \tag{3.2}$$

In shift-invariant sparse coding (SISC), each basis basis vector is allowed to appear at all possible shifts within the signal. (Lewicki & Sejnowski, 1999; Smith & Lewicki, 2005) Given inputs $x_u^{(i)} \in \mathbb{R}^n$, SISC finds basis vectors $\{b_1, b_2, \ldots, b_s\}$ where $b_j \in \mathbb{R}^q$—the basis vectors b_j can be of lower dimension than the input signal itself ($q \leq n$) to allow a basis vector to represent only part of the input vector. To represent the activation of basis vector b_j for input $x_u^{(i)}$ at each time offset, we now need a vector of activations $a_j^{(i)} \in \mathbb{R}^{n-q+1}$, such that the t-th element in this vector $a_j^{(i)}$ represents the activation of basis vector b_j in the input $x_u^{(i)}$ at time offset t. Note that sparse coding as discussed in the previous chapter corresponds to the special case where $n = q$, and the activation $a_j^{(i)} \in \mathbb{R}$ is just a single real number. In our earlier example, if each input $x_u^{(i)} \in \mathbb{R}^{8000}$ is a 500ms-long speech signal, we might choose to avoid redundancy by using 100ms-long basis vectors, in which case $b_j \in \mathbb{R}^{1600}$. Further, the activation corresponding to the input $x_u^{(i)}$ and basis b_j is now a vector $a_j^{(i)} \in \mathbb{R}^{8000-1600+1}$, representing the activation for each possible temporal starting offset for the basis $a^{(j)}$. We will use the notation $a_{j,\tau}^{(i)}$ to represent the coefficient corresponding to the input $x_u^{(i)}$, basis $a^{(j)}$ and temporal offset t.

For shift-invariant sparse coding, we can use the convolution operator $*$ to concisely represent our approximation of the input $x_u^{(i)}$ as a superposition of basis functions: $x_u^{(i)} \approx \sum_j b_j * a_j^{(i)}$.[1]

[1] If $h = f * g$ is the 1-D discrete convolution of two vectors $f \in \mathbb{R}^p$ and $g \in \mathbb{R}^q$, then $h_t = \sum_{\tau=\max(1,t-q+1)}^{\min(p,t)} f_\tau g_{t-\tau+1}$. The dimension of the vector h is given by $\dim(h) = \dim(f) + \dim(g) - 1$. For ease of exposition, we present our SISC model and algorithms only for audio or other sequential

To use ideas recently developed for solving the sparse coding model, we pose the SISC problem as the natural extension to the sparse coding optimization problem (3.1-3.2):

$$\text{minimize}_{b,a} \quad \sum_i \|x_u^{(i)} - \sum_j b_j * a_j^{(i)}\|^2 + \beta \sum_{i,j} \|a_j^{(i)}\|_1 \tag{3.3}$$

$$\text{s.t.} \qquad \|b_j\| \leq 1, \quad \forall j \in 1, ..., s \tag{3.4}$$

Note that by explicitly representing the basis vector at each time offset as a separate basis vector variable, and expanding out the convolution in terms of these new variables, we can, in principle, formulate the above optimization problem as a very large sparse coding problem similar to problem (3.1-3.2)—with the additional constraint that the basis vector variables corresponding to different shifts contain tied parameters. However, such a reformulation would lead to an optimization problem with many more optimization variables—to model 6400 different time offsets (as in the above example), we need 6400 times as many basis vectors. This ignores the special structure in the problem (3.3-3.4), and is computationally infeasible to solve for even moderate problem sizes. Previous solutions to similar SISC optimization problems have thus been based on heuristics. (Lewicki & Sejnowski, 1999; Smith & Lewicki, 2005; Blumensath & Davies, 2006) Instead, we use techniques from our sparse coding algorithms to efficiently solve the SISC problem.

3.2 Efficient SISC Algorithm

We solve the optimization problem (3.3-3.4) by alternately solving two large convex optimization problems: minimizing over the activations $a_j^{(i)}$ given a fixed basis set, and minimizing over the basis vectors b_j given the activations. We now describe efficient algorithms for each of these problems.

(1-D) signals. However, the model and algorithm can also be straightforwardly extended to other input signals with spatial and/or temporal extent (such as images or videos), by using higher-order convolution operators.

3.2.1 Solving for activations

Given a fixed set of basis vectors b, the optimization problem (3.3–3.4) over activations a decomposes over $i = 1, \ldots, k$ into a set of k independent optimization problems. In other words, the activations $\{a_j^{(i)},\ j = 1, \ldots, s\}$ corresponding to an input $x^{(i)}$ can be found independently of the activations corresponding to other inputs. Thus, we will focus on the problem of finding the activations a corresponding to a single input $x^{(i)} \in \mathbb{R}^n$:

$$\text{minimize}_a \quad \|x^{(i)} - \textstyle\sum_j b_j * a_j\|^2 + \beta \sum_j \|a_j\|_1 \tag{3.5}$$

Here, $a_j \in \mathbb{R}^{n-q+1}$ represents the activations associated with basis b_j. Optimizing (3.5) with respect to a is difficult because there are many optimization variables, and they are highly coupled. (For instance, recall that the activation $a_{j,\tau}^{(i)}$ for a basis vector at one time instant and the activation $a_{j,\tau+1}^{(i)}$ for the same basis vector at the next instant are two distinct variables. A basis vector typically correlates quite highly with the same basis vector shifted by one timestep, and this makes it hard to determine which of the two activations better "explains" the input signal $x^{(i)}$.) Previous work (Smith & Lewicki, 2005; Blumensath & Davies, 2006) computed activations using gradient descent on the objective function (3.5). Gradient descent does not typically work well with problems whose variables are tightly coupled. Most existing implementations, therefore, use a heuristic to select a subset of the activations to optimize, and set the other activations to zero. As we demonstrate in the experiments section, the tight coupling between activations makes it difficult to heuristically select a small subset of variables to optimize, and as a result, such heuristic techniques typically lead to suboptimal solutions.

Our approach will efficiently find the exact optimum with respect to all the activations by taking advantage of the "feature-sign" trick described briefly in the previous chapter: the L_1-regularized least squares problem (3.5) reduces to an unconstrained quadratic optimization problem over just the nonzero activations, if we are able to correctly guess the signs (positive, zero or negative) of the optimal values of the activations. Such a quadratic optimization problem can then be easily solved in closed

form using standard numerical methods. This feature-sign trick has been formalized in the *feature-sign search* algorithm, which greedily searches the space of nonzero activations and their signs, and provably converges to the optimal solution. (Lee et al., 2007a)

The feature-sign search algorithm can be modified to efficiently compute activations for short signals (i.e., when $x^{(i)}$ is low-dimensional), as shown in Algorithm 2.[2] For example, if fewer than 1000 activations are nonzero over the course of the optimization for problem (3.5) (and at its optimal solution), then each of the quadratic optimization problems solved in the inner loop of feature-sign search will also involve at most 1000 variables, so that they can be solved efficiently. However, we are often interested in solving for the activations corresponding to fairly long signals (such as if $x^{(i)}$ is a 1 minute long speech signal). Empirically, the number of nonzero activations in the optimal solution grows roughly linearly with the length of the signal (i.e., the dimensionality of $x^{(i)}$). Since solving each least squares problem takes about $O(Z^3)$ time for Z nonzero activations, the standard feature-sign search algorithm becomes expensive for long signals.

To address this problem, we use an iterative sliding window approach as shown in Algorithm 3 to solve a series of smaller problems using the feature-sign search algorithm. These smaller problems are generated by attempting to solve for only $2q$ activations at one time, while keeping the other activations fixed, and iterating till convergence. In solving for these activations using feature-sign search, we can also set the signs of the activations to enable the feature-sign trick: activations which were nonzero keep their sign, all other activations that are in the current window W are assigned a sign opposite to the sign of their partial derivative (so that if an activation has a negative partial derivative of the quadratic term, it is assigned a positive sign for feature-sign search), and any other activations are set to zero. Since the objective function in problem (3.5) is convex, this method is guaranteed to

[2]Other details: Feature-sign search activates activations one at a time, because this is necessary for guaranteeing a descent direction. In our implementation, for each iteration, we simultaneously activate the $T = 300$ zero activations with the largest partial derivatives. This is not guaranteed to give a descent direction, but in the (extremely rare) case where it does not, we simply revert to choosing a single activation for that particular iteration. This preserves the theoretical convergence guarantee of feature-sign search.

Algorithm 2 FS-EXACT

input Input $x^{(i)} \in \mathbb{R}^n$, basis vectors $b_1, b_2, \ldots, b_s \in \mathbb{R}^q$, step size parameter T.
output Optimal activations $a_j \in \mathbb{R}^{n-q+1}$ for problem (3.5).
algorithm
Initialize $a_j := 0$, or to value from previous iteration.
while true **do**
$S := \{a_{j,\tau}^{(i)} | a_{j,\tau}^{(i)} \neq 0\}$
$S := S \cup \{$up to T activations not in S with the largest (magnitude) partial derivatives of the quadratic term $\|x^{(i)} - \sum_j b_j * a_j^{(i)}\|^2\}$.
Solve (3.5) exactly for the activations in S using FS-EXACT, assuming all activations not in S are set to zero.
Break if the partial derivatives of the quadratic term w.r.t. all the activations are smaller than β.
end while
return the optimal activations $a_j^{(i)}$.

Algorithm 3 FS-WINDOW

input Input $x^{(i)} \in \mathbb{R}^n$, basis vectors $b_1, b_2, \ldots, b_s \in \mathbb{R}^q$. (Assume for simplicity that $n - q + 1$ is divisible by q.) Algorithm parameters: N_{passes}, $N_{windows}$.
output Estimated activations $a_j^{(i)} \in \mathbb{R}^{n-q+1}$ for problem (3.5).
algorithm
Initialize $a_j^{(i)}$ arbitrarily, or to value from previous iteration.
$numwindows := (n - 2q + 1)/q$.
for $pass = 1$ to N_{passes} **do**
for $w = 1$ to $N_{windows}$ **do**
$W := \{a_j^{(i)} | q(w-1) + 1 \leq i \leq q(w+1)\}$
Solve problem (3.5) exactly for the activations in W using feature-sign search, keeping all activations not in W fixed.
end for
end for
return the estimated activations $a_j^{(i)}$.

converge to the optimal solution. We will refer to plain feature-sign search (without the sliding window) as FS-EXACT and feature-sign search with sliding window as FS-WINDOW.

Importantly, even though in the worst case the sliding window approach would only be expected to converge linearly, and require a large number of passes through the signal to estimate the optimal activations, in all of our experiments (images, speech, and music), the value obtained for the optimization objective after only two passes through the signal was only a tiny fraction of a percent worse than the optimal value. This is because the activation values that correspond to very different time offsets (for example, if the offsets are further than q time offsets apart), are generally not very tightly coupled, and can thus be optimized sequentially rather than jointly. With a small, fixed number of passes through the signal, the observed performance for optimizing over a single window still depends on the number of nonzero activations Z_w in that window as $O(Z_w^3)$, but does not grow as $O(Z^3)$ if Z is the number of nonzero activations in the full signal. Empirically, FS-WINDOW is much faster than FS-EXACT with very little loss in accuracy.

3.2.2 Solving for basis vectors

Lee et al. (2006) presented an efficient method to optimize the sparse coding optimization problem (3.1-3.2) with respect to the basis vectors b_j for fixed activations:

$$\text{minimize}_b \quad \sum_i \|x_u^{(i)} - \sum_j a_j^{(i)} b_j\|^2 \tag{3.6}$$

$$\text{s.t.} \quad \|b_j\| \leq 1, \quad \forall j \in 1, ..., s \tag{3.7}$$

Their algorithm used the insight that the quadratic objective function can be written as a sum of s quadratic terms, each penalizing the reconstruction error for one element of $x_u^{(i)}$, and depending only on a subset of all the basis vector elements $\{b_{1,t}, b_{2,t}, , \ldots, b_{s,t}\}$ for some fixed element number t ($1 \leq t \leq q$), where $b_{j,t}$ denotes the t-th element of basis vector b_j. This therefore decomposes the optimization problem (3.6-3.7) into many smaller, nearly-independent problems (that are coupled only through the normalization constraint in Equation 3.7). By transforming the problem

into the equivalent, dual optimization problem, it could then be solved very efficiently.

Unfortunately, the same is not true for SISC. Solving the SISC optimization problem (3.3-3.4) for the basis vectors b keeping the activations a fixed reduces to a constrained quadratic optimization problem:

$$\text{minimize}_b \quad \textstyle\sum_i \|x_u^{(i)} - \sum_j b_j * a_j^{(i)}\|^2 \tag{3.8}$$

$$\text{s.t.} \quad \|b_j\| \leq 1, \quad \forall j \in 1, ..., s \tag{3.9}$$

In this problem, because each basis vector can appear in any possible shift (temporal offset), each component of the basis vector contributes to reconstructing many different elements of an input $x_u^{(i)}$, and thus contributes to many different terms in the objective function. Therefore, unlike sparse coding, the different components of the basis vectors are more tightly coupled in the objective. However, as we now demonstrate, this problem is much easier to solve when transformed into the frequency domain.

For a basis vector $b_j = (b_{j,1}, b_{j,2}, \ldots, b_{j,q})$, let the discrete Fourier transform (DFT) be denoted by $\hat{b}_j = (\hat{b}_{j,1}, \hat{b}_{j,2}, \ldots, \hat{b}_{j,q})$, where each element $\hat{b}_{j,\tau}$ is a complex number, representing the frequency component τ.[3] We will use the following two facts from signal processing theory to simplify optimization problem (3.8-3.9): (i) Parseval's theorem (Oppenheim et al., 1996) implies that the DFT $\hat{b}_j$ of a vector b_j scales the L_2 norm by a constant factor; in other words, $\|\hat{b}_j\| = K\|b_j\|$, where K is a known constant.[4] Since our objective and constraints both consist of L_2 terms, we can apply the DFT to them to obtain an equivalent optimization problem over $\hat{b}_j$ instead of b_j. (ii) The Fourier transform of a convolution is the elementwise product of the Fourier transforms. Using (i) and (ii), and denoting the elementwise product of vectors f and

[3]Following standard practice, we apply the DFT after padding the basis vector b_j with zeros so as to make it the same length n as the inputs x. In this case, the DFT is also of length n. Due to space constraints, we refer the reader to standard texts such as Oppenheim et al. (Oppenheim et al., 1996) for further details on Fourier transforms.

[4]Note that the DFT may contain complex numbers. We use $\mathbb{C}$ to denote the set of complex numbers, and y^* to denote the conjugate transpose of a complex vector $y \in \mathbb{C}^n$. The L_2 norm of a complex vector $\hat{y} \in \mathbb{C}^n$ is defined as $\|\hat{y}\| = \sqrt{\hat{y}^*\hat{y}}$.

g by $f \cdot g$, the optimization problem becomes:

$$\begin{aligned} \text{minimize}_{\hat{b}} \quad & \textstyle\sum_i \|\hat{x}_u^{(i)} - \sum_j \hat{b}_j \cdot \hat{a}_j^{(i)}\|^2 \\ \text{s.t.} \quad & \|\hat{b_j}\| \leq \hat{c} = K, \quad \forall j \in 1, ..., s \end{aligned}$$

where the optimization is now over the vector of complex variables $\hat{b}_j \in \mathbb{C}^n$, and $\hat{x}_u^{(i)} \in \mathbb{C}^n$ and $\hat{a}_j^{(i)} \in \mathbb{C}^n$ represent the complex-valued DFT for the input $x_u^{(i)}$ and (padded) activations $a_j^{(i)}$ respectively. Now, for this problem, the variables are no longer tightly coupled, and the Lagrangian can be decomposed as a sum of quadratic terms, each depending on a single frequency component τ:

$$\mathcal{L}(\hat{b}, \lambda) = \sum_\tau \left(\|\hat{x}_\tau - \hat{A}_\tau \hat{v}_\tau\|^2 + \hat{v}_\tau^* \Lambda \hat{v}_\tau \right) - \hat{c} \sum_j \lambda_j,$$

with dual variables $\lambda \in \mathbb{R}^s$ and

$$\hat{x}_\tau = \begin{pmatrix} \hat{x}_{u,\tau}^{(1)} \\ \vdots \\ \hat{x}_{u,\tau}^{(k)} \end{pmatrix} \in \mathbb{C}^k, \quad \hat{v}_\tau = \begin{pmatrix} \hat{b}_{1,\tau} \\ \vdots \\ \hat{b}_{s,\tau} \end{pmatrix} \in \mathbb{C}^s, \quad \Lambda = \text{diag}(\lambda) \in \mathbb{R}^{s \times s},$$

$$\hat{A}_\tau = \begin{pmatrix} \hat{a}_{1,\tau}^{(1)} & \hat{a}_{2,\tau}^{(1)} & \cdots \\ \hat{a}_{1,\tau}^{(2)} & \hat{a}_{2,\tau}^{(2)} & \cdots \\ \vdots & \vdots & \ddots \end{pmatrix} \in \mathbb{C}^{k \times s}$$

The Lagrangian $\mathcal{L}(\hat{b}, \lambda)$ is a function of complex variables $\hat{b}$, but can be expressed as a function of only real variables by representing the real and imaginary parts of $\hat{b}$ as separate real-valued variables. Further, since $|y|^2 = |\text{Re}(y)|^2 + |\text{Im}(y)|^2$ for a complex number y, we can analytically compute $\hat{b}^{\min} = \arg\min_{\hat{b}} \mathcal{L}(\hat{b}, \lambda)$ by optimizing over $\text{Re}(\hat{a})$ and $\text{Im}(\hat{a})$ to obtain:[5]

$$\hat{a}_\tau^{\min} = \left(\hat{A}_\tau^* \hat{A}_\tau + \Lambda \right)^{-1} \hat{A}_\tau^* \hat{x}_\tau \tag{3.10}$$

[5]This can be proved by closely following the derivation for the Lagrangian with real-valued variables, as demonstrated by Lee et al. for the sparse coding algorithm (Lee et al., 2007a).

Substituting this expression for $\hat{a}$ into the Lagrangian, we analytically derive the dual optimization problem $\max_\lambda D(\lambda)$, where $D(\lambda) = \sum_\tau \left(\|\hat{x}_\tau\|^2 - \hat{x}_\tau^* \hat{A}_\tau M_\tau^{-1} \hat{A}_\tau^* \hat{x}_\tau \right) - \hat{c} \sum_j \lambda_j$ and $M_\tau = \hat{A}_\tau^* \hat{A}_\tau + \Lambda$. The dual problem is an unconstrained optimization problem, and can be solved efficiently using Newton's method, with update rules computed using the following gradient and Hessian:

$$\begin{aligned} \frac{\partial D(\lambda)}{\partial \lambda_i} &= \sum_\tau \|e_i^T M_\tau^{-1} \hat{A}_\tau^* \hat{x}_\tau\|_2^2 - \hat{c} \\ \nabla_\lambda^2 D(\lambda) &= -2 \sum_\tau \left(M_\tau^{-1} \hat{A}_\tau^* \hat{x}_\tau \hat{x}_\tau^* \hat{A}_\tau M_\tau^{-1} \right) \cdot \bar{M}_\tau^{*-1}, \end{aligned}$$

where e_i is the i^{th} unit vector, $\cdot$ represents the elementwise product and $\bar{Y}$ represents the elementwise complex conjugate for a complex-valued matrix Y. Once the optimal dual variables λ are computed, the optimal basis vectors can be recovered using Equation (3.10).

Efficient implementation

The update rules derived above rely on the matrices $\hat{A}_\tau$, which contain a given frequency component of the Fourier transform of the activation vectors $a_j^{(i)}$ for all k inputs and all s basis vectors. It would seem straightforward to precompute the Fourier transform of every activation vector and construct each $\hat{A}_\tau$ from its corresponding entries. Unfortunately, while the time domain activations $a_j^{(i)}$ are sparse (i.e., many of the $a_{j,\tau}^{(i)}$ values are zero), their Fourier representations are not. Therefore, the Fourier representations would require $O(ks)$ storage for each frequency component, and these representations cannot all be stored in memory at once for large problems. On the other hand, it is inefficient to compute each component of $\hat{A}_\tau$ directly from the definition of the Fourier integral each time it is used. Thus, the two most straightforward implementations of the above algorithm do not scale to large problems.

To address this, we note that the Newton updates can be computed efficiently if we have precomputed the matrices $\hat{A}_\tau^* \hat{A}_\tau$ and $\hat{A}_\tau^* \hat{x}_\tau$. These matrices are small enough to fit in memory, with $O(s^2)$ and $O(s)$ nonzero entries respectively for each frequency component. Importantly, unlike the $O(ks)$ space required for storing the Fourier

transforms of all activation vectors, these figures do not depend on the number of input signals k. Two further optimizations were used for our largest scale experiments: (i) Because the discrete Fourier transform of a real signal is conjugate symmetric, $\hat{A}_\tau^* \hat{A}_\tau$ and $\hat{A}_\tau^* \hat{x}_\tau$ need to be explicitly computed and cached only for half of the frequencies τ. (ii) Since $\hat{A}_\tau^* \hat{A}_\tau$ is Hermitian, it suffices to cache only the entries in the lower-triangular part.

3.3 Constructing features using unlabeled data

We now describe an application of SISC to self-taught learning, where the goal is to use unlabeled data to improve performance on a classification task. Here, the unlabeled data may not share the classification task's labels.

In self-taught learning, we are given a labeled training set $\{(x_l^{(1)}, y_l^{(1)}), \ldots, (x_l^{(m)}, y_l^{(m)}\}$ together with k unlabeled examples $\{x^{(1)}, \ldots, x^{(k)}\}$. In the previous chapter, we proposed the following algorithm for self-taught learning: sparse coding is applied to the unlabeled data $x^{(i)}$ to learn the basis vectors b_j, by solving the optimization problem (3.1-3.2). These learnt basis vectors are then used to construct features for each input $x_l^{(i)}$ to the classification task by computing:

$$\hat{a}(x_l^{(i)}) = \arg\min_a \|x_l^{(i)} - \sum_j b_j a_j\|^2 + \beta \|a\|_1$$

These features $\hat{a}(x_l^{(i)})$ can then be used as input to off-the-shelf classification algorithms such as an SVM or Gaussian discriminant analysis (GDA), and this often produces better generalization performance than using the raw inputs $x_l^{(i)}$ themselves. (Raina et al., 2006; Raina et al., 2007)

However, the above approach is computationally infeasible and conceptually unsatisfactory when applied to representing "large" inputs with spatial and temporal extent, such as images or audio. As a heuristic solution, in the previous chapter, sparse coding was applied to small parts (or "patches") of the input images or audio signals, and then the activations produced for these individual parts were aggregated

(e.g., by taking the sum of squares of all activations corresponding to a basis) to produce a representation for the entire image or audio signal. Further, the learnt feature representation $\hat{a}(x_l^{(i)})$ is not invariant to shifts of the input signal, and different basis vectors might capture the same pattern occurring at different shifts.

To address these problems, we propose the following algorithm for self-taught learning using SISC: We first apply SISC to the unlabeled data $x_u^{(i)}$ to learn shift-invariant basis vectors b_j. The learnt basis vectors are then used to construct features for the labeled inputs $x_l^{(i)}$ by solving the SISC optimization problem:

$$\tilde{a}^{(i)} = \arg\min_a \|x_l^{(i)} - \sum_j b_j * a_j\|^2 + \beta \|a\|_1. \tag{3.11}$$

Here, we will write $\tilde{a}_{j,t}^{(i)} \in \mathbb{R}$ to represent the activation found for basis b_j at time t, and $\tilde{a}_{\cdot,t}^{(i)} = [\tilde{a}_{1,t}^{(i)}, \tilde{a}_{2,t}^{(i)}, \ldots, \tilde{a}_{s,t}^{(i)}]^T \in \mathbb{R}^s$ to represent the vector of all activations (one activation value per basis vector $b_1, \ldots, b_s$) at time t. As in sparse coding, we expect the SISC features $\tilde{a}^{(i)}$ to capture higher-level patterns than the raw input $x_l^{(i)}$. These features are also robust to shifts and translations of the inputs in the following sense: if the input signal is shifted by a certain amount in time, the features are also shifted by the same amount, *without* any change in their relative values. Using these features $\tilde{a}^{(i)}$ to represent the data, we will apply standard, off-the-shelf classification algorithms (SVM and GDA) to learn a classifier.

We delve deeper into the application of the GDA learning algorithm to SISC features. GDA posits that the conditional distribution of the features given the class label is Gaussian. By assuming that the features $\tilde{a}_{\cdot,t}^{(i)}$ at time t are conditionally independent of the features $\tilde{a}_{\cdot,t'}^{(i)}$ at some other time t' given the label $y_l^{(i)}$, we get:

$$P(\tilde{a}^{(i)}|y_l^{(i)} = y) = \prod_t P(\tilde{a}_{\cdot,t}^{(i)}|y_l^{(i)} = y) \tag{3.12}$$

where $P(\tilde{a}_{\cdot,t}^{(i)}|y)$ is modeled as a multivariate Gaussian (whose parameters $\mu_y \in \mathbb{R}^s, \Sigma_y \in \mathbb{R}^{s \times s}$ depend on y): $\tilde{a}_{\cdot,t}^{(i)} \sim \mathcal{N}(\mu_{y^{(i)}}, \Sigma_{y^{(i)}})$. The GDA parameters μ_y and Σ_y, and the label priors $P(y)$, are learnt using maximum likelihood on the labeled training data, and test examples x are then classified by picking the label $y^* = \arg\max_y P(y|\tilde{a}) ==$

$\arg\max_y P(\tilde{a}|y)P(y)$, where $\tilde{a}$ are the SISC features for input x.

In our experiments, we found that the SISC features $\tilde{a}^{(i)}$ are poorly modeled by a multivariate Gaussian generative distribution as used in GDA—a large number of features are zero and the nonzero feature distributions have long tails.[6] The nonzero features empirically appear to follow an exponential distribution. We thus propose an additional classification algorithm for SISC features, based on the following two-step generative model for the features $\tilde{a}^{(i)}$: each feature's sign (positive, negative, or zero) is determined, and if its sign is nonzero, its value is then determined according to an exponential distribution. Concretely, given y, for each $\tilde{a}^{(i)}_{j,t}$, we imagine that first a random variable $Z^{(i)}_{j,t} \in \{+, 0, -\}$ is drawn from a 3-way multinomial distribution governed by parameter $\phi^y_j \in \mathbb{R}^3$. $Z^{(i)}_{j,t}$ will determine the sign of $\tilde{a}^{(i)}_{j,t}$. Then, if $Z^{(i)}_{j,t} =$ "+", we generate $\tilde{a}^{(i)}_{j,t} \sim \text{Exponential}(\rho^{y,+}_j)$; if $Z^{(i)}_{j,t} =$ "0", we set $\tilde{a}^{(i)}_{j,t} = 0$; and lastly if $Z^{(i)}_{j,t} =$ "−", we generate $-\tilde{a}^{(i)}_{j,t} \sim \text{Exponential}(\rho^{y,-}_j)$. Here, ϕ^y_j, $\rho^{y,+}_j$ and $\rho^{y,-}_j$ are the parameters of the model, and define a naive Bayes like generative model: $P(\tilde{a}^{(i)}|y) = \prod_t \prod_j P(\tilde{a}^{(i)}_{j,t}|y)$. The maximum likelihood parameters for the generative model are straightforward to obtain,[7] and are then used to compute label probabilities $P(y|\tilde{a}^{(i)})$ using Bayes' rule. We call this model "Exp," and present results on all domains using the SVM, GDA and Exp classification algorithms.

Self-taught Learning Details

We apply the above self-taught learning algorithm to audio classification tasks. Rather than use entire speech sentences or songs for the input vectors $x^{(i)}_u$, we found it was much more efficient to divide the signals into medium-sized excerpts of 500 ms, which would be treated as independent. This way, given a fixed set of basis vectors, the optimal activations could be computed efficiently for each excerpt. To reduce edge effects, each segment was multiplied by a window function which decays smoothly to

[6] Some of the baseline features presented in the Experiments section, such as MFCCs, are most often modeled with a Gaussian distribution.

[7] Each multinomial parameter is estimated as a (smoothed) fraction of the occurrences of the feature with negative/zero/positive sign. Each exponential scale parameter ρ is estimated as the absolute value of the (smoothed) average of the feature values with the corresponding negative/positive sign.

zero near the start and end points. For faster convergence, we randomly divided the training data into 2 batches and alternately optimized with respect to each batch.

3.4 Algorithm Efficiency

We begin by evaluating the running-time of our algorithm, described in Section 3.2.1, for solving for the activations given a fixed basis set. To the best of our knowledge, all previous algorithms for large-scale shift-invariant sparse coding have learned the activations using a heuristic to preselect a subset of activations to optimize for (setting all other activations to zero). Smith & Lewicki (2005) used matching pursuit and filter threshold algorithms to select a subset of the activations to optimize for; we will refer to the matching pursuit heuristic as the SL heuristic. Blumensath & Davies (2006) used a heuristic which iteratively chooses the activation with the largest magnitude gradient, and removes its "neighbors" (activations corresponding to the same basis with a slightly different shift) from consideration; we will call this the BD heuristic. In our implementation of each of these heuristics, we used gradient descent with line search to optimize for the selected activations.[8] We will compare these heuristics with our exact activation learning algorithm (FS-EXACT) and gradient descent applied to all the activations without any preselection (GD-FULL).[9]

Figure 3.2(a) shows the convergence rates of these four algorithms when applied to learning SISC activations for a one-second (time-domain) speech signal using 32 basis vectors.[10] The suboptimality of an algorithm achieving objective f_{alg} for problem (3.5) with optimal objective f^* is defined as $(f_{\text{alg}} - f^*)/f^*$. FS-EXACT clearly outperforms

[8]Our gradient descent algorithm for solving $\min_s f(s) + \beta\|s\|_1$ (for a differentiable function f) transforms it to the equivalent problem $\min_{s^+,s^-} f(s^+ - s^-) + \beta 1^T(s^+ + s^-)$ with the constraints $s^+, s^- \geq 0$. The algorithm then performs a line search with exponential backoff along the negative gradient of the new objective function, handling the constraints by projecting all points considered during the line search into the feasible space. The algorithm exits when the cumulative decrease in the objective function over 3 iterations is less than a fixed threshold. This gradient descent algorithm was faster than a gradient descent algorithm using a constant step size.

[9]We do not present running time results for the faster sliding window algorithm FS-WINDOW as the exact algorithm FS-EXACT is usable at the scales for which results have been reported for previous algorithms.

[10]Each speech basis was 188ms long. Similar results were obtained when a straightforward extension of our method was applied to the case of 2-D convolution for images.

the other algorithms. For example, after 8 seconds, FS-EXACT is 10^{-2}-suboptimal, but it takes the best other algorithm 40 seconds to reach this level of suboptimality. Further, even when given sufficient time to run the heuristics to convergence, both the heuristic methods converge to suboptimal solutions, which are significantly poorer than the solutions found by FS-EXACT. This is true even when the heuristic is allowed to choose a substantial fraction of the activations to be nonzero (which slows the heuristic methods further).

We next assess the effectiveness of using the dual problem formulation (in the Fourier domain) for learning the basis vectors. We compare the overall running time of basis learning using four possible algorithms, comprising combinations of two methods for solving for the activations—FS-EXACT and GD-FULL—and two methods for updating the basis vectors—Newton's method with the dual formulation (DUAL) and stochastic gradient descent (GD-BASIS) on the original problem (3.3-3.4). Figure 3.2(b) shows the convergence results for all four algorithms on the SISC image task (similar results are achieved for the speech task). FS-EXACT + DUAL outperforms the other algorithms. For example, it achieves an objective value of 1.74×10^5 within 10 minutes, but the best other algorithm takes over 2 hours.

The overall time for solving the SISC optimization problem is dominated by the time for learning activations. We also note that the two basis vector update methods (DUAL and GD-BASIS) individually take comparable amounts of time per iteration, even though the DUAL method computes the optimal basis vectors for the fixed activations at each iteration, whereas GD-BASIS just updates the basis vectors using a small gradient step at each iteration. This contributes to faster overall convergence of basis learning using DUAL.

3.5 Self-taught Learning Results

We apply our SISC based self-taught learning algorithm to two audio classification tasks: (i) Speaker identification on the TIMIT speech corpus (Garofolo et al., 1993) given a small amount of labeled data (one sentence per speaker), and a large amount of unlabeled data comprising speech from *different speakers from different dialect*

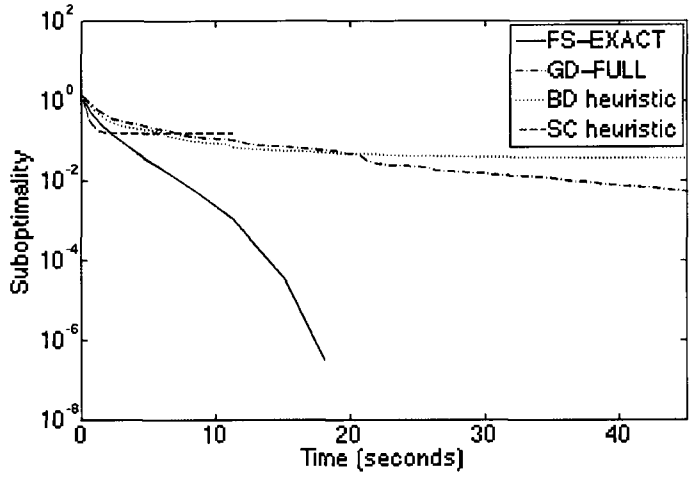

(a)

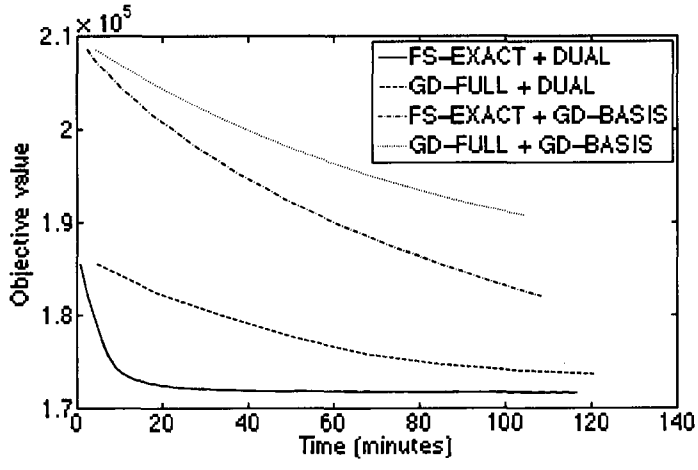

(b)

Figure 3.2: (a) Convergence of activation learning for speech data. The plot shows the "suboptimality" achieved by the algorithms vs. the time taken (seconds). Similar results are obtained for 2-D image data. (b) Convergence of the SISC optimization problem for image data. The plot shows the objective value attained by different combinations of activation learning and basis learning algorithms vs. the time taken (minutes). Since the problem is not jointly convex in the activations and basis vectors jointly, we could not compute a suboptimality relative to the global minimum. (Best viewed in color.)

regions than the ones in the labeled data. (ii) Musical genre classification with a small number of labeled song snippets (6 seconds of music per genre), and a large amount of unlabeled data comprising songs from *different genres* of music than the ones in the labeled data.[11] In both of these classification tasks, the unlabeled data is easy to obtain, and does not share the labels associated with the task. We compute SISC features for both tasks by learning basis vectors on the unlabeled data.[12]

For speaker identification, we compare our SISC features against both spectral and cepstral features—i.e., against the raw spectrogram, and against the MFCC features that are widely used in audio applications. For music classification, we compare against using the raw spectrogram, the MFCC features, and also a set of custom, hand-engineered features designed specifically for this task by Tzanetakis & Cook (Tzanetakis & Cook, 2002).[13]

For each of these features, we apply the SVM, GDA and Exp classification algorithms to learn a classifier on the labeled training set. For an SVM, the input features were aggregated over all time offsets t in the entire input signal, with the aggregation method picked out of several choices using cross-validation on a development set.[14] For the generative algorithms GDA and Exp, each input feature was constructed by averaging the features over overlapping time "windows" of W_T timesteps (where W_T was picked by cross-validation). (Thus, for example, $\tilde{a}^{(i)}_{\cdot,t}$ in Equation 3.12 is now replaced by an average of $\tilde{a}^{(i)}_{\cdot,t}$ over W_T time offsets t.) Each of these windows is assumed to be independently sampled from the generative model distribution. Consequently,

[11]The classification task was based on a genre-labeled music corpus obtained from the Magnatune website (`http://www.magnatune.com`).The unlabeled data was extracted from songs from other genres not represented in the training/test sets.

[12]We picked the sparsity penalty β for basis learning by searching for the smallest value (leading to the most nonzero activations) for which basis vectors could still be learned efficiently (within 1-2 days); the same value of β was used to construct SISC features.

[13]Tzanetakis & Cook also proposed other features based on advanced, highly specialized music concepts, such as automatic rhythm and beat detection. In this paper, we use only their 19 timbral features, since they measure "sound quality" as opposed to longer-time functions of the music signal, such as beats. The other features would still be essential for constructing a truly state-of-the-art system.

[14]The aggregation methods we considered for SISC features $\tilde{a}^{(i)}_{j,t}$ were: count of the average number of times each feature was nonzero; average of square roots of individual features; average of absolute values of individual features; and, average of squares of individual features. The average values refer to an average over the time offset t, and normalize for the total length of the input signal.

at test time, these algorithms output the label that maximizes the product of the generative probability for each feature window. We also augment the Exp algorithm by trading off the multinomial and exponential terms using an additional parameter α, while still learning the other parameters using the usual maximum likelihood estimates.[15] The parameters of the classifiers were picked using cross-validation on a separate development set.[16] This additional aggregation step and reweighting term were also applied to the baseline features in the reported results, with the best aggregation/reweighting picked using cross-validation. All the reported test results are averaged over 2500 random choices of the training and test set.

Table 3.1 shows the test results obtained for musical genre classification with two different training set sizes.[17] The SISC features achieve the highest classification accuracy. We note that MFCCs comprise a carefully engineered feature set that has been specifically designed to capture the discriminative features of audio. In contrast, the SISC features were discovered fully *automatically* using unlabeled data, but still lead to comparable or superior performance.

Speaker identification can be done fairly accurately using standard methods when the audio samples are clean and noiseless (and when the number of speakers is relatively small), since each speaker's unique vocal tract properties often make it easy to distinguish between speakers. (Jurafsky & Martin, 2000) However, the most challenging, and perhaps important, setting for speaker identification is identification even in

[15] Using slightly informal notation, the reweighting results in writing the generative model as $P(\tilde{a}^{(i)}_{j,t}|y;\phi,\rho,\alpha) \propto \left(P(Z^{(i)}_{j,t}|y;\phi)\right)^{\alpha} P(\tilde{a}^{(i)}_{j,t}|y, Z^{(i)}_{j,t};\rho)$, where $Z^{(i)}_{j,t} \in \{+,0,-\}$ corresponds to the sign of $\tilde{a}^{(i)}_{j,t}$. Such a "reweighting" term is often used in speech recognition systems to balance the language model and the acoustic model (Jurafsky & Martin, 2000), and has also been used to reweight probabilistic models in other contexts (Raina et al., 2004).

[16] We tuned all the standard parameters for each algorithm by cross-validation. For SVM, this includes the kernel and regularization parameters; for GDA, the regularization parameters and choice of diagonal or full covariance matrix; for Exp, the smoothing parameters and the reweighting parameter α.

[17] Other details: We applied SISC over the spectrogram representation of the input, with shift-invariance over time only (and not over frequencies). We learnt 128 basis vectors of length 500 ms from 3,000 unlabeled spectrogram excerpts of length 1.5 seconds each. The spectrogram was computed with MATLAB's built-in spectrogram function, with window length 25 ms (400 samples) and 50 percent overlap; we used 300 frequencies evenly spaced from 20 to 6000 Hz. The training and test sets were always drawn from different songs.

Feature Set	GDA	SVM	Exp
SISC	51.0	**56.6**	55.7
TC	49.3	47.0	45.8
MFCC	43.6	54.0	34.2
Raw	44.2	48.4	42.9
SISC	37.9	**41.8**	39.7
TC	38.9	39.2	37.8
MFCC	34.4	**41.7**	37.5
Raw	38.8	38.2	36.3

Table 3.1: Classification accuracy on 5-way musical genre classification with 3 (top half) or 1 (bottom half) training song per genre, and three 2-second excerpts per song. For each half, the results in bold are statistically significantly better than the other results ($p \leq 0.01$).

the presence of substantial amounts of noise (for example, imagine trying to hear a person's voice on the phone over loud background noise). Such a speaker identification system has also been used for the STAIR (STanford AI Robot) robotic platform, as part of the robot's dialog system (see (Krsmanovic et al., 2006) for details); thus, our experiments will emphasize this more interesting, noisy setting.

We evaluated our speaker ID system under a variety of noise conditions. We recorded five kinds of household noises: two electric shavers, a printer, running water, and a fan. These noise types were chosen based on noise conditions encountered by STAIR. (Krsmanovic et al., 2006) Classification was performed with the corpus data (no added noise), and under three additional conditions: first, the same kind of noise was added to all training and test examples (SAME); second, all examples had a type of noise chosen randomly and independently (RAND); third, in the most difficult condition, for each speaker, all training examples contain one kind of noise, and all the test examples contain a different kind of noise (DIFF). For each noise type, we evaluate two intensity levels of noise, as measured by the signal/noise ratio (SNR) for the noise relative to the input signal; higher SVN implies lower added noise.

Noise condition	SISC			MFCC			Raw		
	SVM	GDA	Exp	SVM	GDA	Exp	SVM	GDA	Exp
No added noise	71.2	74.2	70.7	46.0	71.6	62.6	64.9	**78.9**	46.1
SAME, SNR=20	58.6	60.6	58.9	37.7	64.6	53.2	53.5	**66.9**	41.6
SAME, SNR=10	55.3	56.3	53.8	33.5	57.9	48.6	50.7	**61.8**	40.4
RAND, SNR=20	51.8	51.0	**55.6**	34.3	**55.8**	42.1	42.1	51.1	35.2
RAND, SNR=10	42.0	**48.7**	**48.7**	29.2	43.8	31.9	33.1	38.5	27.5
DIFF, SNR=20	44.1	**50.8**	**50.3**	31.0	48.3	33.6	28.7	40.0	28.5
DIFF, SNR=10	32.3	**41.0**	**41.3**	20.3	31.5	19.7	21.7	23.3	27.1

Table 3.2: Classification accuracy on 5-way speaker identification, using 1 training sentence per speaker. The results in bold are statistically significantly better than the other results in the same row ($p \leq 0.01$).

Table 3.2 shows the test results for speaker identification.[18] SISC features outperform the other features under two of the three noise conditions tested.

3.6 Discussion

In this chapter, we presented an efficient algorithm for the SISC optimization problem. Our algorithm solves for the activations by searching over their signs; and solves for the basis vectors by mapping an optimization problem with highly-coupled parameters to a set of much smaller, weakly-coupled problems in the Fourier domain, thus allowing it to be solved efficiently. We also showed that this method performs well in self-taught learning applications to audio classification tasks.

In our experiments, we learned 128 basis vectors for each classification tasks. We expect that learning larger basis sets would allow us to capture more structure in the signals and therefore improve classification accuracy. Currently, the main bottleneck to learning larger basis sets is memory, since efficient basis learning depended heavily on the caching of intermediate results ($\hat{S}_t^* \hat{S}_t$ and $\hat{S}_t^* \hat{x}_t$). To cache these values for

[18]Further details: We learned a set of 128 SISC basis vectors over a log-frequency spectrogram with 128 frequencies evenly spaced on a log-scale from 300 to 8000 Hz. Basis vectors were learned from dialect regions 1 through 4 of the Timit corpus, while regions 5 and 6 were used for development, and regions 7 and 8 for testing. For classification, each training and test instance consisted of a 1.5-second sample from a speaker.

significantly larger numbers of basis vectors or for larger inputs would have required more than the 4GB RAM that was available on the machines used to run these experiments. However, our algorithm can be easily parallelized. With N processors, each processor could compute the respective terms for its own subset of the frequencies, and would therefore only need to store these quantities for the frequencies it is responsible for. This is a promising direction for future investigation.

Chapter 4

Self-taught Learning for Discrete Inputs

In the previous chapters, we have demonstrated that sparse coding algorithms can improve classification accuracy for several self-taught learning problems. These algorithms perform especially well on continuous, real-valued input data, such as images or audio. However, when these algorithms are applied to discrete data (such as text documents), in many cases the resulting classifiers are not significantly better than the classifiers obtained using supervised learning alone. In hindsight, this is not surprising—sparse coding is based on an optimization problem with a quadratic loss function (in which we attempt to minimize the squared error distance between a given input and the model's reconstruction of that input), which does not apply naturally to discrete input data. Sparse coding based on this quadratic loss function can be interpreted as performing maximum-a-posteriori learning in a specific generative probabilistic model for the inputs x; in particular, the model assumes Gaussian noise for the inputs (details in Section 4.1), which is a poor model for discrete-valued data. These sparse coding models were devised to explain low-level human perception of real-valued signals (such as images and audio) (Atick, 1992; Olshausen & Field, 1996a), and do not directly fit symbolic or discrete data (such as text documents). In our view, the restriction to a Gaussian noise model severely limits the applicability of sparse coding in a general self-taught learning algorithm.

As a running example, consider the application of self-taught learning to text classification: suppose we would like to classify sports webpages as "Baseball" or "Football" using only very few labeled webpages and many unlabeled text documents, which may or may not be about Baseball or Football, and can be obtained randomly from the Internet (say). A natural representation of text documents is often as a binary "bag-of-words" vector $x \in \{0,1\}^n$, where the i-th feature is 1 if the i-th word in our vocabulary occurred in the document, or as a word-counts vector $x \in \{0,1,2,\dots\}^n$, where the i-th feature represents the number of times the i-th word occurred in the document. In either case, such input vectors are very poorly modeled by a continuous Gaussian distribution (which could take fractional, or negative values). It is thus hardly surprising that when sparse coding is applied to a self-taught learning task involving text data, it only leads to very small improvements in accuracy.

The above problem is not unique to text classification. Sparse coding with the Gaussian noise distribution assumption may be too restrictive to model the wide variety of inputs that we might encounter in machine learning problems, including point clouds or depth maps, discrete data, etc.

To address this problem, we generalize the Gaussian probabilistic model behind sparse coding in a principled way to include most standard distributions. We draw on the widely studied idea of the "exponential family" of distributions. This class of distributions includes the Gaussian, Bernoulli and Poisson distribution, among others, while still providing guarantees useful for efficient learning and inference. Our generalization is analogous to the way in which generalized linear models (GLMs) generalize least squares regression (which relies on a Gaussian assumption) to other kinds of regression, including logistic regression (for binary inputs) or softmax regression (for multivalued inputs) (McCullagh & Nelder, 1989). We call our model *exponential family sparse coding*, and to differentiate it from the previous model, we call that model "Gaussian sparse coding" throughout this chapter.

Our generalization makes the parameter learning problem significantly harder.

However, we show that the optimization problem can be solved via a series of L_1-regularized least squares problems, each of which can be solved using algorithms similar to the ones used for Gaussian sparse coding. In fact, our optimization procedure can also be applied to other L_1-regularized optimization problems, and is especially efficient for problems that have very sparse optimal solutions.

We apply our model successfully to two self-taught learning problems—text classification and a robotic perception task—even though Gaussian sparse coding produces poor performance for both.

4.1 A probabilistic model for sparse coding

We consider the self-taught learning problem considered in the previous chapters. We are given a small labeled training set a classification problem with a small labeled training set $\{(x_l^{(1)}, y^{(1)}), (x_l^{(2)}, y^{(2)}), \ldots, (x_l^{(m)}, y^{(m)})\}$, and a large set of unlabeled examples $\{x_u^{(1)}, x_u^{(2)}, \ldots, x_u^{(k)}\}$. In previous chapters, we assumed that the input x (labeled or unlabeled) is specified as a real-valued vector $x \in \mathcal{X} = \mathbb{R}^n$, but we no longer place this restriction on the input. For example, text documents can be represented as a binary vector $x \in \mathcal{X} = \{0,1\}^n$ or as an integer-valued vector $x \in \mathcal{X} = \{0,1,2,\ldots\}^n$.

In Gaussian sparse coding, as discussed earlier, we estimate basis vectors from unlabeled data $x_u^{(i)}$ by solving the optimization problem (2.2-2.3). In Chapter 2, we presented probabilistic justification for posing this optimization problem, based on a generative model for inputs x. In that model, we assume that x is generated from a Gaussian distribution with mean $\eta = \sum_j b_j a_j$, and (known) covariance $\sigma^2 I$, and that the activation vector a follows a Laplacian prior $P(a) \propto \prod_j \exp(-\beta'|a_j|)$ for some (known) constant β'. The Laplacian prior encourages sparse activations by giving low prior probability to large nonzero values for the activations. Given unlabeled examples $x_u^{(i)}$, the maximum-a-posteriori estimate of the corresponding activations

$a^{(i)}$ and the basis vectors b_j would be obtained by solving:[1]

$$\max_{b,a} \prod_i P\left(x_u^{(i)} | b, a^{(i)}\right) P\left(a^{(i)}\right) \tag{4.1}$$

By taking logarithms to convert products to sums, and setting $\beta = 2\sigma^2\beta'$, this reduces to exactly the optimization problem (2.2-2.3) used earlier.

4.2 Self-taught Learning for Discrete Inputs

To motivate the algorithms introduced in this paper, consider the application of the Gaussian sparse coding algorithm to binary input vectors $x \in \{0,1\}^n$, say for text classification. The Gaussian sparse coding model makes the probabilistic assumption that $P(x \mid \eta = \sum_j b_j a_j)$ is a Gaussian distribution, which is a poor fit to binary data. Stated otherwise, the Gaussian sparse coding model tries to enforce the decomposition $x \approx \sum_j b_j a_j$, even though the unconstrained sum $\sum_j b_j a_j$ is a particularly poor approximation to a binary vector x. Thus, a straightforward application of Gaussian sparse coding does not lead to very useful basis vectors or features.

Instead, loosely speaking, we might want to find an approximation of the form $x \approx \sigma(\sum_j b_j a_j)$, where $\sigma(v) = [\frac{1}{1+e^{-v_1}}, \frac{1}{1+e^{-v_2}}, \ldots]$ represents the elementwise logistic function for a vector v. This promises to be a better approximation, since the logistic function always lies in the interval $(0,1)$.

We now present a systematic generalization of the Gaussian sparse coding model. Our generalization includes both Gaussian sparse coding and our seemingly arbitrary logistic function approximation as special cases, and will directly suggest models for other input types, such as when the inputs consist of nonnegative integer counts $x \in \{0,1,2,\ldots\}^n$.

[1]Following our sparse coding model, we use the norm constraint $\|b_j\| \leq 1$ on the basis vectors to disallow degenerate solutions in which the activations can be scaled down as long as the basis vectors are scaled up by the same number. We assume a uniform prior on the feasible basis vectors.

4.3 Exponential Family Sparse Coding

The exponential family is a widely used class of distributions in statistics, and in its most general form, is represented as: $P(x|\eta) = h(x)\exp(\eta^T T(x) - \psi(\eta))$. Here, η represents the natural parameter for the model, and the functions h, T and ψ together define a particular member of the family. For example, it is easy to verify that the multivariate Gaussian distribution $\mathcal{N}(\mu, I)$ with fixed covariance I and (unknown) mean parameter $\mu \in \mathbb{R}^n$ is equivalent to the exponential family distribution defined by $h(x) = e^{-\|x\|^2/2}/(2\pi)^{n/2}$, $T(x) = x$ and $\psi(\eta) = \eta^T\eta/2$ (with natural parameter $\eta = \mu$). The exponential family of distributions is broad enough to include most standard distributions (Gaussian, Bernoulli, Poisson, exponential, and others), but also restrictive enough to provide useful guarantees. Importantly, it guarantees that the log-likelihood is concave in the natural parameter η, making maximum likelihood learning of parameters tractable (McCullagh & Nelder, 1989).

To apply sparse coding to discrete inputs, we modify the Gaussian sparse coding model to allow any distribution from the exponential family:

$$P(x|b,a) = h(x)\exp(\eta^T T(x) - \psi(\eta)), \quad \eta = \sum_j b_j a_j \tag{4.2}$$

where we use the basis vectors b_j and the activations a_j to construct the natural parameter η for the family.[2] Our new generative model includes the earlier Gaussian generative model for $P(x|b,a)$ as a special case, since the Gaussian model can be obtained by a specific choice of the functions $h(x)$, $T(x)$ and $\psi(\eta)$. In fact, our model extends Gaussian sparse coding in the same way that generalized linear models (GLMs) extend the notion of regression with least squares loss to other loss functions, including logistic regression and softmax regression as special cases.

Given unlabeled examples $\{x_u^{(1)}, x_u^{(2)}, \ldots, x_u^{(k)}\}$, we can apply Equation (4.1) to

[2]Note that the input x does not need to have a vector representation, and can be in a more general input space $x \in \mathcal{X}$. We assume that $T(x) \in \mathbb{R}^n$, and thus that $b_j \in \mathbb{R}^n$.

compute the maximum-a-posteriori estimates of the basis vectors b_j and the activations $a^{(i)}$:[3]

$$\text{minimize}_{B,a} \quad \sum_i -\log h(x^{(i)}) - a^{(i)T} B^T T(x^{(i)}) + \psi(Ba^{(i)}) + \beta \sum_i \|a^{(i)}\|_1 \quad (4.3)$$

$$\text{s.t.} \quad \|b_j\| \leq 1, \quad \forall j \in 1, ..., s \quad (4.4)$$

where we define the basis matrix B such that its j-th column is the basis vector b_j, implying that $\eta = \sum_j b_j a_j = Ba$. We call this the "exponential family sparse coding" problem. As for Gaussian sparse coding, the value of β controls the number of nonzero activations at the optimal solution (Tibshirani, 1996b); by definition, we want the model to produce sparse activations, and we will set β large enough to produce only a small number of nonzero values per activation vector $a^{(i)}$ on average.

Since the exponential family guarantees convexity of $\log P(x|\eta)$ with respect to η, we can show that the above optimization problem is convex with respect to a for fixed B, and with respect to B for fixed a (though it is not jointly convex). This again suggests an alternating minimization procedure iterating the following two steps till convergence, starting at random initial values for a and B: (i) fix basis matrix B, and compute the optimal activations a; and, (ii) fix the activations a, and compute the optimal basis matrix B.

Step (ii) involves a constrained optimization problem over B with a differentiable objective function. We can thus apply projective gradient descent updates, where at each iteration we perform a line search along the direction of the (negative) gradient, projecting onto the feasible set before evaluating the objective function during the line search. In our case, the projection operation is especially simple: we just need to rescale each basis vector to have norm 1 if its norm is greater than 1. In our experiments, we find that such a projective gradient descent scheme is sufficiently fast for basis learning.[4] We thus focus now on the algorithm for computing the optimal activations in Step (i).

[3] As in Gaussian sparse coding, we assume a Laplacian prior on a: $P(a) \propto \prod_j \exp(-\beta|a_j|)$, and a uniform prior on b_j.

[4] We note that it is also possible to solve for B by solving the dual optimization problem (similar to the derivation for Gaussian sparse coding).

Step (i) computes the optimal activation a given fixed basis vectors. The resulting problem involves a non-differentiable L_1-regularized objective function, to which straightforward gradient descent methods are not applicable. This problem appears somewhat more complex than the L_1-regularized problem obtained for Gaussian sparse coding, because in that case, the only other term in the objective function was quadratic in a, and that allowed very efficient specialized solutions (e.g., given the sign of each activation a_j, we can compute the optimal activations for Gaussian sparse coding in closed form; but this is not true in general for exponential family sparse coding). Recently, many sophisticated algorithms have been developed for general L_1-regularized optimization, including specialized interior point methods (Koh et al., 2007), quasi-Newton methods (Andrew & Gao, 2007; Yu et al., 2008) and coordinate descent methods (Friedman et al., 2007). When these methods are used for computing activations with 1000 basis vectors, the activations can be estimated in a few seconds *per unlabeled example.* Since we often need to solve for the activations of tens of thousands of unlabeled examples repeatedly in the inner loop of the overall alternating minimization procedure, these solvers turn out to be too slow for self-taught learning.

We now present a simple optimization algorithm for L_1-regularized optimization problems. We later show that, when the optimal solution is very sparse (as in Equation 4.3-4.4) our method is much faster than classical L_1-regularized solvers (Koh et al., 2007; Andrew & Gao, 2007; Yu et al., 2008; Friedman et al., 2007).

4.3.1 Computing optimal activations

As before, we note that since the optimal values for the activation vector $a^{(i)}$ for example $x_u^{(i)}$ do not depend on other examples, we can optimize separately over each activation vector, and it is sufficient to consider the following optimization problem for a single input x and its activation a:

$$\min_a \quad \ell(a) + \beta\|a\|_1 \tag{4.5}$$

where a corresponds to a vector of activations, and $\ell(a)$ is a specific convex function of a.

The choice of exponential family distribution defines the function $\ell(a)$ here. In the special case of Gaussian sparse coding, $\ell(a)$ is simply a quadratic function, and the optimization problem is a L_1-regularized least squares problem that can be solved efficiently (Efron et al., 2004; Lee et al., 2007a). This suggests an iterative algorithm for general exponential family distributions: at each iteration, we compute a local quadratic approximation $\hat{\ell}(a)$ to the function $\ell(a)$, and optimize the objective function $\hat{\ell}(a) + \beta\|a\|_1$ instead.[5] Using this insight, Lee et al. proposed the IRLS-LARS algorithm (Lee et al., 2006) for the case of L_1-regularized logistic regression, using Efron et al.'s LARS algorithm (Efron et al., 2004) in the inner loop to solve the approximated problem.

This idea can be generalized beyond just logistic regression, and can be applied to other L_1-regularized optimization problems for which a local quadratic approximation can be efficiently computed. Indeed, for the case of the L_1-regularized exponential family in Equation (4.3-4.4), we can show that the local quadratic approximation at a point a is:

$$\hat{\ell}(a) \;=\; \left\|\Lambda^{1/2}Bs' - \Lambda^{1/2}z\right\|^2 \tag{4.6}$$

where $\Lambda_{ii} = \psi''\left((Ba)_i\right)$ for a diagonal matrix Λ, and $z = \Lambda^{-1}(T(x) - \psi'(Ba)) + Ba$.[6]

Further, if the objective function $\ell(a)$ is reasonably approximated by a quadratic function, the solutions to the successive quadratic approximations should be close to each other. However, the LARS algorithm used in IRLS-LARS cannot be initialized at an arbitrary point, and thus has to rediscover the solution from scratch while solving each successive approximation. In contrast, the feature-sign search algorithm (that we developed in the context of Gaussian sparse coding) can be initialized at

[5]This method is an instance of a general method called Iteratively Reweighted Least Squares (IRLS) in the literature (Green, 1984).

[6]To show that $\hat{\ell}$ is a local quadratic approximation to ℓ at the point a, it suffices to show that ℓ and $\hat{\ell}$ have the same gradient and Hessian at a. Indeed, we have: $\nabla\ell = \nabla\hat{\ell} = -B^T T(x) + B^T\psi'(Ba)$, and $\nabla^2\ell = \nabla^2\hat{\ell} = B^T\Lambda B$.

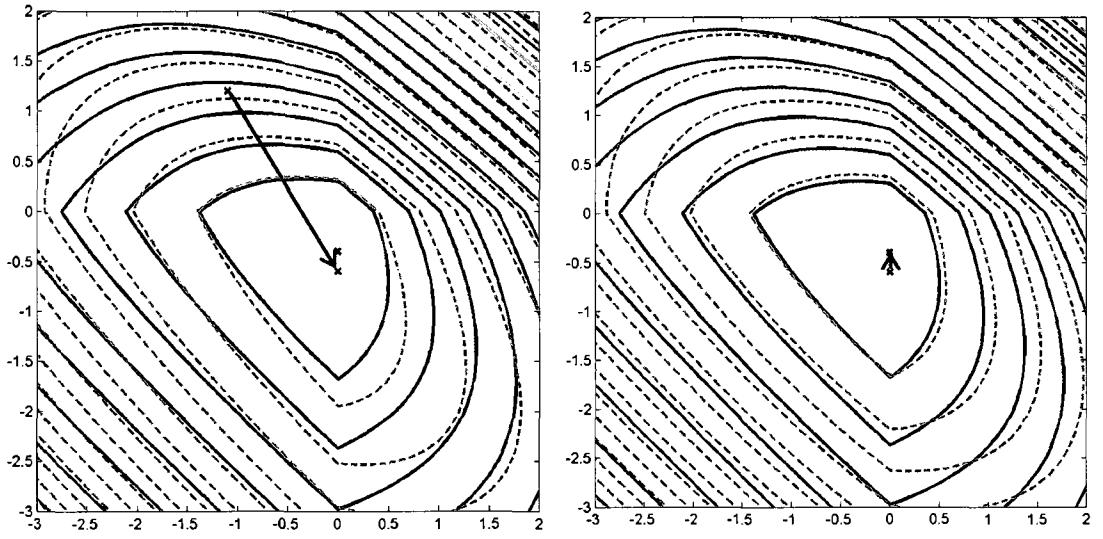

Figure 4.1: Illustration of the IRLS-FS algorithm for L_1-regularized optimization. Solid contours show the true objective function, dashed lines show the IRLS approximation at each iteration. The red cross is the true minimum. Left: First iteration update shown by arrow. Right: In the second iteration, the IRLS approximation is more accurate near the minimum, and the algorithm converges close to the true minimum. (Best viewed in color.)

an arbitrary point (Lee et al., 2007a), and can thus potentially solve the successive approximations much faster. We propose to use the feature-sign search algorithm to optimize each quadratic approximation.

The final algorithm, which we call IRLS-FS, is described below. The algorithm is guaranteed to converge to the global optimum in a finite number of iterations. (Proof similar to IRLS-LARS.)

4.3.2 Computational Efficiency

We compare the IRLS-FS algorithm against state-of-the-art algorithms for optimizing the activations, focusing on the case of binary sparse coding (i.e., $x \in \{0,1\}^n$, with

Algorithm 4 IRLS-FS algorithm for L_1-regularized exponential family problems

Input: Input $x \in \mathcal{X}$, with an exponential family distribution over $\mathcal{X}$ defined by the functions h, T and ψ as in Equation 4.2, where $T(x) \in \mathbb{R}^n$. $B \in \mathbb{R}^{n \times s}$. Sparsity parameter β. Convergence threshold ϵ. Initialize $a \in \mathbb{R}^s$ as $a := \vec{0}$.

while decrease in objective value at last step $> \epsilon$ **do**

Compute $n \times n$ diagonal matrix Λ with $\Lambda_{ii} = \psi''((Ba)_i)$,

Compute vector $z = \Lambda^{-1}(T(x) - \psi'(Ba)) + Ba$.

Initializing feature-sign search at a, compute:

$\hat{a} = \arg\min_{a'} \left\|\Lambda^{1/2} B a' - \Lambda^{1/2} z\right\|^2 + \beta \|a'\|_1$

Set $a := (1-t)a + t\hat{a}$, where t is found by backtracking line-search (Boyd & Vandenberghe, 2004) to minimize the objective function in Eqn (4.3).

end while

the Bernoulli distribution used as the particular exponential family distribution). This case is especially interesting because this leads to an L_1-regularized logistic regression problem. Note that the activation vector $a \in \mathbb{R}^s$ for a single example has s values, where s is the number of basis vectors used; in other words, the number of "features" in the L_1-regularized logistic regression problem is equal to the number of basis vectors used, but is *independent* of the dimensionality of inputs x (or more generally, the dimensionality of the sufficient statistics $T(x)$) in the original problem. This problem is of general interest (e.g., see Ng, 2004), and customized algorithms have also been developed for it.

We consider five recent algorithms: the IRLS-LARS algorithm (Lee et al., 2006) and the l1-logreg interior point method (Koh et al., 2007) specifically for logistic regression, the Coordinate Descent method (Friedman et al., 2007) with successive IRLS approximations (constructed locally as in IRLS-FS), and the OWL-QN (Andrew & Gao, 2007) and SubLBFGS (Yu et al., 2008) algorithms for L_1-regularized convex optimization problems.[7] All algorithms were evaluated on nine L_1-regularized logistic regression problems which arise in the course of solving Equations (4.3-4.4) with

[7]Other baseline algorithms: Previous published work (Lee et al., 2006) has shown that IRLS-LARS outperforms several previous algorithms, including grafting (Perkins & Theiler, 2003), SCGIS (Goodman, 2004), GenLasso (Roth, 2004) and Gl1ce (Lokhorst, 1999). IRLS-FS, IRLS-LARS, l1-logreg and CoordDesc were implemented in Matlab, and OWL-QN and SubLBFGS were compiled in C++ with optimization flags. Code for all baselines was obtained from the respective authors.

Dataset	Small1	Small2	Small3	Med1	Med2	Med3	Large1	Large2	Large3
IRLS-LARS	4.6	4.9	4.3	12.8	12.5	13.2	1131	1270	1214
l1-logreg	18.3	18.9	17.7	181	188	185	3277	3101	3013
CoordDesc	3.6	3.4	5.6	20.7	20.7	31.0	787	653	723
OWL-QN	7.1	7.0	10.3	27.1	31.4	25.6	1018	739	906
SubLBFGS	33.0	22.3	23.1	101	142	57.2	1953	2717	1627
IRLS-FS	**2.5**	**2.3**	**2.2**	**5.3**	**5.5**	**5.4**	**117**	**108**	**109**

Table 4.1: Running time in seconds for computing activations for binary sparse coding. Each column corresponds to a different binary sparse coding problem.

binary sparse coding (the inputs $x_u^{(i)} \in \{0,1\}^n$ were bag-of-words vectors representing unlabeled text documents, details in Section 4.4.1). The sparsity parameter β was set to produce 20 nonzero activations per example on average.[8] We measured the running time taken by each algorithm to converge within a specified tolerance of the optimal objective value.[9]

Table 4.1 shows the running time for computing activations for 50 input examples, for 9 exponential family sparse coding problems with different input dimensions and number of basis vectors. The problems labeled "Small" each had 200 basis vectors and input dimension 369, the "Med" problems had 600 basis vectors and dimension 369, and the "Large" problems had 1000 basis vectors and dimension 3891. All results were averaged over 50 trials. IRLS-FS outperforms the other algorithms on the task of computing activations, showing that it well-suited to exponential family sparse coding. When a large number of basis vectors are used, IRLS-FS can be 5 to 7 times faster than the best baseline algorithm.

This poses the question: can IRLS-FS be a useful algorithm for general L_1-regularized optimization problems (not necessarily ones generated by the sparse coding problem)? We compare the algorithms above on 14 moderate-size benchmark

[8] In our experiments, this value of β produced reasonable basis vectors during basis learning.

[9] Details: Since IRLS-LARS solves the dual or Lasso version of our problem (i.e., with a constraint $\|a\|_1 \leq C$ on the L_1 norm of the activations rather than a penalty $\beta\|a\|_1$), we first use the KKT conditions to convert between a constraint value C and the equivalent penalty β for that problem (Lee et al., 2006). We ran all algorithms until they reached an objective value of $(1+\epsilon)f^{opt}$ where f^{opt} is the optimal objective value (we used $\epsilon = 10^{-6}$).

Dataset	col	alo	dul	due	arr	mad	hep	spf	pro	wbc	ion	spl	spc	spa
Sparsity	0.2	0.5	0.8	1.4	3.5	3.6	26	30	32	40	46	57	64	67
IRLS-LARS	2.1	3.3	6.2	35.6	2.2	26	0.5	5.0	2.1	5.0	3.5	18.3	2.6	57.8
l1-logreg	18.3	16.8	13.6	14.4	34.8	509	1.0	3.0	2.0	3.8	2.7	12.8	2.0	37.1
CoordDesc	83.3	54.1	63.8	129	7.7	101	0.2	**2.0**	0.6	**2.6**	**1.4**	**4.5**	**0.8**	**14.2**
OWL-QN	27.4	29.4	16.9	79.6	7.7	634	**0.1**	3.4	**0.4**	13.4	1.9	7.1	0.9	39.3
SubLBFGS	114	80.8	60.5	311	24.3	261	0.7	9.3	2.7	14.4	4.5	13.4	2.1	43.0
IRLS-FS	**1.9**	**1.9**	**2.5**	**7.1**	**1.5**	**14**	0.3	2.3	1.3	2.9	2.0	10.4	1.9	50.8

Table 4.2: Running time in seconds for 50 trials of learning parameters of various L_1-regularized logistic regression benchmarks (obtained from Lee *et al.*, 2006). The sparsity is measured by the percentage of nonzero parameters at the optimal solution. The datasets are ordered left-to-right by increasing sparsity (e.g., the leftmost problem *Col* had only 0.2% nonzero parameters at the optimal solution).

classification datasets (obtained from Lee et al., 2006), and apply L_1-regularized logistic regression to them. The value of β on each benchmark was picked to optimize the generalization error of the resulting logistic regression classifier; unlike the earlier experiment, β was not set explicitly to obtain sparse solutions. Table 4.2 shows the running time of the algorithms to compute the optimal parameters. IRLS-FS outperforms the other algorithms on 6 out of 14 of these benchmark datasets; more specifically, it performs best when the optimal parameters have a very small number of nonzero values. While IRLS-FS may not be well-suited to very large scale applications (e.g., with millions of features), it appears to be a useful tool for general L_1-regularized optimization, especially in cases where the optimal solution is expected to be sparse.

When IRLS-FS is used for updating the activations (given fixed basis vectors) in combination with projective gradient descent for updating the basis vectors (given fixed activations), we are able to learn the basis vectors used in our self-taught learning experiments (next section) in about a day on a single computer. This is comparable to the running time for our Gaussian sparse coding experiments in Chapter 2.

4.4 Application to self-taught learning

The exponential family sparse coding model generalizes Gaussian sparse coding, and the activations produced by this model can similarly be used as higher-level features for self-taught learning problems. The model is also closely related to exponential family PCA (Collins et al., 2001), which corresponds to setting the sparsity penalty β to zero, and additionally constraining the basis vectors b_j to be orthogonal to each other. We now show that the exponential family sparse coding model can produce better self-taught learning performance than both Gaussian sparse coding and exponential family PCA.

We also compare our model with Latent Dirichlet Allocation (LDA), a probabilistic generative model for integer-valued (counts) data that is widely applied to unsupervised learning with text documents (Blei et al., 2003). For text documents, the LDA model posits that the document is generated by first picking a distribution over "topics," and then sampling individual words from that topic distribution. Once the model is learnt, a new document can be represented by its inferred distribution over topics. This suggests a self-taught learning algorithm where we learn the topic model over unlabeled documents, and then use the inferred topic distributions for labeled documents as features. In our experiments, we show that our sparse coding model outperforms such a topic model, even though topic models are highly specialized to model text documents.

4.4.1 Text classification

We first apply the exponential family sparse coding algorithms to two self-taught learning problems in text classification: one using binary-valued input vectors with the Bernoulli distribution as the exponential family distribution, and another using integer-valued (word count) vectors with the Poisson distribution as the exponential family distribution.

The self-taught learning problems are based on five standard webpage classification problems (Do & Ng, 2006), and a newsgroup classification problem (20 newsgroups dataset, Lang, 1995). We used 470,000 unlabeled news articles (from the Reuters

corpus, Rose et. al, 2002) to learn basis vectors according to the binary and Poisson sparse coding models.[10] Table 4.3 gives examples of basis vectors obtained from Poisson sparse coding—each column shows the five word stems that were most highly active (i.e., had the highest magnitude weight) for some basis vector. Many basis vectors appear to encode related words and capture various "topics" (Blei et al., 2003). The learnt representation transforms a high-dimensional word-based representation (the bag-of-words input vector) into a succinct representation based on only a few topics that best describe the document. With this succinct topic-based representation, we should be able to learn well even with very few labeled examples (loosely speaking, by associating topics with labels, instead of attempting to associate individual words with labels).

free	share	pharmaceut	estat	paint	actor	novel	audio
market	exchange	drug	real	pictur	actress	literari	video
polici	stock	product	sale	portrait	film	poet	dvd
power	secur	share	loss	museum	comedi	fiction	digit
peopl	commiss	stock	loan	rule	star	univers	softwar

Table 4.3: Examples of basis vectors trained for the classification problems in the Business (left 4 columns) and Arts (right 4 columns) webpage subcategories, using unlabeled Reuters corpus documents with Poisson sparse coding.

Using the learnt basis vectors, we computed features for each classification task using the binary and Poisson sparse coding model. We call our model "ExpSC" and compare against several baselines: the raw words themselves ("Raw"), Gaussian sparse coding ("GSC"), exponential family PCA with the same binary or Poisson exponential family assumption ("ExpPCA"), and also Latent Dirichlet Allocation

[10]Details: The webpage classification problems were obtained from the subcategories of the Arts, Business, Health, Recreation and Sports categories of the DMOZ webpage hierarchy (`http://www.dmoz.org`). Each of them consisted of 10 separate binary classification problems over a 500 word vocabulary; the problems were preprocessed with stopword removal and stemming. The newsgroup classification problem consisted of 10 binary classification problems constructed by picking random newsgroup pairs from 20 newsgroups dataset. We used 600 basis vectors, and picked β to achieve roughly 10% nonzero activations. We did not tune these numbers. For learning, we used stochastic updates with mini-batches of 2000 randomly sampled examples, and stopped learning when the objective value did not decrease for 10 consecutive mini-batch iterations.

Training set size		Raw	ExpSC	ExpSC +Raw	GSC	GSC +Raw	ExpPCA	ExpPCA +Raw	LDA +Raw
Binary	4	34.3%	**27.9%**	30.0%	-	-	29.1%	31.3%	-
	10	23.0%	20.5%	**20.4%**	-	-	22.3%	22.66%	-
	20	17.7%	17.4%	**16.1%**	-	-	19.3%	17.7%	-
Poisson	4	29.6%	25.4%	**25.0%**	31.2%	26.4%	32.9%	30.4%	33.2%
	10	24.3%	18.9%	**18.6%**	26.1%	22.7%	26.3%	23.8%	24.7%
	20	18.4%	15.2%	**14.9%**	21.4%	17.6%	24.2%	21.2%	17.6%

Table 4.4: Aggregate test error across all text classification problems (webpages/newsgroups), represented either using binary vectors (Binary) or word count vectors (Poisson). Gaussian sparse coding (GSC) and LDA work better with word counts, so we show results only for this case. LDA+Raw performed better than LDA alone.

(LDA), a widely-used topic model for text documents (Blei et al., 2003). All baselines (except the raw features) were trained using the same unlabeled data as our model. For LDA, we tried 20, 50 and 100 topics, and picked the best result. We also consider combinations of the raw word features with the other types of features (e.g., "ExpSC+Raw" indicates a combination of the ExpSC features and the raw features). All features were evaluated using standard supervised-learning classifiers over 100 trials each for 4, 10 and 20 labeled training documents.[11]

Table 4.4 shows the average test error over all problems for the binary and Poisson case. The exponential family sparse coding features alone frequently outperform the other features, and produce slightly better results when used in combination with the raw features (ExpSC+Raw). The results for Poisson sparse coding are particularly striking, showing 20-30% error reduction in some cases. The other three methods for using unlabeled data (GSC, ExpPCA, LDA) perform poorly in many cases. Figure 4.2 shows the test errors (with standard error bars) plotted against the training set size for both binary and Poisson sparse coding.

[11]We focused on three standard classifiers—SVM, GDA and kernel dependency estimation (KDE)—that performed best for the raw bag-of-words features out of several generic classifiers, including k-NN and decision trees. We report average results of the best performing classifier for each feature. We picked the β value used for computing the features by cross-validation.

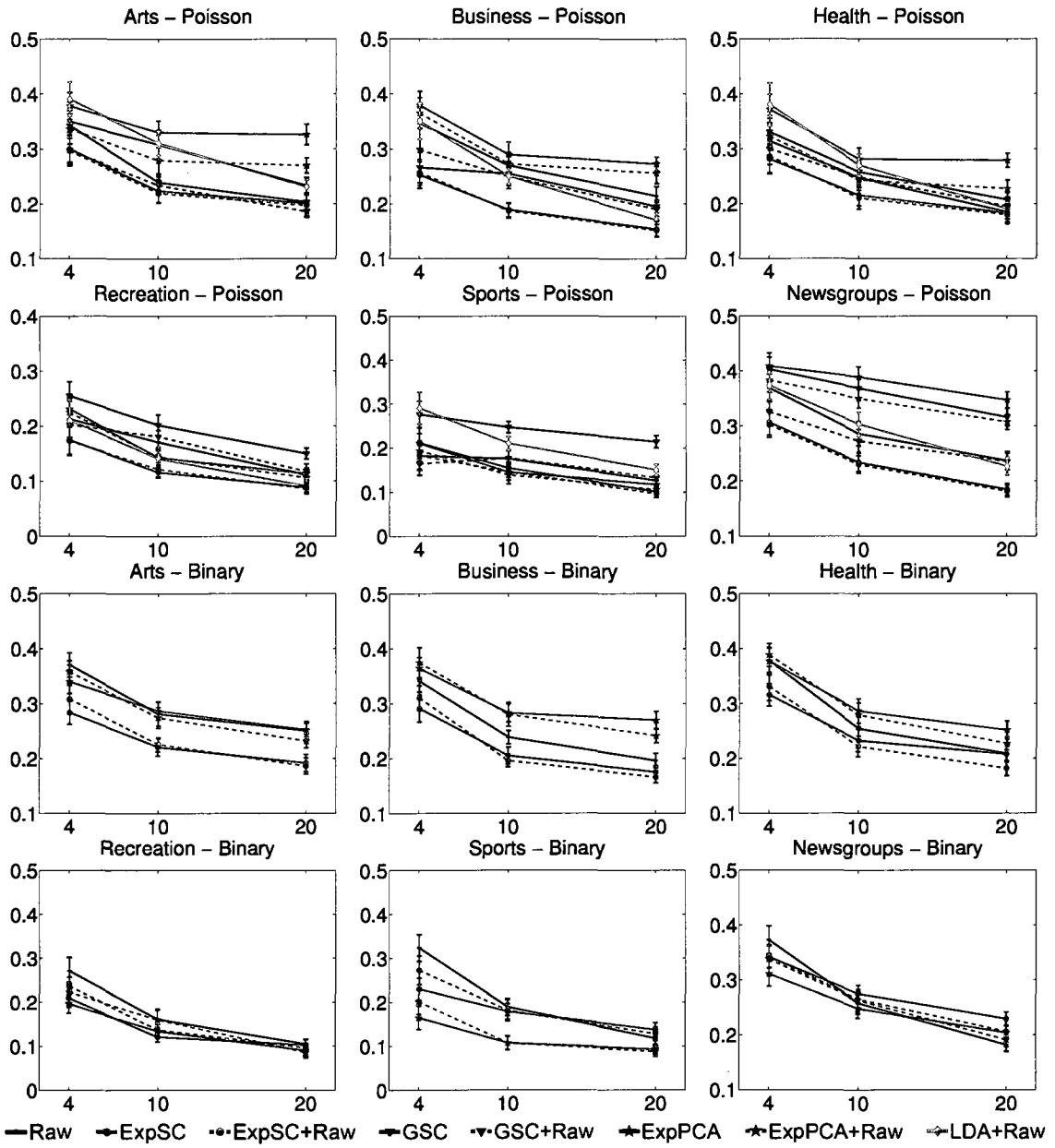

Figure 4.2: Test error vs. training set size for the webpage and newsgroup classification tasks. Poisson sparse coding was used for the ExpSC results. Our algorithm is plotted in red color. (Best viewed in color.)

4.4.2 Robotic perception

We also applied the exponential family sparse coding algorithm to a very different self-taught learning problem: object recognition from 3D range data (see Figure 4.3 for an example of the 3D range data view of a test car). The data was collected with a laser range finder (Velodyne lidar) mounted on a car. The data was obtained by driving the car in a parking lot environment; at each instant, the laser range finder produces a point-cloud representation of the environment. Given a 3D box in this point-cloud space, the task is to predict whether the box contains a car or not.

A standard, robust represenation for such 3D point cloud data is the "spin-image" representation (Johnson & Hebert, 1999). A detailed description of spin-images is beyond the scope of this thesis; but informally, for our application, a spin-image can be thought of a 2D view of a 3D point cloud, when viewed from a given point in 3D space. Specifically, spin images can be thought of as generated by a sheet spinning about the vertical z vector at a point, accumulating counts of other points in each pixel as it rotates (see Figure 4.3). Spin-images describe the 3D surfaces around a reference point using a 2D array of counts (20x10 array in our case), and can represent 3D volumes robustly. For example, we would expect that since cars have similar 3D volume profiles, the spin image computed around a similar point on two different cars would still bear significant similarities.

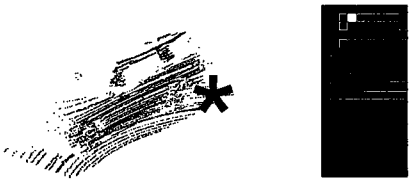

Figure 4.3: Left: A view of a point cloud for a car produced by the laser range finder. Right: A spin-image generated around the point marked with a red star on the left (dark pixels denote zero counts, bright pixels denote larger counts).

Given a large number of unlabeled spin-images (which can be obtained very easily by taking unlabeled point clouds and random reference points within them) and a small number of spin-images from regions manually labeled as car or non-car, our task is to predict whether a new spin image represents a car or non-car region. Since

Training set size	Raw	ExpSC	ExpSC +Raw	GSC	GSC +Raw	ExpPCA	ExpPCA +Raw
4	34.2%	**23.7%**	25.2%	36.8%	36.0%	38.5%	34.6%
10	22.4%	**20.2%**	20.7%	31.3%	27.5%	31.4%	22.2%
20	18.4%	19.2%	**16.9%**	28.7%	19.5%	23.7%	18.0%

Table 4.5: Test error for various algorithms and training set sizes for classifying spin-images from the laser range finder.

the spin-image is a count-based representation, we can apply Poisson sparse coding to this problem. Basis vectors were learnt using 31,000 unlabeled spin-images, and manual examination of the result reveals that certain basis vectors capture various 3D features of cars, roads, trees, and other objects.

Table 4.5 shows the test error for varying training set size. When compared with using the raw spin-image alone, the Poisson sparse coding features reduce test error by 30% with 4 training examples, and by 8-10% for the other cases.

4.5 Discussion

In this paper, we presented a general method for self-taught learning, that extends the previous sparse coding models in a natural way. The extensions can still be solved efficiently using the IRLS-FS algorithm, which we showed to be an efficient algorithm for medium-sized L_1-regularized learning problems with sparse optimal solutions. We showed that our model achieves better self-taught learning performance than previous methods on two very different tasks. We believe our model will extend the applicability of self-taught learning to new, previously difficult problems.

Our extension to Gaussian sparse coding is conceptually similar to the extension proposed for PCA by Collins *et al.*, 2001. However, PCA itself defines a linear transform of the features, unlike Gaussian sparse coding, and does not work as well on self-taught learning tasks. In this chapter, we demonstrated that the exponential family extension of sparse coding also outperforms exponential family PCA in most cases.

Compared to LDA, our model is more general because it can be applied to non-text and non-exchangeable domains. Further, it has been pointed out that when LDA topics are viewed as defining a simplex over word distributions, the exact topics learnt by LDA can vary a lot—the only constraint is that the simplex defined by the topics still spans all the training documents (Blei et al., 2003). In our view, the additional sparsity constraints in the sparse coding model help reduce this ambiguity, and allow large numbers of "topics" to be learnt robustly.

Chapter 5

Large-scale Deep Unsupervised Learning

In the first few chapters of this thesis, we have considered variants of the sparse coding model for unsupervised learning of representations. In this chapter, we consider a more general setting, where we are interested in learning not just a single layer of representation (obtained by the activations or features in our sparse coding algorithms), but in multiple layers of representation, with each layer using the previous layer as input to build successively more abstract concepts. Learning algorithms for multiple layers of representation are often called "deep learning" algorithms.

In this chapter, we consider two well-known unsupervised learning models, deep belief networks (DBNs) and sparse coding, that can learn hierarchical representations of their input (Olshausen & Field, 1996b; Hinton & Salakhutdinov, 2006). With the invention of increasingly efficient learning algorithms over the past decade, these models have been applied to a number of machine learning applications, including computer vision (Larochelle et al., 2007), text modeling (Salakhutdinov & Hinton, 2007) and collaborative filtering (Salakhutdinov et al., 2007), among others. We have already discussed some such applications of sparse coding in previous chapters. These models are especially well-suited to problems with high-dimensional inputs, over which they can learn rich models with many latent variables or layers. When applied to images, these models can easily have tens of millions of free parameters,

and ideally, we would want to use millions of unlabeled training examples to richly cover the input space. Unfortunately, with current algorithms, parameter learning at this scale can take weeks using a conventional implementation on a single CPU. Partly due to such daunting computational requirements, typical applications of DBNs and sparse coding considered in the literature generally contain many fewer free parameters (e.g., see Table 5.1), or are trained on a fraction of the available input examples.

5.1 Deep learning algorithms

Many classical machine learning algorithms, such as support vector machines or logistic regression, can be viewed as learning a single function h that transforms an input vector x into the output label prediction y. In practice, the leap from the input vector x to the abstract prediction y can be hard to achieve via a single function h. For example, for image classification, these algorithms might have to learn a function h that maps the pixel intensities x in an image directly to a prediction about whether the image contains an elephant or not. Or, for text classifications, the algorithms might learn a function that maps the raw words occuring in a document to a prediction about whether the document is a Sports document. Such applications often use various hand-designed features to be computed on the inputs first, so that the mapping from those features to the output label can be reasonably computed in a single step. The learned function h is a single step of representation, and does not capture composition of functions directly. Such algorithms that rely on a single step (or layer) of representation are often called "shallow" learning algorithms.

In contrast, learning algorithms that attempt to learn a sequence of functions h_1, h_2, ..., h_k, and then make a final prediction using the composition $h(x) = h_1(h_2(\ldots h_k(x)))$, do not need to learn everything about the input-to-label mapping in a single step. Each composition can slowly abstract from low-level input dimensions, towards the high-level output label. Thus, for images, we could first learn to detect edges from the pixels in an image, then we could use the edges to learn angles and corners, till ultimately we can learn high-level concepts after several layers of abstraction. To contrast these algorithms with shallow algorithms that learn a single

layer of representation, such algorithms are often called "deep" learning algorithms.

Neural networks with multiple layers of representation are an example of a deep learning algorithm (Rumelhart et al., 1987). However, supervised learning of deep neural networks with many layers of representation is often prone to local minima, and such networks are usually extremely difficult to train using only labeled data. There has been significant recent work on deep learning algorithms, including the development of several practical algorithms for learning deep models using unlabeled data (Hinton & Salakhutdinov, 2006; Bengio et al., 2006). These algorithms are based on learning the deep model a single layer at a time, by gaining a slightly more abstract representation at each layer. Further, recent theoretical work demonstrates that deep learning has significant theoretical advantages—loosely speaking, it can be shown that there are learning problems for which a shallow learning algorithm would require an exponential number of free parameters to be learned, but for which a deep learning model might require only a linear number of free parameters (Bengio & Lecun, 2007). Intuitively, shallow learning algorithms that attempt to capture the label in one step are subject to a combinatorial problem of capturing all variations in the input data, but deep learning algorithms can sometimes avoid these problems by learning simple concepts first, and then combining these concepts to learn more complex concepts.

We consider two specific algorithms for unsupervised learning of deep models, deep belief networks (Hinton & Salakhutdinov, 2006) and sparse coding (Olshausen & Field, 1996a), though many of our observations extend more generally to other unsupervised learning algorithms for deep models, such the autoencoder-based algorithms for learning deep neural networks (Bengio et al., 2006). In our view, the power of deep learning algorithms can be best utilized when we can learn large, deep models with many millions of parameters, and train such models using massive amounts of unlabeled data. This requires that we consider algorithms for large-scale learning of such deep models.

5.2 Large-scale learning

Current learning algorithms for deep unsupervised learning methods, including DBNs and sparse coding, are extremely slow for learning large models, or for learning with large numbers of unlabeled examples. In our view, if the goal is to deploy better machine learning applications, the difficulty of learning large models is a severe limitation. To take a specific case study, for two widely-studied statistical learning tasks in natural language processing—language modeling and spelling correction—it has been shown that simple, classical models can outperform newer, more complex models, just because the simple models can be tractably learnt using orders of magnitude more input data (Banko & Brill, 2001b; Banko & Brill, 2001a; Brants et al., 2007).

Analogously, in our view, scaling up existing DBN and sparse coding models to use more parameters, or more training data, might produce very significant performance benefits. For example, it has been shown that sparse coding exhibits a qualitatively different and highly selective behavior called "end-stopping" when the model is large, but not otherwise (Lee et al., 2007a). There has been a lot of recent work on scaling up DBN and sparse coding algorithms, sometimes with entire research papers devoted to ingenious methods devised specifically for each of these models (Hinton et al., 2006; Bengio et al., 2006; Murray & Kreutz-Delgado, 2006; Lee et al., 2007a; Kavukcuoglu et al., 2008). In our view, better self-taught learning performance can also be achieved just by having the ability to train larger scale models, using larger numbers of training examples.

Meanwhile, the raw clock speed of single CPUs has begun to hit a hardware power limit, and most of the growth in processing power is increasingly obtained by throwing together multiple CPU cores, instead of speeding up a single core (Gelsinger, 2001; Frank, 2002). Recent work has shown that several popular learning algorithms such as logistic regression, linear SVMs and others can be easily implemented in parallel on multicore architectures, by having each core perform the required computations for a subset of input examples, and then combining the results centrally (Dean & Ghemawat, 2004; Chu et al., 2006). However, standard algorithms for DBNs and sparse coding are difficult to parallelize with such "data-parallel" schemes, because

Published source	Application	#Params
Hinton et al., 2006	Digit images	1.6mn
Hinton & Salakhutdinov, 2006	Face images	3.8mn
Salakhutdinov & Hinton, 2007	Semantic hashing	2.6mn
Ranzato & Szummer, 2008	Text	3mn
Our model		100mn

Table 5.1: A rough estimate of the number of free parameters (in millions) in some recent deep belief network applications reported in the literature, compared to our desired model. To pick the applications, we looked through several research papers and picked the ones for which we could reliably tell the number of parameters in the model. All the models do not implement exactly the same algorithm, and the applications cited may not have used the largest-scale models possible, so this is not an exact comparison; but the order of magnitude difference between our desired model and recent work is striking.

they involve iterative, stochastic parameter updates, such that any update depends on the previous updates. This makes the updates hard to massively parallelize at a coarse, data-parallel level (e.g., by computing the updates in parallel and summing them together centrally) without losing the critical stochastic nature of the updates. It appears that *fine-grained parallelism* might be needed to successfully parallelize these tasks.

In this chapter, we exploit the power of modern graphics processors (GPUs) to tractably learn large DBN and sparse coding models. The typical graphics card shipped with current desktops contains *over a hundred* processing cores, and has a peak memory bandwidth several times higher than modern CPUs. The hardware can work concurrently with thousands of threads at any time, and is able to schedule these threads on the available cores with very little overhead. Such fine-grained parallelism makes graphics processors (GPUs) increasingly attractive for general-purpose computation that is hard to parallelize on other distributed architectures.

There is of course a tradeoff—this parallelism is obtained by devoting many more transistors to data processing, rather than to caching and control flow operations, as in a regular CPU core. This puts specific constraints on the types of instructions and memory accesses that can be efficiently implemented (discussed further in Section 5.3). Thus, the main challenge in successfully applying GPUs to a machine

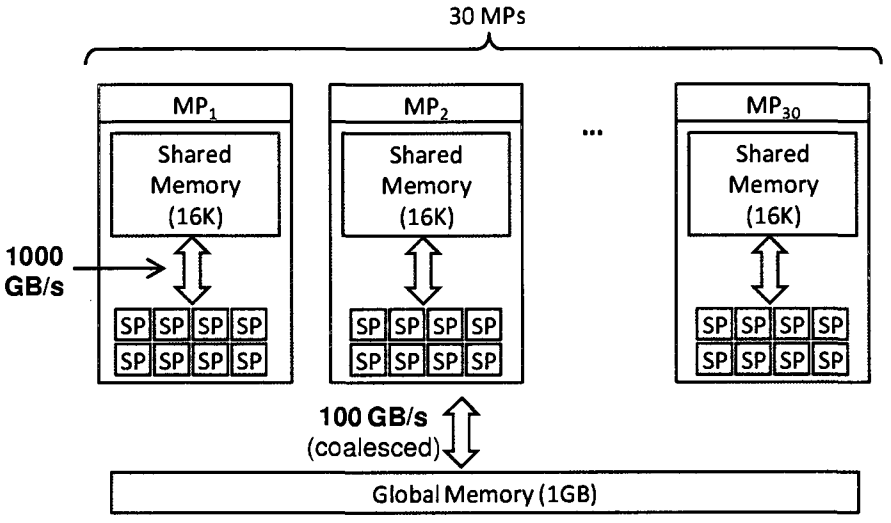

Figure 5.1: Simplified schematic for the Nvidia GeForce GTX 280 graphics card, with 240 total cores (30 multiprocessors with 8 stream processors each).

learning task is to redesign the learning algorithms to meet these constraints as far as possible. While a thorough introduction to graphics processor architecture is beyond the scope of this thesis, we now review the basic ideas behind successful computation with GPUs.

5.3 Computing with graphics processors

We illustrate the principles of GPU computing using Nvidia's CUDA programming model (Harris, 2008). Figure 5.1 shows a simplified schematic of a typical Nvidia GPU. The GPU hardware provides two levels of parallelism: there are several multiprocessors (MPs), and each multiprocessor contains several stream processors (SPs) that run the actual computation. The computation is organized into groups of threads, called "blocks", such that each block is scheduled to run on a multiprocessor, and within a multiprocessor, each thread is scheduled to run on a stream processor.

All threads within a block (and thus executing on the same multiprocessor) have

shared access to a small amount (16 KB) of very fast "shared memory," and they can synchronize with each other at different points in their execution. All threads also have access to a much larger GPU-wide "global memory" (currently up to 4 GB) which is slower than the shared memory, but is optimized for certain types of simultaneous access patterns called "coalesced" accesses. Briefly, memory access requests from threads in a block are said to be coalesced if the threads access memory in sequence (i.e., the k-th thread accesses the k-th consecutive location in memory).[1] When memory accesses are coalesced, the hardware can perform them in parallel for all stream processors, and the effective access speed (between the stream processors and the global memory) is several times faster than the access speed between a CPU and RAM.

Since GPU computation and within-GPU memory accesses themselves are highly parallel, in many algorithms, the main bottleneck arises in transferring data between RAM and the GPU's global memory. For example, the total time taken to multiply two 1000x1000 matrices using our GPU configuration (and a vendor-supplied linear algebra package) is roughly 20 milliseconds, but the actual computation takes only 0.5% of that time, with the remaining time being used for transfer in and out of global memory. A partial solution is to perform memory transfers only in large batches, grouped over several computations. In our example, if we were doing 25 different matrix multiplications and were able to perform memory transfers in large chunks (by transferring all inputs together, and transferring all outputs together), then as much as 25% of the total time is spent in computation. Thus, efficient use of the GPU's parallelism requires careful consideration of the data flow in the application.

[1]For simplicity, we ignore certain other technical conditions that are easy to obey in practice. We also omit discussion of two other types of memory—constant and texture memory—that are optimized for other specific types of access patterns that we do not use in our applications.

5.4 Preliminaries

We consider an unsupervised learning task where we are given a large unlabeled dataset $\{x^{(1)}, x^{(2)}, \ldots, x^{(k)}\}$, where each input $x^{(i)} \in \mathbb{R}^n$.[2] The goal is to learn a model for the inputs x, and to subsequently apply the model to specific machine learning tasks (as in a self-taught learning setup). For example, each unlabeled input $x^{(i)} \in \mathbb{R}^{900}$ might represent a 30x30 pixel image of a handwritten character (represented as a vector of pixel intensities). We might want to learn a model for the complex 900-dimensional space of inputs, and then use this model for classifying new handwritten characters using only very little labeled data.

5.4.1 Deep Belief Networks

DBNs are multilayer neural network models that learn hierarchical representations for their input data. Hinton et al. (2006) proposed an unsupervised algorithm for learning DBNs, in which the DBN is greedily built up layer-by-layer, starting from the input data. Each layer is learnt using a probabilistic model called a restricted Boltzmann machine (RBM). Briefly, an RBM contains a set of stochastic hidden units h that are fully connected in an undirected model to a set of stochastic visible units x. Assuming binary-valued units, the RBM defines the following joint distribution:

$$P(x, h) \propto \exp\left(\sum_{i,j} x_i w_{ij} h_j + \sum_i c_i x_i + \sum_j b_j h_j\right)$$

where the weights w and biases b and c are parameters to be tuned. The conditional distributions can be analytically computed:

[2]For simplicity, we drop the subscript u in our previous notation $x_u^{(i)}$ for unlabeled examples, and represent unlabeled examples just as $x^{(i)}$ in this chapter.

$$P(h_j|x) = \text{sigmoid}(b_j + \sum_i w_{ij} x_i) \tag{5.1}$$

$$P(x_i|h) = \text{sigmoid}(c_i + \sum_j w_{ij} h_j) \tag{5.2}$$

Maximum likelihood parameter learning for an RBM can be efficiently approximated by contrastive divergence updates (Hinton, 2002), where we start with the unlabeled examples as the visible units, alternately sample the hidden units h and visible units x using Gibbs sampling (Equations 5.1-5.2), and update the parameters as:

$$w_{ij} := w_{ij} + \eta \left(\langle x_i h_j \rangle_{\text{data}} - \langle x_i h_j \rangle_{\text{sample}} \right) \tag{5.3}$$

$$c_i := c_i + \eta \left(\langle x_i \rangle_{\text{data}} - \langle x_i \rangle_{\text{sample}} \right) \tag{5.4}$$

$$b_j := b_j + \eta \left(\langle h_j \rangle_{\text{data}} - \langle h_j \rangle_{\text{sample}} \right) \tag{5.5}$$

where η is the learning rate, $\langle \cdot \rangle_{\text{data}}$ represents expectations with the visible units tied to the input examples, and $\langle \cdot \rangle_{\text{sample}}$ represents expectations after $T \geq 1$ iterations of Gibbs sampling. Since each update requires a Gibbs sampling operation, and the updates have to be applied over many unlabeled examples to reach convergence, unsupervised learning of the parameters can take several days to complete on a modern CPU.

5.4.2 Sparse Coding

We briefly revisit the sparse coding model introduced in Chapter 3. Sparse coding is an algorithm for constructing succinct representations of input data (Olshausen & Field, 1996b). Using our earlier example, if each input $x^{(i)} \in \mathbb{R}^{900}$ represents a handwritten character image, sparse coding attempts to learn that each handwritten character is composed of only a few building blocks, such as pen strokes (instead of 900 arbitrary intensity values).

Specifically, given inputs $x \in \mathbb{R}^n$, sparse coding attempts to find basis vectors $b = \{b_1, b_2, \ldots, b_s\}$, $b_j \in \mathbb{R}^n$ such that each input x can be represented as a linear combination of a few basis vectors: $x \approx \sum_j a_j b_j$, where $a_j \in \mathbb{R}$ represents the activation of basis b_j, and most of the a_j values are zero (or, the vector a is sparse). The basis vectors are found by solving the following optimization problem (Lee et al., 2007a):

$$\begin{array}{ll} \text{minimize}_{b,a} & \frac{1}{2}\sum_i \|x^{(i)} - \sum_j a_j^{(i)} b_j\|^2 + \beta \sum_{i,j} |a_j^{(i)}| \\ \text{s.t.} & \|b_j\| \leq 1, \quad \forall j \in \{1, ..., s\} \end{array}$$

where the first term in the objective function encourages good reconstruction ($x^{(i)} \approx \sum_j b_j a_j^{(i)}$), and the second term encourages sparsity by penalizing non-zero activations (Tibshirani, 1996a). The optimization problem is *not* jointly convex in both b and a variables, but it is convex in either one of those variables, if the other is kept fixed. In Chapter 2, we discussed an alternating minimization algorithm which iterates over two steps: first, keeping b fixed, we optimize over a, which leads to an L_1-regularized least squares problem, that can be solved using custom-designed solvers (Efron et al., 2004; Lee et al., 2007a; Andrew & Gao, 2007). Then, we keep a fixed, and optimize over b using convex optimization techniques (Lee et al., 2007a). For problems with high-dimensional inputs and large numbers of basis vectors, the first step is particularly time consuming as it involves a non-differentiable objective function, and the overall learning algorithm can take several days.

5.5 GPUs for unsupervised learning

Both the above algorithms repeatedly execute the following computations: pick a small number of unlabeled examples, compute an update (by contrastive divergence or by solving a convex optimization problem), and apply it to the parameters. To successfully apply GPUs to such unsupervised learning algorithms, we need to satisfy two major requirements. First, memory transfers between RAM and the GPU's global memory need to be minimized, or grouped into large chunks. For machine learning

applications, we can achieve this by storing all parameters permanently in GPU global memory during learning. Unlabeled examples usually cannot all be stored in global memory, but they should be transferred only occasionally into global memory in as large chunks as possible. With both parameters and unlabeled examples in GPU global memory, the updates can be computed without any memory transfer operations, with any intermediate computations also stored in global memory.

A second requirement is that the learning updates should be implemented to fit the two level hierarchy of blocks and threads, in such a way that shared memory can be used where possible, and global memory accesses can be coalesced. Often, blocks can exploit data parallelism (e.g., each block can work on a separate input example), while threads can exploit more fine-grained parallelism because they have access to very fast shared memory and can be synchronized (e.g., each thread can work on a single coordinate of the input example assigned to the block). Further, the graphics hardware can hide memory latencies for blocks waiting on global memory accesses by scheduling a ready-to-run block in that time. To fully use such latency hiding, it is beneficial to use a large number of independently executing blocks. In some cases, as discussed for sparse coding in Section 5.7, we might benefit from completely redesigning the updates to be inherently parallel and requiring less synchronization between threads.

Using these principles, we arrive at the following template algorithm for applying GPUs to unsupervised learning tasks:

Algorithm 5 Parallel unsupervised learning on GPUs

Initialize parameters in global memory.
while convergence criterion is not satisfied **do**
  Periodically transfer a large number of unlabeled examples into global memory.
  Pick a few of the unlabeled examples at a time, and compute the updates in parallel using the GPU's two-level parallelism (blocks and threads).
end while
Transfer learnt parameters from global memory.

5.6 Learning large deep belief networks

We apply Algorithm 5 to learning large DBNs using the contrastive divergence updates in Equations (5.3-5.5). The parameters w, c and b for all the DBN layers are maintained permanently in global memory during training. The updates require repeated Gibbs sampling using the distributions in Equations (5.1-5.2). These distributions can be rewritten using matrix notation:

$$\begin{aligned} P(h|x) &= \text{vectorSigmoid}(b + w^T x) \\ P(x|h) &= \text{vectorSigmoid}(c + wh) \end{aligned}$$

where vectorSigmoid$(\cdot)$ represents the elementwise sigmoid function, and x, h are vectors containing an element corresponding to each visible and hidden unit respectively. The above computations can be batched together for several examples for further efficiency. The matrix operations can be performed in parallel using optimized linear algebra packages for the GPU, and the sigmoid computation and sampling can be done by a simple parallelization scheme where each block works on a single example, and each thread in the block works on a single element of the example. Finally, once the samples have been generated, the updates can again be applied in parallel using linear algebra packages: e.g., $w := w + \eta \left(\langle x^T h \rangle_{\text{data}} - \langle x^T h \rangle_{\text{sample}} \right)$

We extend our method to learning deep belief networks with "overlapping patches" as shown in Figure 5.2. This model is most easily understood with hidden and visible units arranged in a 2-D array (e.g., when the input is an image and each visible unit is a pixel). The input image is fully tiled by equally-spaced, equal-sized patches (or receptive fields), and each patch is fully connected to a unique group of hidden units. There is no sharing of weights in this model, and each connection is parameterized by a free parameter. Each group of hidden units is connected only to a local window (or patch, or receptive field) of visible units, with each connection parameterized by a free parameter (and no weight sharing). Because of the overlapping patches, all the parameters in the model depend on each other, making learning hard. However, Gibbs

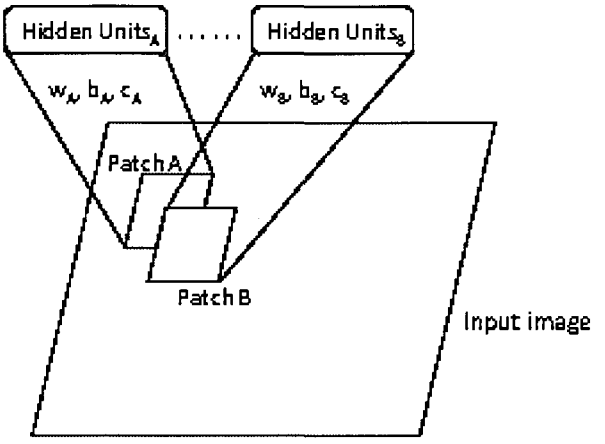

Figure 5.2: A schematic diagram of the overlapping patches model for deep belief networks. Two patches A and B in the input image are shown, with each patch connected to a different set of hidden units. The connections are parameterized by their own sets of parameters w_A, b_A, c_A and w_B, b_B, c_B.

sampling can still be performed in parallel for this model: each visible unit depends on hidden units at many different locations, but the sampling operation $x|h$ can be implemented using only coalesced global memory accesses (implementation details: this can be achieved by using the shared memory available in graphics processors, as shared memory accesses do not need to be coalesced for efficient access). The upward sampling operation $h|x$ still uses a local patch of pixels, and can be implemented using coalesced accesses. Finally, once the sampling operations are performed, weight updates can be applied by considering the cross products $x_i h_j$ in the samples, and this can be done efficiently in parallel as well.

These overlapping patch RBMs can be stacked on top of each other, such that the second-layer RBM contains hidden units connected locally to first-layer hidden units, and so on. The resulting deep networks have a very large number of units, but only sparse, local connections, which make learning tractable even for models with more than 100 million parameters.

5.6.1 Experimental Results

We compare our GPU-based algorithm against CPU-based methods using the following multicore hardware:

- **GPU**: Nvidia GeForce GTX 280 graphics card with 1GB memory. The machine had a dual-core CPU @ 3.16GHz. The reported running time results show the total running time (including all computation, memory transfer, etc.).
- **Single CPU**: Single core @ 3.16GHz.
- **Dual-core CPU**: Two cores, each @ 3.16GHz. (Identical machine as for the GPU result.)
- **Quad-core* CPU**: Four cores, each @ 2.40GHz.[3]

The CPU-based method was implemented using two highly optimized multi-threaded linear algebra packages: ATLAS BLAS (Whaley et al., 2001) and Goto BLAS (Goto & van de Geijn, 2007). Consistent with previous results, we found that Goto BLAS was faster (Bengio, 2007), so we report CPU results using it. As input, we used a large dataset of natural images (van Hateren & van der Schaaf, 1998) and obtained input examples by randomly extracting square image patches of the required size. Following previous work, we used Gaussian visible units and binary hidden units, and trained a sparse RBM by adding an additional penalty term to the objective (Lee et al., 2007b)—however, these modifications do not affect the running time results significantly. For learning, we performed one-step contrastive divergence updates using a mini-batch of 192 examples.

Table 5.2 shows the running time for processing 1 million examples for RBMs of varying size (denoted by number of visible units $\times$ number of hidden units). The GPU method is between 12 to 72 times faster. The speedup obtained is highest for large RBMs, where the computations involve large matrices and can be more

[3]Note that each core in our quad-core machine is somewhat slower than the single CPU core, so that the peak processing power of the quad-core is a little more than three times that of the single CPU. For this reason, the quad-core machine does not always perform better than the single/dual-core machine. We put an asterisk on quad-core* everywhere to remind the reader of this distinction.

Package	Architecture	576x1024	1024x4096	2304x16000	4096x11008
Goto BLAS	Single CPU	563s	3638s	172803s	223741s
Goto BLAS	Dual-core CPU	497s	2987s	93586s	125381s
Goto BLAS	Quad-core* CPU	777s	3785s	70175s	95537s
GPU		38.6s	184s	1376s	1726s
GPU Speedup		**12.9x**	**16.2x**	**51.0x**	**55.4x**

Table 5.2: Average running time in seconds for processing 1 million input examples for learning an RBM, with contrastive divergence updates applied in batches of 192 examples each. The size of the RBM in each column is denoted by the number of visible units $\times$ number of hidden units. The GPU speedup is computed w.r.t. the fastest CPU-based result.

efficiently parallelized by using a large number of concurrent blocks (which allows the graphics hardware to better hide memory latencies). The largest model in Table 5.2 has 45 million parameters, and our GPU method can update these parameters using a million examples in about 29 minutes. In comparison, our multicore CPU takes more than a day per million examples. Since we would ideally want to use tens of millions of training examples for learning such a large model, the CPU method is impractical for such tasks.

Table 5.3 shows a similar running time comparison for two "overlapping patch" models (see table caption for details). The GPU method is about 10 times faster than the dual-core CPU. This speedup is somewhat lower than the speedup observed for a fully connected RBM (Table 5.2), because Gibbs sampling in the overlapping patch model requires many operations involving small matrices (one weight matrix per patch), instead of only a few operations involving large matrices.[4] Using the overlapping patch model, we can learn a four-layer DBN with 96 million parameters, and 25600, 82944, 8192, 4608 and 1024 units respectively in the input layer and the four successive hidden layers. Such models are at least an order of magnitude larger than previously published work on DBNs.

[4]The quad-core* machine was much slower for learning these models, taking 51698s and 104057s respectively, presumably because of the lower raw-clock speed per core. Because the dual-core BLAS performance is also only 16% better than the single core BLAS, even when both cores are at the same clock-speed, it appears that this problem is relatively difficult to efficiently parallelize with multithreaded BLAS, probably because of the small-size per-patch matrix operations involved.

Package	Arch.	20736x49152	36864x92928
Goto	Single CPU	38455s	77246s
Goto	Dual-core	32236s	65235s
GPU		3415s	6435s
GPU Speedup		**9.4x**	**10.1x**

Table 5.3: Average time in seconds for processing 1 million examples for the overlapping patch model, with contrastive divergence updates applied in batches of 192 examples each. The model size in each column is denoted by the number of visible units $\times$ number of hidden units (but note that the units are not fully connected). The two models were created by taking 144x144 pixel and 192x192 pixel inputs respectively; the size of each patch is 24x24 pixels, there are 192 hidden units connected to each patch, and neighboring patches are 8 pixels apart. Overall, the models have 28 million and 54 million free parameters respectively.

Finally, we note that the overlapping patches model can be modified to share parameters in all patches, such that, for example, $w_A = w_B$ in Figure 5.2. If overlapping patches are tiled one pixel apart, this model is identical to the convolutional RBM model (Desjardins & Bengio, 2008; Lee et al., 2009a). Contrastive divergence learning in this model can be implemented by using convolutions to perform the Gibbs sampling operation $h|x$. For small to medium filter (patch) sizes, spatial convolution can be implemented very efficiently using GPUs, by having each block read a filter into shared memory, then reading the input image column-by-column into shared memory, and finally aggregating the output elements affected by that filter and that input image column. It can be shown that by ordering operations in this way, we use only fast shared memory accesses and coalesced global memory accesses.[5] For example, on computing the convolution of 32 128x128 images with 32 16x16 filters, our GPU implementation of spatial convolution (including the time to transfer images/filters into GPU memory) is over 100 times faster than either spatial convolution implemented in C or FFT-based convolution in Matlab.

[5]For larger filter sizes FFT-based convolution is generally better, and a GPU FFT package can be used.

5.7 Parallel sparse coding

We now consider the sparse coding optimization problem discussed in Section 5.4.2. Following the template in Algorithm 5, we maintain the basis parameters b permanently in global memory, and transfer input examples to GPU global memory periodically in large batches. Following the alternating minimization method, each update itself consists of two steps: the first, simpler part of the update involves optimizing over b, given fixed a. This leads to the following constrained optimization problem:

$$\text{minimize}_b \quad \sum_i \|x^{(i)} - \sum_j a_j^{(i)} b_j\|^2 \quad \text{s.t.} \|b_j\| \leq 1, \forall j$$

We solve this problem using projected gradient descent, where we follow the gradient of the quadratic objective function, and project at each step to the feasible set.[6] This method is guaranteed to converge to the optimal b and can be straightforwardly implemented using a GPU linear algebra package.

The other part of the update involves optimizing over a, given fixed b. Since the activation $a^{(i)}$ for each example $x^{(i)}$ is now independent of the activations for other examples, it suffices to consider the following canonical L_1-regularized least squares problem for a single input example x:

$$\text{minimize}_a \quad \tfrac{1}{2}\|x - \sum_j a_j b_j\|^2 + \beta \sum_j |a_j| \tag{5.6}$$

The objective function is not differentiable because of the L_1-penalty term. This problem has recently received wide attention because of its robust feature selection properties (Tibshirani, 1996a; Ng, 2004), and several custom algorithms have been designed to solve it (Efron et al., 2004; Lee et al., 2007a; Andrew & Gao, 2007). Some of these algorithms use sparse linear algebra operations to achieve efficiency. We instead present a very different two-stage algorithm that is inherently parallel,

[6] The projection operation is particularly simple: for each basis vector b_j, if $\|b_j\| > 1$ then rescale b_j to have norm 1, otherwise keep b_j unchanged.

and is thus able to use the GPU hardware more efficiently.

5.7.1 Parallel L_1-regularized least squares

Our algorithm is based on the observation that in the optimization problem in Equation (5.6), if we vary only one of the activations a_j, while keeping the other activations fixed, the optimal value a_j^* can be easily computed (Friedman et al., 2007). Letting B be a matrix with b_j as its j-th column, and $r_j = b_j^T b_j$:

$$a_j^* = \begin{cases} 0 & \text{if } |g_j - r_j a_j| \leq \beta \\ (-g_j + r_j a_j + \beta)/r_j & \text{if } g_j - r_j a_j > \beta \\ (-g_j + r_j a_j - \beta)/r_j & \text{if } g_j - r_j a_j < -\beta \end{cases}$$

$$\text{where } g = \nabla_a \frac{1}{2}\|x - \sum_j a_j b_j\|^2 = B^T B a - B^T x.$$

The updates can be efficiently performed in parallel by having thread j compute just one coordinate a_j^*. Further, since we usually batch several examples together, we can precompute the matrix $B^T B$, the vector $B^T x$ and the vector r once in parallel, store the result in global memory, and perform only efficient accesses to compute all a_j^* values.[7]

Thus, we propose the following iterative algorithm: at each iteration, starting at the current activation values $a = \hat{a}$, we compute all the optimal coordinate values a_j^* *in parallel* as outlined above. Then, we perform a line search in the direction of vector $d = a^* - \hat{a}$. The line search consists of finding a step size $t > 0$ such that the value of the objective function at the point $a = \hat{a} + td$ is lower than the value at $a = \hat{a}$. This line search, including the function evaluations, can be run in parallel.[8] We then move

[7]To see why, note that to compute a_j^*, thread j needs to compute $g_j - r_j a_j = \sum_t (B^T B)_{tj} a_t - (B^T x)_j - r_j a_j$. Consider the elements thread j accesses: (i) $(B^T B)_{tj}$: Accesses can be coalesced if $B^T B$ is stored in row-major order. (ii) By maintaining a in shared memory, all threads can access the same element a_t simultaneously, as well as access the elements a_j that are different for each thread. (For the interested reader, we add that this avoids "bank conflicts" in shared memory. See CUDA reference manual for details.) (iii) $(B^T x)_j$ and r_j: Can be coalesced as thread j accesses the j-th location.

[8]Details: By substituting $a = \hat{a} + td$ in the original objective function, the line search reduces

Method	Sparsity≈3%	6%	10%
Single CPU	215s	403s	908s
Dual-core	191s	375s	854s
GPU	37.0s	41.5s	55.8s
Speedup	**5.2x**	**9.0x**	**15.3x**

Table 5.4: Average running time for updating sparse coding parameters on 5000 input examples. The GPU speedup is computed w.r.t. the fastest CPU-based result. Lee et al.'s algorithm appears to be difficult to parallelize using multithreaded Matlab, because it is an active set method that performs only small matrix operations (including inverses) most of the time. The sparsity value refers to the average percentage of the 1024 activations that were nonzero at the optimal solution. Note that 3-10% is a reasonable range as it corresponds to around 30 to 100 nonzero activations per input example.

to the new point $a = \hat{a} + td$, and iterate. We declare convergence when the objective value decreases by less than a 10^{-6} fraction of the previous objective value.

Since the direction d is a nonnegative linear combination of descent directions along the coordinate axes: $d_j = a_j^* - \hat{a}_j$, d must itself be a descent direction for the objective function. Thus, at each iteration, a step size $t > 0$ can always be found that reduces the value of the objective function, and the overall algorithm is guaranteed to converge to the optimal solution.

This algorithm uses fine-grained parallelism by having each thread compute just one coordinate of the solution. Such highly multithreaded execution is especially well-suited for graphics processors, as the hardware is able to hide memory latency (for threads blocked on memory accesses) by scheduling other threads that are not blocked on memory accesses, and leads to high utilization of the available cores.

5.7.2 Experimental Results

We again compare our method against a multicore CPU baseline (Lee et al., 2007a). We used optimized Matlab code provided by Lee et al. For the CPU multicore results, we executed Matlab with multithreading enabled. Since different choices for the

to minimizing a 1-D function of the form $f(t) = \alpha_2 t^2 + \alpha_1 t + \alpha_0 + \beta\|\hat{a} + td\|_1$, where the values $\alpha_2, \alpha_1, \alpha_0$ can be computed in parallel. For the 1-D line search over $f(t)$, we simply try a fixed set of positive step sizes, and pick the largest step size that reduces the value of the objective function.

regularization parameter β produce solutions of different sparsity, we experimented with a range of choices.

Table 5.4 shows the running time[9] for applying sparse coding basis updates (including both basis and activation optimization) for $k = 5000$ examples, with mini-batches of 1000 examples. Each example $x \in \mathbb{R}^{1024}$ was obtained via a randomly sampled 32x32 pixel natural image patch. We used $s = 1024$ basis vectors, initialized randomly. The large majority of sparse coding time in Lee et al.'s method is taken by the activation learning step, especially when many activations are nonzero at the optimum. By effectively parallelizing this step, our GPU method is up to 15 times faster than a dual-core implementation.

We note that in our self-taught learning algorithm, the basis learning can be done offline (before we see any test examples), but activations need to be computed for every new example that we wish to classify. This means that it is especially important that the activation learning procedure be very efficient, as it is used at classification time. When compared just as a method for computing activations (and not in the alternating procedure for basis learning), our GPU method is up to 27 times faster than the CPU baseline.

5.8 Discussion

Graphics processors are able to exploit finer-grained parallelism than current multi-core architectures or distributed clusters. They are designed to maintain thousands of active threads at any time, and to schedule the threads on hundreds of cores with very low scheduling overhead. The map-reduce framework (Dean & Ghemawat, 2004) has been successfully applied to parallelize a class of machine learning algorithms (Chu et al., 2006). However, that method relies exclusively on data parallelism—each core might work independently on a different set of input examples—with no further subdivision of work. In contrast, the two-level parallelism offered by GPUs is much more powerful: the top-level GPU blocks can already exploit data parallelism, and GPU

[9]The quad-core* machine was slower than the dual-core machine for these models, taking 271s, 574s and 1441s respectively, because of the lower raw-clock speed per core.

threads can further subdivide the work in each block, often working with just a single element of an input example.

We note that GPUs have been applied to certain problems in machine learning, including SVMs (Catanzaro et al., 2008), and to supervised learning in convolutional networks (Chellapilla et al., 2006). A general map-reduce framework for GPUs has also been developed (He et al., 2008), but it usually gives lower performance than a customized GPU method. We hope that our experiments will encourage large-scale applications of deep belief networks and sparse coding to self-taught learning problems. XXX.

Chapter 6

Conclusions

Self-taught learning is a new framework for using unlabeled data in supervised classification tasks. This framework does not require that the unlabeled data follow the class labels of the supervised task, or arise from the same generative distribution. Such unlabeled data is often significantly easier to obtain than in previously studied frameworks such as semi-supervised learning. In this thesis, we have demonstrated that self-taught learning can be applied successfully to a variety of hard machine learning problems.

Algorithms for self-taught learning: The centerpiece of our work is a self-taught learning algorithm based on an optimization problem called "sparse coding." This algorithm uses unlabeled data to learn a new representation for complex, high-dimensional inputs, and then applies supervised learning over this representation. The representation captures higher-level aspects of the input, and significantly improves classification performance on many test domains, including computer vision, audio recognition and text classification (Raina et al., 2007). We have also developed efficient sparse coding algorithms for a translation-invariant version of the model, that can be applied to audio and image data (Grosse et al., 2007). We also generalize the model to a much broader class of inputs (the exponential family of distributions), and apply the model to text classification and a robotic perception task (Lee et al., 2009b). Taken together, these experiments demonstrate that machine learning can be applied to much harder problems than previously possible.

Large-scale algorithms: These self-taught learning algorithms work best when they are allowed to learn rich models (with millions of parameters) using large amounts of unlabeled data (millions of examples). Unfortunately, with current methods, it can take weeks to learn such rich models. Further, these methods require fast, sequential updates, and with current algorithms, are not conducive to being parallelized on a distributed cluster, such as the commonly used map-reduce cluster. To apply self-taught learning to such large-scale problems, we show that graphics processor hardware (available in most modern desktops) can be used to massively parallelize the algorithms. Using a new inherently parallel algorithm, the sparse coding algorithm can be easily implemented on graphics processors, and we show that this can reduce the learning time from about three weeks to a single day (Raina et al., 2009).

Learning hierarchical representations: Finally, we consider self-taught learning methods that learn hierarchical representations using unlabeled data. We focus on a particular hierarchical model, the deep belief network, that has received wide attention in the machine learning community in recent years. We develop general principles for unsupervised learning of such hierarchical models using graphics processors, and show that the slow learning algorithms for deep belief networks can be successfully parallelized. This implementation is up to 70 times faster than an optimized CPU implementation, reduces the learning time from weeks to hours, and represents the state-of-the-art in learning deep belief networks (Raina & Ng, 2008).

Learning for the Internet age: The last decade has been characterized by a veritable explosion in the amount of data freely available. It is now possible to almost routinely obtain *hundreds of millions* of images, or even *billions* of English documents on the Web. Websites such as Google and Facebook serve *billions* of webpages every month. Developing machine learning algorithms that can operate at these scales is a challenge.

Further, since a large proportion of the available data is unlabeled, progress in machine learning might well rely on the development of unsupervised learning algorithms that can use large amounts of unlabeled data. In this thesis work, we show that unlabeled data can be used profitably in a variety of applications—the algorithms we describe are almost completely unsupervised, but can perform remarkably

well on image, text and audio data. However, we believe that this work is still just scraping the surface of possibilities, and the potential benefits of using easily available unlabeled data can be truly enormous.

Bibliography

(2005). A sparse texture representation using local affine regions. *IEEE Trans. Pattern Anal. Mach. Intell.*, *27*, 1265–1278. Lazebnik, Svetlana and Schmid, Cordelia and Ponce, Jean.

Ando, R. K., & Zhang, T. (2005). A framework for learning predictive structures from multiple tasks and unlabeled data. *Journal of Machine Learning Research*, *6*, 1817–1853.

Andrew, G., & Gao, J. (2007). Scalable training of L_1-regularized log-linear models. *ICML*.

Atick, J. (1992). Could information theory provide an ecological theory of sensory processing. *Network: Computation in Neural Systems*, *3*, 213–251.

Banko, M., & Brill, E. (2001a). Mitigating the paucity-of-data problem: exploring the effect of training corpus size on classifier performance for natural language processing. *First international conference on Human language technology research* (pp. 1–5).

Banko, M., & Brill, E. (2001b). Scaling to very very large corpora for natural language disambiguation. *ACL*.

Baxter, J. (1995). Learning internal representations. *COLT*. Santa Cruz, California, United States.

Baxter, J. (1997). Theoretical models of learning to learn. In T. Mitchell and S. Thrun (Eds.), *Learning to learn*.

Belkin, M., Niyogi, P., & Sindhwani, V. (2005). On Manifold Regularization. *AISTAT.*

Bell, A. J., & Sejnowski, T. J. (1995). An information-maximization approach to blind separation and blind deconvolution. *Neural Computation, 7,* 1129–1159.

Belongie, S., Malik, J., & Puzicha, J. (2002). Shape matching and object recognition using shape contexts. *IEEE Trans. Pattern Anal. Mach. Intell., 24,* 509–522.

Ben-David, S., Lu, T., & Pál, D. (2008). Does unlabeled data provably help? worst-case analysis of the sample complexity of semi-supervised learning. *COLT* (pp. 33–44).

Ben-David, S., & Schuller, R. (2003). Exploiting task relatedness for multiple task learning. *COLT.*

Bengio, Y. (2007). Speeding up stochastic gradient descent. *NIPS Workshop on Efficient Machine Learning.*

Bengio, Y., Lamblin, P., Popovici, D., & Larochelle, H. (2006). Greedy layer-wise training of deep networks. *NIPS.*

Bengio, Y., & Lecun, Y. (2007). *Scaling learning algorithms towards ai.* MIT Press.

Berg, A., Berg, T., & Malik, J. (2005). Shape matching and object recognition using low distortion correspondence. *CVPR.*

Bishop, C. (1995). *Neural networks for pattern recognition.* Oxford University Press.

Bishop, C. M. (2006). *Pattern recognition and machine learning.* Springer.

Blei, D., Ng, A. Y., & Jordan, M. (2002). Latent Dirichlet allocation. *NIPS.*

Blei, D., Ng, A. Y., & Jordan, M. I. (2003). Latent Dirichlet allocation. *JMLR, 3,* 993–1022.

Blum, A., & Chawla, S. (2001). Learning from labeled and unlabeled data using graph mincuts. *ICML* (pp. 19–26). Morgan Kaufmann Publishers Inc.

Blumensath, T., & Davies, M. (2006). Sparse and shift-invariant representations of music. *IEEE Transactions on Audio, Speech, and Language Processing* (pp. 50–57).

Boyd, S., & Vandenberghe, L. (2004). *Convex optimization.* Cambridge University Press.

Boynton, G., & Hegde, J. (2004). Visual cortex: The continuing puzzles of area v2. *Current Biology, 14*, 523R–524R.

Bradley, D., & Bagnell, J. A. (2008). Differentiable sparse coding. *NIPS.*

Brants, T., Popat, A. C., Xu, P., Och, F. J., & Dean, J. (2007). Large language models in machine translation. *EMNLP-CoNLL.*

Caruana, R. (1997). Multitask learning. *Machine Learning, 28*, 41–75.

Catanzaro, B. C., Sundaram, N., & Keutzer, K. (2008). Fast support vector machine training and classification on graphics processors. *ICML.*

Cavanaugh, J., Bair, W., & Movshon, J. (2002). Nature and interaction of signals from the receptive field center and surround in macaque v1 neurons. *Journal of Neurophysiology, 88*, 2530–2546.

Chapelle, O., Schölkopf, B., & Zien, A. (Eds.). (2006). *Semi-supervised learning.* Cambridge, MA: MIT Press.

Chellapilla, K., Puri, S., & Simard, P. (2006). High performance convolutional neural networks for document processing. *Frontiers in Handwriting Recognition.*

Chu, C. T., Kim, S. K., Lin, Y. A., Yu, Y., Bradski, G. R., Ng, A. Y., & Olukotun, K. (2006). Map-reduce for machine learning on multicore. *NIPS.*

Collins, M., Dasgupta, S., & Schapire, R. E. (2001). A generalization of principal component analysis to the exponential family. In *NIPS.*

Cortes, C., & Vapnik, V. (1995). Support-vector networks. *Machine Learning* (pp. 273–297).

Cozman, F. G., & Cohen, I. (2002). Unlabeled data can degrade classification performance of generative classifiers. *Fifteenth International Florida Artificial Intelligence Society Conference* (pp. 327–331).

Dean, J., & Ghemawat, S. (2004). Mapreduce: Simplified data processing on large clusters. *USENIX Symposium on Operating Systems Design and Implementation* (pp. 137–150).

Deerwester, S. C., Dumais, S. T., Landauer, T. K., Furnas, G. W., & Harshman, R. A. (1990). Indexing by latent semantic analysis. *Journal of the American Society of Information Science, 41*, 391–407.

Desjardins, G., & Bengio, Y. (2008). *Empirical evaluation of convolutional RBMs for vision* (Technical Report).

Do, C., & Ng, A. Y. (2006). Transfer learning for text classification. *NIPS*.

Dupuis-Roy, N., Fortin, I., Fiset, D., & Gosselin, F. (2009). Uncovering gender discrimination cues in a realistic setting. *Journal of Vision, 9*, 1–8.

Efron, B., Hastie, T., Johnstone, I., & Tibshirani, R. (2004). Least angle regression. *Annals of Statistics, 32*, 407–499.

Essen, U., & Steinbiss, V. (1992). Cooccurrence smoothing for stochastic language modeling. *Acoustics, Speech, and Signal Processing, IEEE International Conference on, 1*, 161–164.

Fei-Fei, L., Fergus, R., & Perona, P. (2004). Learning generative visual models from few training examples: an incremental Bayesian approach tested on 101 object categories. *CVPR Workshop on Gen.-Model Based Vision.*

Fisher, R. A. (1936). The use of multiple measurements in taxonomic problems. *Annals of Eugenics, 7*, 179–188.

Frank, D. (2002). Power-constrained CMOS scaling limits. *IBM Journal of Research and Development, 46.*

Freeman, W. T., & Adelson, E. H. (1991). The design and use of steerable filters. *IEEE Transactions on Pattern Analysis and Machine Intelligence, 13*, 891–906.

Friedman, J., Hastie, T., Höfling, H., & Tibshirani, R. (2007). Pathwise coordinate optimization. *Ann. App. Stat., 2.*

Garofolo, J. S., Lamel, L. F., Fisher, W. M., Fiscus, J. G., Pallett, D. S., Dahlgren, N. L., & Zue, V. (1993). *Timit acoustic-phonetic continuous speech corpus.* Linguistic Data Consortium, Philadelphia.

Gelsinger, P. (2001). Microprocessors for the new millennium: Challenges, opportunities and new frontiers. *ISSCC Technical Digest.*

Goodman, J. (2004). Exponential priors for maximum entropy models. *ACL.*

Gool, L. J. V., Moons, T., & Ungureanu, D. (1996). Affine/ photometric invariants for planar intensity patterns. *ECCV '96: Proceedings of the 4th European Conference on Computer Vision-Volume I* (pp. 642–651). London, UK: Springer-Verlag.

Goto, K., & van de Geijn, R. (2007). High performance implementation of the level-3 BLAS. *ACM Transactions on Mathematical Software, 35.*

Grauman, K., & Darrell, T. (2007). The pyramid match kernel: Efficient learning with sets of features. *Journal of Machine Learning Research, 8*, 725–760.

Green, P. J. (1984). Iteratively reweighted least squares for maximum likelihood estimation, and some robust and resistant alternatives. *Journal of the Royal Statistical Society, Series B, Methodological, 46*, 149–192.

Gross, C. G. (2002). Genealogy of the "grandmother cell". *The Neuroscientist, 8*, 512–518.

Grosse, R., Raina, R., Kwong, H., & Ng, A. Y. (2007). Shift-invariant sparse coding for audio classification. *UAI.*

Harris, M. (2008). Many-core GPU computing with NVIDIA CUDA. *International Conference on Supercomputing.*

Harris, Z. S. (1968). *Mathematical structures of language.* Wiley.

Hawkins, J., & Blakeslee, S. (2004). *On intelligence.* Times Books.

He, B., Fang, W., Luo, Q., Govindaraju, N. K., & Wang, T. (2008). Mars: A mapreduce framework on graphics processors. *PACT.*

Hearst, M. A. (1992). Automatic acquisition of hyponyms from large text corpora. *International Conference on Computational Linguistics* (pp. 539–545).

Hinton, G. E. (2002). Training products of experts by minimizing contrastive divergence. *Neural Computation, 14,* 2002.

Hinton, G. E., Osindero, S., & Teh, Y.-W. (2006). A fast learning algorithm for deep belief nets. *Neural Computation, 18.*

Hinton, G. E., & Salakhutdinov, R. R. (2006). Reducing the dimensionality of data with neural networks. *Science, 313,* 504–507.

Hofmann, T. (1999). Probabilistic latent semantic analysis. *UAI* (pp. 289–296).

Holub, A., Welling, M., & Perona, P. (2005). Combining generative models and Fisher kernels for object class recognition. *ICCV.*

Horn, R., & Johnson, C. R. (1985). *Matrix analysis.* Cambridge Press.

Hoyer, P. O., & Hyvrinen, A. (2002). A multi-layer sparse coding network learns contour coding from natural images. *VISION RESEARCH, 42,* 2002.

Hubel, D. H., & Wiesel, T. N. (1962). Receptive fields, binocular interaction and functional architecture in the cat's visual cortex. *The Journal of Physiology, 160,* 106–154.

Hyvärinen, A., & Pajunen, P. (1999). Nonlinear independent component analysis: Existence and uniqueness results. *Neural Networks, 12,* 429–439.

III, H. D., & Marcu, D. (2006). Domain adaptation for statistical classifiers. *Journal of Artificial Intelligence Research, 26,* 101–126.

Ito, M., & Komatsu, H. (2004). Representation of angles embedded within contour stimuli in area v2 of macaque monkeys. *Journal of Neuroscience, 24*, 3313–3324.

Jaakkola, T., & Haussler, D. (1998). Exploiting generative models in discriminative classifiers. *NIPS.*

Joachims, T. (1999). Transductive inference for text classification using support vector machines. *International Conference on Machine Learning (ICML)* (pp. 200–209). Bled, Slowenien.

Johnson, A. E., & Hebert, M. (1999). Using spin images for efficient object recognition in cluttered 3d scenes. *IEEE Transactions on Pattern Analysis and Machine Intelligence, 21*, 433–449.

Jurafsky, D., & Martin, J. (2000). *Speech and language processing.* Prentice Hall.

Kavukcuoglu, K., Ranzato, M., & LeCun, Y. (2008). *Fast inference in sparse coding algorithms with applications to object recognition* (Technical Report).

Ke, Y., & Sukthankar, R. (2004). PCA-SIFT: A more distinctive representation for local image descriptors. *IEEE Computer Society Conference on Computer Vision and Pattern Recognition, 2*, 506–513.

Koenderink, J. J., & van Doom, A. J. (1987). Representation of local geometry in the visual system. *Biol. Cybern., 55*, 367–375.

Koh, K., Kim, S.-J., & Boyd, S. (2007). An interior-point method for large-scale L_1-regularized logistic regression. *JMLR, 8*, 1519–1555.

Krsmanovic, F., Spencer, C., Jurafsky, D., & Ng, A. Y. (2006). Have we met? MDP based speaker id for robot dialogue. *The Ninth International Conference on Spoken Language Processing (InterSpeech–ICSLP).*

Lafferty, J., McCallum, A., & Pereira, F. (2001). Conditional random fields: Probabilistic models for segmenting and labeling sequence data. *Proc. 18th International Conf. on Machine Learning.*

Lanckriet, G., Cristianini, N., Bartlett, P., & Ghaoui, L. E. (2004). Learning the kernel matrix with semidefinite programming. *Journal of Machine Learning Research*, *5*, 27–72.

Lang, K. (1995). Newsweeder: learning to filter netnews. *ICML*.

Larochelle, H., Erhan, D., Courville, A., Bergstra, J., & Bengio, Y. (2007). An empirical evaluation of deep architectures on problems with many factors of variation. *ICML*.

Lasserre, J. A., Bishop, C. M., & Minka, T. P. (2006). Principled hybrids of generative and discriminative models. *CVPR* (pp. 87–94).

Lawrence, N. D., & Jordan, M. I. (2006). Gaussian processes and the null-category noise model. In A. Chapelle and B. Schölkopf (Eds.), *Semi-supervised learning*, 152–165. MIT Press.

Lazebnik, S., Schmid, C., & Ponce, J. (2006). Beyond bags of features: Spatial pyramid matching for recognizing natural scene categories. *CVPR*.

LeCun, Y., & Bengio, Y. (1998). Convolutional networks for images, speech, and time series. 255–258.

Lecun, Y., Bottou, L., Bengio, Y., & Haffner, P. (1998). Gradient-based learning applied to document recognition. *Proceedings of the IEEE* (pp. 2278–2324).

LeCun, Y., & Cortes, C. (1998). The MNIST database of handwritten digits. `http://yann.lecun.com/exdb/mnist/`.

Lee, D. D., & Seung, H. S. (1997). Unsupervised learning by convex and conic coding. *NIPS* (pp. 515–521).

Lee, D. D., & Seung, H. S. (1999). Learning the parts of objects by non-negative matrix factorization. *Nature*, *401*, 788–791.

Lee, H., Battle, A., Raina, R., & Ng, A. Y. (2007a). Efficient sparse coding algorithms. *NIPS*.

Lee, H., Chaitanya, E., & Ng, A. Y. (2007b). Sparse deep belief net model for visual area V2. *NIPS.*

Lee, H., Grosse, R., Ranganath, R., & Ng, A. Y. (2009a). Convolutional deep belief networks for scalable unsupervised learning of hierarchical representations. *ICML.*

Lee, H., Raina, R., Teichman, A., & Ng, A. Y. (2008). Exponential family sparse coding with application to self-taught learning with text documents. *ICML Workshop on Prior Knowledge for Text and Language Processing.*

Lee, H., Raina, R., Teichman, A., & Ng, A. Y. (2009b). Exponential family sparse coding with application to self-taught learning. *IJCAI.*

Lee, L. (1999). Measures of distributional similarity. *Proceedings of the 37th conference on Association for Computational Linguistics* (pp. 25–32). Association for Computational Linguistics.

Lee, S.-I., Lee, H., Abbeel, P., & Ng, A. Y. (2006). Efficient L_1 regularized logistic regression. *AAAI.*

Levitt, B., Kiper, D., & Movshon, J. (1994). Receptive fields and functional architecture of macaque v2. *Journal of Neurophysiology, 71*, 2517–2542.

Lewicki, M. S., & Sejnowski, T. J. (1999). Coding time-varying signals using sparse, shift-invariant representations. *NIPS* (pp. 730–736).

Lin, D. (1998). Automatic retrieval and clustering of similar words. *International Conference on Computational linguistics* (pp. 768–774).

Lokhorst, J. (1999). *The LASSO and Generalised Linear Models.* Honors Project, Department of Statistics, The University of Adelaide, South Australia, Australia.

Lowe, D. G. (1999). Object recognition from local scale-invariant features. *International Conference on Computer Vision* (pp. 1150–1157).

Manning, C. D., & Schütze, H. (1999). *Foundations of statistical natural language processing.* MIT Press.

McCallum, A. (2000). Simulated/Real/Aviation/Auto UseNet data. `http://www.cs.umass.edu/~mccallum/code-data.html`.

McCullagh, P., & Nelder, J. A. (1989). *Generalized linear models.* Chapman & Hall.

Mika, S., Schölkopf, B., Smola, A., Müller, K.-R., Scholz, M., & Rätsch, G. (1999). Kernel PCA and de–noising in feature spaces. *NIPS.*

Mikolajczyk, K., & Schmid, C. (2005). A performance evaluation of local descriptors. *IEEE Transactions on Pattern Analysis & Machine Intelligence, 27,* 1615–1630.

Miller, G. A. (1995). Wordnet: A lexical database for English. *Commun. ACM, 38,* 39–41.

Mountcastle, V. (1978). *An organizing principle for the cerebral function: The unit module and the distributed system.* The MIT Press.

Murray, J. F., & Kreutz-Delgado, K. (2006). Learning sparse overcomplete codes for images. *J. VLSI SPS, 45.*

Ng, A. Y. (2004). Feature selection, L_1 vs. L_2 regularization, and rotational invariance. *ICML.*

Nigam, K., McCallum, A., & Mitchell, T. (2006). Semi-supervised text classification using EM. In A. Chapelle and B. Schölkopf (Eds.), *Semi-supervised learning.* MIT Press.

Nigam, K., McCallum, A., Thrun, S., & Mitchell, T. (2000). Text classification from labeled and unlabeled documents using EM. *Machine Learning, 39,* 103–134.

Olshausen, B. A., & Field, D. J. (1996a). Emergence of simple-cell receptive field properties by learning a sparse code for natural images. *Nature, 381,* 607–609.

Olshausen, B. A., & Field, D. J. (1996b). Emergence of simple-cell receptive field properties by learning a sparse code for natural images. *Nature, 381,* 607–609.

Olshausen, B. A., & Field, D. J. (1997). Sparse coding with an overcomplete basis set: A strategy employed by V1? *Vision Research, 37*, 3311–3325.

Oppenheim, A. V., Willsky, A. S., & Nawab, S. H. (1996). *Signals & systems (2nd ed.)*. Prentice-Hall, Inc.

Osborne, M., Presnell, B., & Turlach, B. (2000a). On the lasso and its dual. *Journal of Computational and Graphical Statistics, 9*, 319–337.

Osborne, M. R., Presnell, B., & Turlach, B. A. (2000b). A new approach to variable selection in least squares problems. *IMA Journal of Numerical Analysis, 20*, 389–404.

Pantel, P., & Lin, D. (2000). An unsupervised approach to prepositional phrase attachment using contextually similar words. *ACL* (pp. 101–108).

Pearson, K. (1901). On lines and planes of closest fit to systems of points in space. *The London, Edinburgh and Dublin Philosophical Magazine and Journal of Science, 2*, 559–572.

Perkins, S., Lacker, K., & Theiler, J. (2003). Grafting: Fast, incremental feature selection by gradient descent in function space. *Journal of Machine Learning Research, 3*, 1333–1356.

Perkins, S., & Theiler, J. (2003). Online feature selection using grafting. *ICML*.

Quiroga, Q. Q., Reddy, L., Kreiman, G., Koch, C., & Fried, I. (2005). Invariant visual representation by single neurons in the human brain. *Nature, 435*, 1102–1107.

Rabiner, L., & Juang, B.-H. (1993). *Fundamentals of speech recognition.* Prentice-Hall, Inc.

Raina, R., Battle, A., Lee, H., Packer, B., & Ng, A. Y. (2006). Self-taught learning. *NIPS Workshop on Learning when test and training inputs have different distributions.*

Raina, R., Battle, A., Lee, H., Packer, B., & Ng, A. Y. (2007). Self-taught learning: Transfer learning from unlabeled data. *ICML.*

Raina, R., Madhavan, A., & Ng, A. Y. (2009). Large-scale deep unsupervised learning using graphics processors. *ICML.*

Raina, R., & Ng, A. Y. (2008). Learning large deep belief networks using graphics processors. *NIPS Workshop on Parallel Implementations of Learning Algorithms.*

Raina, R., Shen, Y., Ng, A. Y., & McCallum, A. (2004). Classification with hybrid generative/discriminative models. In *Nips.* MIT Press.

Ranzato, M. A., & Szummer, M. (2008). Semi-supervised learning of compact document representations with deep networks. *ICML.*

Rose, T., Stevenson, M., & Whitehead, M. (2002). The reuters corpus volume 1 - from yesterday's news to tomorrow's language resources. *In Proceedings of the Third International Conference on Language Resources and Evaluation* (pp. 29–31).

Roth, V. (2004). The generalized lasso. *IEEE Trans. Neural Networks, 15,* 16–28.

Roweis, S. T., & Saul, L. K. (2000). Nonlinear dimensionality reduction by locally linear embedding. *Science, 290.*

Rumelhart, D. E., Hinton, G. E., & Williams, R. J. (1987). Learning internal representations by error propagation. In D. E. Rumelhart, J. L. McClelland et al. (Eds.), *Parallel distributed processing: Volume 1: Foundations,* 318–362. Cambridge: MIT Press.

Salakhutdinov, R., & Hinton, G. (2007). Semantic Hashing. *SIGIR workshop on Information Retrieval and applications of Graphical Models.*

Salakhutdinov, R., Mnih, A., & Hinton, G. (2007). Restricted boltzmann machines for collaborative filtering. *ICML.*

Sceniak, M. P., Hawken, M. J., & Shapley, R. (2001). Visual spatial characterization of macaque V1 neurons. *The Journal of Neurophysiology, 85,* 1873–1887.

Schaffalitzky, F., & Zisserman, A. (2002). Multi-view matching for unordered image sets, or "how do i organize my holiday snaps?". *ECCV '02: Proceedings of the 7th European Conference on Computer Vision-Part I* (pp. 414–431). London, UK: Springer-Verlag.

Schölkopf, B., & Smola, A. J. (2001). *Learning with kernels: Support vector machines, regularization, optimization, and beyond.* Cambridge, MA, USA: MIT Press.

Seeger, M. (2001). *Learning with labeled and unlabeled data*Technical Report). Edinburgh University.

Series, P., Lorenceau, J., & Fregnac, Y. (2003). The silent surround of v1 receptive fields: theory and experiments. *Journal of Physiology - Paris, 97*, 453–474.

Serre, T., Wolf, L., & Poggio, T. (2005). Object recognition with features inspired by visual cortex. *CVPR.*

Sharma, J., Angelucci, A., & Sur, M. (2000). Induction of visual orientation modules in auditory cortex. *Nature, 404*, 841–847.

Smith, E., & Lewicki, M. S. (2005). Efficient coding of time-relative structure using spikes. *Neural Computation, 17*, 19–45.

Snow, R., Jurafsky, D., & Ng, A. Y. (2005). Learning syntactic patterns for automatic hypernym discovery. In *Nips*, 1297–1304.

Srebro, N. (2004). *Learning with matrix factorizations.* Doctoral dissertation, Massachusetts Institute of Technology.

Srebro, N., & Jaakkola, T. (2001). Sparse matrix factorization for analyzing gene expression patterns. *NIPS Workshop on on Machine Learning Techniques for Bioinformatics.*

Szummer, M., & Jaakkola, T. (2003). Information regularization with partially labeled data. *NIPS.* MIT Press.

Taskar, B. (2004). Database of ocr images. `http://ai.stanford.edu/~btaskar/ocr/`.

Tenenbaum, J. B., de Silva, V., & Langford, J. C. (2000). A global geometric framework for nonlinear dimensionality reduction. *Science, 290*, 2319–2323.

Thrun, S. (1996). Is learning the n-th thing any easier than learning the first? *NIPS*.

Tibshirani, R. (1996a). Regression shrinkage and selection via the lasso. *Journal of the Royal Statistical Society, Series B, 58*, 267–288.

Tibshirani, R. (1996b). Regression shrinkage and selection via the lasso. *Journal of the Royal Statistical Society, Series B, 58*, 267–288.

Tipping, M. E., & Bishop, C. M. (1999). Probabilistic principal component analysis. *Journal of the Royal Statistical Society, Series B, 61*, 611–622.

Torralba, A., Murphy, K. P., & Freeman, W. T. (2007). Sharing visual features for multiclass and multiview object detection. *IEEE Transactions on Pattern Analysis and Machine Intelligence, 29*, 854–869.

Tsuda, K., Kin, T., & Asai, K. (2002). Marginalized kernels for biological sequences. *Bioinformatics, 18*.

Tzanetakis, G., & Cook, P. (2002). Musical genre classification of audio signals. *IEEE transactions on Speech and Audio Processing*.

van Hateren, J. H., & van der Schaaf, A. (1998). Independent component filters of natural images compared with simple cells in primary visual cortex. *Proceedings of the Royal Society London B, 265*, 359–366.

Vapnik, V. N. (1998). *Statistical learning theory*. Wiley-Interscience.

Vidal-Naquet, M., & Ullman, S. (2003). Object recognition with informative features and linear classification (pp. 281–288.).

Weston, J., Collobert, R., Sinz, F., Bottou, L., & Vapnik, V. (2006). Inference with the universum. *ICML.*

Whaley, R. C., Petitet, A., & Dongarra, J. J. (2001). Automated empirical optimization of software and the ATLAS project. *Parallel Computing, 27,* 3–35.

Yu, J., Vishwanathan, S. V. N., Günter, S., & Schraudolph, N. N. (2008). A quasi-Newton approach to nonsmooth convex optimization. *ICML.*

Zhang, H., Berg, A., Maire, M., & Malik, J. (2006). SVM-KNN: Discriminative nearest neighbor classification for visual category recognition. *CVPR.*

Zhou, D., Bousquet, O., Lal, T. N., Weston, J., & Schölkopf, B. (2003). Learning with local and global consistency. *NIPS* (pp. 321–328). MIT Press.

Zhu, X. (2005). *Semi-supervised learning literature survey* (Technical Report 1530). Computer Sciences, University of Wisconsin-Madison.

Zou, H., Hastie, T., & Tibshirani, R. (2004). Sparse principal component analysis. *Journal of Computational and Graphical Statistics, 15.*